Experimental Studies of CAI combustion in a Four-stroke GDI Engine with an Air-assisted Injector

A thesis submitted for the degree of Doctor of Philosophy

by

Nikolaos P. Brouzos

School of Engineering and Design
Brunel University
United Kingdom

February 2007

In memory of my father

Brunel University
School of Engineering and Design
United Kingdom

Nikolaos P. Brouzos

Experimental Studies of CAI combustion in a Four-stroke GDI Engine with an Air-assisted Injector

February 2007, PhD

Abstract

CAI combustion and the factors affecting it were intensively investigated in a single cylinder, air-assisted gasoline direct injection engine. CAI was achieved by means of residual gas trapping by utilising low-lift short duration camshafts and early closing of the exhaust valves. The effects of EVC (Exhaust Valve Closure) and IVO (Inlet Valve opening) timings, spark timing, single and split injection timings, coolant temperature, compression ratio, cam lift and duration on exhaust emissions and CAI operation were investigated experimentally. Engine speed throughout the course of the experiments, was varied from 1200rpm to 2400rpm and the air/fuel ratio was altered from stoichiometric to the misfire limit.

The results show that the EVC timing, compression ratio, cam lift and duration had significant influences on CAI combustion and emissions. Early EVC when combined with higher compression ratio and higher cam lift, enhance CAI combustion operation and stability. IVO timing had minor effect on CAI combustion while spark timing hardly affects CAI operation as soon as fully-developed CAI conditions were established. Coolant temperature was revealed to have substantial impact on CAI combustion when the coolant temperature was below 65°C.

The results also show the importance of injection timing. Early injection gave faster and more stable combustion, less HC and CO emissions, but more prone to knocking combustion and higher NOx emissions. Furthermore, CAI operation range could considerably be extended with injection during the recompression process. Late injection led to slower and unstable combustion, higher HC and CO emissions but lower combustion noise and NOx emissions. Split injection gave even further extension of CAI range in both

stoichiometric and lean mixture operations. All the above clearly suggest, that optimising injection timing and using split injection is an effective way to control and extend CAI operation in a direct injection gasoline engine.

Contents

Page Number

Abstract

Acknowledgements

Nomenclature

Chapter 1 – Introduction **1**

1.1 – Introduction 1
1.2 – Objectives of Project 4
1.3 – Outline of Thesis 4

Chapter 2 – Literature Review **6**

2.1 – Emissions Legislation 7
2.2 – The Present and the Future in Automotive Industry Research and Development 11
2.3 – Controlled Auto– Ignition Combustion 14
2.3.1 – Introduction and Current Strategies 14
2.3.2 – Overview of CAI Combustion 15
2.3.3 – Approaches towards CAI Combustion in four-stroke gasoline engines 20
– Effects of Engine Operating Parameters on CAI Combustion 25
– CAI Combustion in DI Gasoline Engines 26
2.4 – Exhaust Emissions 29
2.5 – Summary 31

Chapter 3 – Experimental Test Facility **33**

3.1 – Ricardo Hydra Research Engine 34
3.1.1 – General Description 34
3.1.2 – Cylinder Head 35
3.1.3 – Crankshaft Position System 36
3.1.4 – Air– Assisted Fuel Injection System 36

3.1.5 – Ignition System 40
3.1.6 – Sandwich adapter plate 40
3.1.7 – Cylinder Liner and Piston 42
3.1.8 – Gasketing 43
3.1.9 – Fuel Supply System 44
3.1.10 – Injector Calibration 45
3.1.11 – Engine modifications for CAI operation 46
3.2 – Summary 47

Chapter 4 – Experimental Set– up and Data Analysis for CAI and SI Engine Tests **48**

4.1 – Introduction 49
4.2 – Engine variables and test parameters 49
4.2.1 – Camshafts 49
4.2.2 – Compression ratio 51
4.2.3 – Injection timing 51
4.2.4 – Spark timing 52
4.3 – Engine Testing and Measurement Equipment 53
4.3.1 – Introduction 53
4.3.2 – In-Cylinder Pressure Data Acquisition System 53
4.3.2.1– Pressure Transducer 54
4.3.3 – In-Cylinder Pressure and Heat Release Analysis 55
4.3.3.1 – In-Cylinder Pressure Measurements 55
4.3.3.2 – Data Processing and Heat Release Analysis 57
4.3.4 – Calculation of Trapped Mass of Exhaust Products 63
4.3.5 – Exhaust Emissions 64
4.3.5.1 – CO_2, CO, O_2 and Air/Fuel Ratio Measurements 64
4.3.5.2 – NO_x Measurements 66
4.3.5.3 – Unburned Hydrocarbon Measurements 67
4.3.5.4 – Calculation of Specific Exhaust Emissions 68
4.3.6 – Engine Efficiency Calculations 69
4.3.7 – Combustion Efficiency Calculations 70
4.3.8 – Temperature Measurements 70
4.4– Summary 70

Chapter 5 – CAI Combustion Experimental Strategies, Results and Analysis Part I **71**

5.1 – Introduction 72
5.2 –Experimental Strategies 72
5.2.1 – Valve Timing Strategy for CAI Combustion 72
5.2.2 – Injection timing strategy 74
5.2.3 – Compression ratio 76
5.2.4 – Engine coolant 77
5.3 – Test Methodology 77
5.3.1 – Introduction 77
5.3.2 – Experimental practice 78
5.4 – Discussion of Results 82
5.4.1 – CAI Operation Performance 82
5.4.1.1 – General/Overall Performance 82
5.4.2 – CAI and SI Combustion Comparison and Analysis 83
5.4.3 – Spark Ignition Effect 91
5.4.4 – IVO Timing Effect 95
5.4.5 – Coolant temperature effect 96
5.5 – Summary 98

Chapter 6 – CAI Combustion Experiments, Results and Analysis Part II **100**

6.1 – Introduction 101
6.2 – Effect of single injection on CAI operation 101
6.2.1 – Overview 101
6.2.2 – Results and Analysis 103
6.2.2.1 – Effects of Single Injection on CAI Operation Performance and emissions at λ=1 103
6.2.2.2 – Effect of Injection Timing on CAI Combustion at stoichiometric operation at λ=1 108
6.2.2.3 – Effect of Injection Timing on CAI Combustion at Various A/F Ratios 112
6.3 – Effect of split injection on CAI operation 120
6.3.1 – Overview 120
6.3.2 – Results and Analysis 121

6.4 – Effect of EVC timing on CAI operation 127
6.4.1 – Overview 127
6.4.2 – Results and Analysis 128
6.5 – Effect of Compression Ratio (CR) on CAI operation 131
6.5.1 – Overview 131
6.5.2 – Results and Analysis 132
6.6 – Effect of Valve Lift and Cam Duration on CAI operation 135
6.6.1 – Overview 135
6.6.2 – Results and Analysis 136
6.7 – Summary 139

Chapter 7 – Conclusions and Recommendations for Further Work 142

7.1 – Conclusions 143
7.1.1 – Engine Experiments with CAI Combustion 143
7.2 – Variable Timing Parameters' Effect on CAI combustion 144
7.2.1 – Spark Timing Effect 144
7.2.2 – IVO Timing Effect 144
7.2.3 – Fuel Injection Timing Effect 145
– Single injection effect 145
– Double injection effect 145
7.2.4 – EVC timing effect 146
7.3 – Engine Related Parameters' Effect 147
7.3.1 – Coolant Media Temperature Effect 147
7.3.2 – Compression Ratio Effect 147
7.3.3 – Cam Lift and Valve Duration effect 147
7.4 – Further Work Recommendations 148

References

Appendix A – Engine Component Detail Drawings

Appendix B – Fuel Injector Calibration Curve

Appendix C – Compression Ratio Calculations

Appendix D – Source Code of Calculations Software Used

Acknowledgements

Taking this opportunity I would like to express me deepest gratitude to my supervisor Professor Hua Zhao for all the help and guidance I received from the very first day of this project which he gave me the opportunity to be a part of. By becoming his student, I was given the chance to broaden my knowledge horizons in a field I've always sought working in.

In addition, I would like to thank my colleague Dr Yufeng Li for the enormous and precious help I received ever since I was involved in this project. Working with him was a real pleasure and an invaluable experience for which I'm deeply grateful.

A big part of this work wouldn't have been accomplished without the help and contribution of the technical stuff responsible for the Engine laboratories at Brunel University. My deepest gratitude goes out to Mr Bob Webb and Mr John Langdon who have always ensured that the project was never short of supplies. I would also like to thank Mr Clive Barratt for his fast response and endless help on every electronics problem emerging as the project was going on and for manufacturing and maintaining all the necessary control boxes and drives required for the correct engine operation. I'm also sincerely grateful to Mr Len Soanes, Mr Andrew Selway and Mr Paul Yates for ensuring every component used during the project, was fabricated and maintained adequately. Their help has been invaluable.

I owe great gratitude to my mother who has never failed to support me and help me in every way possible from the very first moment I took the decision to join Brunel University for my PhD.

Last but not least, I'm deeply indebted to my partner Magda, as well as her family, for all the direct and indirect support and affection shown throughout the good and bad times that I have been through during the time spent in the UK for my PhD. I strongly believe that I wouldn't be able to complete my PhD if it hadn't been for her to help me in every way possible with my work on this project.

Nomenclature

General Abbreviations

A/F	Air/Fuel
AFR	Air /Fuel Ratio
ABDC	After Bottom Dead Centre
ARC	Active Radical Combustion
ATAC	Active Thermo-Atmospheric Combustion
ATDC	After TDC
BBDC	Before Bottom Dead Centre
BMEP	Brake Mean Effective Pressure
BS	British Standard
BTDC	Before Top Dead Centre
CA	Crank Angle
CAI	Controlled Auto Ignition
CARB	California Air Resources Board
CI	Compression Ignition
COVimep	Coefficient of Variation in IMEP
CR	Compression Ratio
DAQ	Data Acquisition
DI	Direct Injection
EGR	Exhaust gas Recirculation
EGT	Exhaust Gas Temperature
EVC	Exhaust Valve Closure
Ex	Exhaust
FID	Flame Ionisation Detector
GDI	Gasoline Direct Injection
HC	Hydrocarbons
HCCI	Homogenous Charge Compression Ignition
Hz	Hertz
kW	Kilowatt
IC	Internal Combustion
IEGR	Internal Exhaust Gas Recirculation
IMEP	Indicated Mean Effective Pressure

IVC	Intake Valve Closure
LIEF	Laser Induced Exiplex Fluorescence
MBT	Minimum Spark Advance for Best Torque
MFB	Mass Fraction Burned
MPI	Manifold Port Inector/Injection
m	Mass
m/s	metres per second
NEDC	New Emission Drive Cycle
NMOG	Non-Methane Organic Compounds
NDIR	Non-Dispersive Infrared
ON	Octane Number
PC	Personal Computer
PCCI	Premixed Charge Compression Ignition
PFI	Port Fuel Injector/Injection
PIV	Particle Image Velocimetry
PM	Particulate Matter
ppm	parts per million
RAM	Random Access Memory
RON	Research Octane Number
RPM	Revolutions per Minute
SI	Spark Ignition
SOI	Start of Injection
SRS	Spontaneous Raman Scattering
SULEV	Super Low Emissions Vehicle
TDC	Top Dead Centre
TLEV	Transitional Low Emissions Vehicle
UK	United Kingdom
ULEV	Ultra Low Emissions Vehicle
uHC	Unburned Hydrocarbons
VCA	Vehicle Certification Agency
VOC	Volatile Organic Compounds
VVA	Variable Valve Actuation
WOT	Wide Open Throttle
ZEV	Zero Emissions Vehicle

General Notation

λ, lambda	Relative air/fuel ratio
γ	Ratio of specific heats
σ	Standard deviation
θ	Crank angle
a	Crank radius, wet molar fraction of fuel
B	Constant
b	H/C ratio of fuel
c	O/C ratio of fuel
c_p	Specific heat capacity at constant pressure
c_v	Specific heat capacity at constant volume
D	Displacement vector
d	Wet molar fraction of intake air
d_i	Generic displacement in direction I
E_b	Bias voltage
f	Wet molar fraction of exhaust products in intake mixture
g	Wet molar fraction of CO_2
h	Wet molar fraction of CO
i	Numerical index, denotes intake species
j	Wet molar fraction of O_2
k	Wet molar fraction of N_2
l	Connecting rod length, Wet molar fraction of H_2O, litre
M	Magnification Factor
m	Wet molar fraction of NO
m_f	Mass flow rate of fuel
m_r	Mass flow rate of reactants
m_x	molecular mass (where x is CH_bO_c, CO_2, CO, O_2, N_2, H_2O, CH_4 or O)
N	Engine speed, number of cycles
n	Polytropic coefficient, number of crank revolutions per power stroke
n_f	Number of moles of fuel in intake charge
n_r	Number of moles of reactants
n_p	Number of moles of products
P,p	Pressure
P_c	In-cylinder pressure

P_i	Indicated power
Q	Heat transfer
Q_{hv}	Lower heating value of fuel
q	Heat transfer
δQ_{hr}	Heat released during combustion
δQ_{ht}	Heat exchange with chamber walls
R	Universal gas constant
s	Wet molar fraction of unburned hydrocarbons, distance between crank and piston pin axis
T	Temperature
ΔT	Time interval
t	Time, Wet molar fraction of H_2
$\vec{U}$	Veclocity vector
dU	Systematic change in internal energy
u	Velocity component on the x direction
V	Volume
V_c	Clearance Volume
V_d	Displacement volume
v	Velocity component in the y direction
W, w	Work transfer
δW	Work done by cylinder gases on the piston
x	Generic wet molar fraction

Chemical Symbols and Abbreviations

C_1, C_2	Carbon
CH_4	Methane
CH_bO_c	Generic fuel type
CO	Carbon monoxide
CO_2	Carbon dioxide
DMA	Dimethylaniline
H_2O	Water
NO	Nitrogen oxide
NO_2	Nitrogen dioxide
NO_x	Combined oxides of nitrogen

O	Oxygen Radical
O_2	Oxygen
O_3	Ozone

Chapter 1

Introduction

Chapter 1 Introduction

1.1 Introduction

It is universally accepted, that ever since the internal combustion engine was invented, it became the indispensable means to fulfil everyday transportation needs and thus contributing to the improving of many aspects of social and economic life. As years went by and need for transportation evolved, so did the way internal combustion engines responded by adopting new technologies.

However, the benefits of internal combustion engines came to a cost as in the last decades the impact of pollutant exhaust gaseous emissions on the environment has continuously become a hazard to the environment; these concerns involved the effect of CO_2 emissions on the reduced atmospheric air quality leading to the phenomenon called "greenhouse effect" as well as harmful pollutants of HC, NOx and PM. Governments in collaboration with environmental awareness organisations have been focusing their attempts since then in setting the frame for production of engines with minimum possible emissions in an attempt to protect the future air pollution. Simultaneously, the alerting levels of fossil fuels have increased interest in seeking alternative fuels that would replace conventional fuels and thus reduce harmful gaseous emissions. Consequently the automotive industry and everyone involved in it, had to invest into time, money and effort to come up with environmentally friendly engines that would not only combine low emissions but also increased fuel economy without sacrificing as little power output as possible. At the moment, even though these techniques have been investigated intensively providing with encouraging results, they have never been put into any kind of production engine mainly because of practicality and cost efficiency reasons; therefore ICE have been the predominant type of engines used in vehicles.

Consequently, attention was paid to the fact that ICE had to be further optimised to further reduce emission levels so that the vehicles they were fitted in, could comply with the strict regulations imposed concerning maximum permitted emission levels of NOx, CO_2, unburnt HC and particulate matter (PM). Two main approaches in meeting these targets were followed towards this direction:

- Direct fuel injection at high pressure into the engine cylinder; examples include the emerging GDI - direct injection gasoline engines, refined direct injection diesel engines operating with multiple injections and direct injection natural gas engines

- Controlled auto-ignition (CAI) combustion of premixed mixtures of gasoline/diesel with excess air or exhaust gas recirculation (EGR), also known as homogeneous charge compression ignition (HCCI) combustion.

The GDI engine represents, at present, the state-of-the-art in engine research and development in reducing fuel consumption or CO_2 emissions from gasoline engines. The potential fuel economy benefit of a GDI engine is achieved by employing necessary stratification with lean-burn operation at part-load in order to burn an overall very lean or diluted mixture, inherently keeping pumping losses at part-load at a minimum. It is achieved by placing a rich mixture near the spark plug by means of in-cylinder flow (tumble or swirl), piston geometry, spray pattern, and accurate fuel injection control.

However, combustion of the stratified charge in a GDI engine presents a number of obstacles such as optimisation of fuel injection, in-cylinder flow, and piston geometry all crucial parameters to the stratified charge operation by placing the combustible charge near the spark plug at the right time (fuel injection timing and spark timing). But it is notoriously difficult to control the stratified charge combustion over the required operating range. Unsynchronised timing of the above events, leads to excessive unburned hydrocarbons (uHC) and smoke emissions. Secondly, as combustion takes place in the stratified stoichiometric mixture, larger amount of NOx is produced in the stratified charge operation than the homogeneous lean-burn operation. In addition, because the spark timing is strongly linked to injection timing, it is often too advanced for minimising in-cylinder NOx formation. Furthermore, the lean-burn operation necessitates the use of less efficient, expensive, and fuel sensitive NOx after-treatment. These factors make it difficult for the current DI gasoline engines to meet future emission legislation. Therefore, automotive industry needs concentrate on new techniques that will assist in production of a GDI engine that will have both low fuel consumption and low emissions.

CAI engines on the other hand boast for low NOx emission levels and high engine efficiencies directly comparable to the merits of SI and CI engines respectively. The potential to meet current and future emissions legislation, without the need for expensive, complex and inefficient exhaust gas aftertreatment systems, has attracted attention from the automotive industry and the research groups around the world. Even though CAI combustion hasn't been a particularly popular concept for production engines, with the exception of the Honda two-stroke ARC250 engine, its application to four stroke power units presents a notable challenge especially for passenger vehicles.

Various methods of achieving CAI combustion have been discussed and investigated so far; however the method that has emerged as most suitable for a multi cylinder unit capable of the good transient response essential for automotive applications, is the use of large scale valve timings that allow trapping of large amounts of burned gases before fresh charge induction takes place. In this way, both the thermal energy needed to initiate the combustion and the high levels of charge dilution required to maintain the subsequent heat release rate to sustainable levels, are provided. This procedure as it may be expected reduces the space available for the fresh charge, significantly minimising the power output capacity of the engine. As a likely solution the operation of the engine at both SI and CAI mode has been proposed initiating either combustion type according to the load conditions, via a fully variable valve train mechanism.

Unlike conventional SI combustion, where the combustion timing is controlled by the spark timing, the start of autoignition combustion is mainly affected by the temperature history experienced by the fuel/air mixture. Valve timing plays an important role in controlling engine load as the closing of the exhaust defines the quantity of exhaust gas residuals in the cylinder that can blend with the fresh charge and form a mixture with increased overall temperature that burns during the following cycle. It was therefore necessary to obtain a clear opinion on the role various valve timings had on mixture formation, emission levels and operating region.

In addition to the injection timing control before and during the intake process described above, the fuel injection process in the compression stroke is also expected to affect the autoignition combustion process. Unlike the fuel injection process before and during the intake process, a stratified charge will form when fuel is injected during the compression

stroke, which will further influence the start of autoignition and its subsequent combustion process. It is known that a stratified combustible charge will burn faster than a homogeneous charge of the same air/fuel ratio. But it is unknown if the delayed injection will lead to advanced or retarded autoignition combustion, which needs to be investigated. Furthermore, double injections split between an early injection during intake and a later injection during compression shall be investigated on its effect on autoignition combustion and pollutant emission from the CAI combustion process.

1.2 Objectives

The objectives of this project are to:

(i) to research the self-initiated CAI combustion process and its control in a direct injection gasoline engine,
(ii) to investigate the effect of fuel injection timing on CAI combustion,
(iii) to investigate how changing valve timings affects CAI combustion
(iv) to research the effects of other engine parameters on CAI combustion.

1.3 Outline of Thesis

Following the Introduction in Chapter 1, Chapter 2 summarises in four parts the literature published in relation to the objectives of this study. The first part outlines the current and future emissions' legislation and the ways they affect automotive research and development. In the next section, state of the art technologies that either are or may be employed in the future in order to comply with the emissions regulations are reviewed. The third section provides with an introduction to CAI combustion as well as a summary of the literature devoted to it so far. In the fourth section, challenges that need to overcome along with methods employed in order to provide accurate control over the CAI operation are discussed in detail.

Chapter 3 gives a general overview of the engine set-up and its components. Specifications of the engine and test bed are discussed, along with details of the cylinder head, the air assisted fuel injector and the ignition system.

Chapter 4 includes details of the engine components that are varied throughout the course of the experiments (camshafts profiles and valve times, compression ratio, spark and injection timing) along with analytical description of the engine components that had to be modified so that the engine could be operated for CAI experiments. In the same chapter, a summary of the measurement components and methods employed for data recording and analysis is given.

Chapter 5 outlines the experimental strategies concerning valve and injection timing, compression ratio as well as coolant temperature. After describing the experimental schedule and how engine tests were performed, results involving SI/CAI comparison and effects of spark timing, IVO timing and coolant temperature on CAI combustion are presented and discussed.

Chapter 6 contains discussions of the results obtained with changes in single and double injection timings, changes in compression ratio as well as changes in valve lift and duration and their effect on CAI combustion.

Chapter 7 summarises the conclusions that have been drawn from previous chapters. Suggestions and recommendations for further work are also included. This section summarises the necessary steps to be taken so that the aspects of CAI combustion that haven't been studied and require further study, to be investigated and analysed.

Appendix A contains detailed drawings of various engine components manufactured during the project. Appendix B includes the results of the fuel injector calibration procedure. Appendix C lists the compression ratio calculations that took place during the course of the experiments. The aforementioned are included as a reference resource for researchers that may use the equipment in the future. Furthermore in Appendix D the source code of the program used for data processing is presented.

Chapter 2

Literature Review

Chapter 2 Literature Review

2.1 Vehicle Emissions Legislation

Combustion engines development in the post World War II industrial world has helped towards the production of a wider range of vehicles such as passenger cars, trucks and buses that not only consume the planet's fossil fuels resources but also produce harmful emissions gradually reducing the air quality and putting human health into risk. The advantages however offered by vehicles and their widespread use all around the world have turned them into one of the most important means of transportation. One should anticipate in the future that the current worldwide status is more likely to expand than to shrink as emerging economies continue to exhibit impressive growth rates. In addition the introduction of modern technologies, the electronics embedded into engines plus the customers' demand for greater power output will eventually lead to higher fuel consumption rates, higher emission levels and faster fossil fuel consumption.

Over the past decades the main guidelines of automotive research have been concentrating on coming up with solutions that would minimise the recurring damage caused by the use of combustion engines to the environment. With controversy going on about how vehicle emissions contribute towards climate via the greenhouse effect, the necessity for technologies that would facilitate the production of "cleaner" engines becomes greater. Recent statistics [1], illustrate the increased trend of greenhouse gas (GHG) production in the EU with the power industry being the main contributor and with transport following. GHG arising from transport consist of CO_2, NOx and volatile organic compounds (VOC). In worldwide attempt to respond to the increased alarm over climate change, many nations have pledged under the Kyoto protocol to reduce in the following years their GHG production each one at a different percentage e.g UK has committed to reduce them by 12% by 2010. [2]

The resolutions, however, that came out of the Kyoto protocol were not only targeting atmospheric pollution directly associated with emissions from hydrocarbon fuel combustion on a global scale but also on a localised scale mainly including countries'

capitals and industrially developed regions where there's great likelihood that emissions such as NOx and VOC are likely to react with the atmospheric oxygen under the presence of sunlight forming the so called photochemical smog. Air becomes polluted with components such as airborne particles (called particulate matter) and ground-level ozone that can be hazardous to public health when inhaled. In addition, under conditions of restricted oxygen supply, carbon molecules included in the fuel cannot be completely oxidised to CO_2 leading to the formation of CO which can cause symptoms such as drowsiness and headache, followed by unconsciousness, respiratory failure, and even fatality [3]. Further health risks such us impaired respiratory function, may occur when particulate matter (PM) or other carcinogenic hydrocarbon products like benzene are inhaled.

On the bright side though, a significant effort has been made over the last three decades by the involved parties (legislation bodies and vehicle manufacturers) towards minimizing the harmful products emitted by internal combustion engines. A range of lastingly stringent legislation on the reduction of these harmful emissions has been implemented in the United States, Japan and in the EU. Exhaust gas after-treatment systems such as catalytic converter that turn toxic combustion by-products (NOx, CO_2 and VOC) to less harmful gases, have been introduced by the vehicle manufacturers. Table 2.1 provides a summary of the emissions' legislation currently applying in the EU and California Air Resources Board (CARB) for passenger cars.

Table 2.1 Present and Proposed Emission Levels Legislated in the EU and CARB for Passenger Cars[4][5]

Euro Standard	Year	Engine Type	CO (g/km)	HC/NMOG (g/km)	NOx (g/km)	HC+NOx (g/km)	PM (g/km)
Euro III	2001	SI	2.3	0.2	0.15	-	-
		CI	0.64	-	0.5	0.56	0.05
Euro IV	2005	SI	1.00	0.2	0.08	-	-
		CI	0.5	-	0.25	0.3	0.025
Euro V	2009[b]	SI	1.0	0.10[c]	0.06	-	0.005[d]
		CI	0.5	-	0.18	0.23	0.005
Euro VI	2014	SI	1.0	0.10[c]	0.06	-	0.005[d]
		CI	0.5	-	0.08	0.17	0.005
CARB (LEV II)	**2004-10**		**2**	**0.033**	**0.04**		**-**
TLEV			-	-	-		-
LEV			4.2	0.056	0.07		0.01
ULEV			2.1	0.034	0.07		0.01
SULEV			1	0.006	0.02		0.01

*After 100,000 Miles
b – 2010.09 for vehicles > 2,500 kg
c - and NMHC = 0.068 g/km
d - applicable to vehicles using DI engines

Even though the above data exhibit the maximum emission levels allowed for a passenger car, there appear to be a substantial amount of differences in the way this legislation is applied. In the EU each manufacturer is obliged to produce passenger cars that have to comply with the legislation valid at the time of production. Furthermore the maximum levels allowed in the EU are normalised over a modal driving cycle known as New European Driving Cycle (NEDC) that represents the typical usage of a car in Europe. CARB legislation is currently far more stringent than the EU and it is based upon a "fleet-averaged" which essentially means that the average emissions output from the sum of cars sold by a manufacture has to lie within the predefined limits. This instruction allows car manufacturers to use the sales of SULEVs for example to counteract for the higher emissions from TLEVs in order to stay within the allowed emissions range. Furthermore CARB emissions legislation is normalised under transient driving cycle procedures known as Federal Test Procedure 75 (FTP-75) and Supplemental Federal Test Procedures (SFTP) that addresses shortcomings of the earlier. It is therefore understood that these different legislations aren't immediately comparable so that a combined, widely accepted legislation can be established. Johnson [6] in a study published, attempted a normalization of the EU

and CARB regulations and concluded that the HC emission levels in EURO IV and LEV II standards can be considered to be similar. In addition it was noted that the US NOx emissions permitted are 50% less compared to the EU ones; a fact that is likely to further delay the launching of HSDI Diesel and GDI engines in the US market unless satisfactory aftertreatment of exhaust gases is introduced.

Additional measures targeting reductions in local GHG levels have been introduced in EU countries including the UK in the form of heavy motor fuel taxation as illustrated in Table 2.2.

Table 2.2. Minimum levels of taxation applicable to motor fuels in the EU[7]

-	**Minimum excise rates prior to 1.1.2004**	**Minimum excise rates from 1.1.2004**	**Minimum excise rates from 1.1.2010**
Petrol (/1000 l.)	337	421	421
Unleaded petrol (/1000 l.)	287	359	359
Diesel (/1000 l.)	245	302	330
Kerosene (/1000 l.)	245	302	330
LPG (/1000 l.)	100	125	125
Natural gas	100 (/1 000 kg)	2.6 (/gigajoule)	2.6 (/gigajoule)

(The volumes are measured at a temperature of 15° C)

These range of measures also involve granting tax advantages to businesses and engine manufacturers that take specific measures to reduce their emissions as well as introduction of heavier 'company car tax' that imposes greater penalties to the operation of vehicles of high CO_2 emissions along with obligatory publication of the CO_2 emission levels for all new cars manufactured. Recently the EU proposed legally binding fleet average CO_2 emissions of 130 g/km from 2012 onward based on the NEDC, for class M1 vehicles (4 wheels, driver plus max. 8 passengers, Gross Vehicle Weight Rating (GVWR) <3,500kg or

7,700lbs). This implies a fleet average fuel consumption of just 5.4 L/100km (43.4 mpg US) for gasoline and 4.8 L/100km (48.9 mpg US) for diesel vehicles if the market share of petrol and diesel cars is considered to be more or less equal [8]. A similar range of measures have been introduced in the US since the 1970's aiming at achieving certain reduced levels of fleet average fuel consumption for passenger cars and light trucks. However, the reasoning behind this set of action had been the concern regarding oil supply rather than the harmful results of high CO_2 emissions.

2.2 The Present and the Future in Automotive Industry Research and Development

It is unanimously accepted that the target for introducing an engine that would possess significantly better properties than the existing ones should be the ultimate goal of the automotive industry. An engine that ideally would not rely on fossil fuels, would produce no harmful emissions, would be more fuel efficient and practical at the same time. Table 2.3 provides the classification of the various types of vehicles known as Low Emission Vehicles (LEV) and their capability in emission reduction is exhibited. It could be claimed that the answer to the above stated issues, lies in the terms "fuel cell"; a technology that looks rather attracting and promising in theory. Existing technologies in theory enable the production of Zero Emission Vehicles (ZEV) with the use of a fuel cell that would consume hydrogen produced from water by electricity generated from renewable sources. Unfortunately, though, a series of practical issues such as high costs, problems with on-board hydrogen storage and the lack of hydrogen infrastructure haven't been resolved yet meaning that such a propulsion technology would take at least twenty years to be realised and implemented into production vehicles. In addition, reports mentioning that the well-to-wheel efficiency of fuel cell power trains with all the necessary auxiliary equipment is estimated to be similar, or even lower, than that of optimised Diesel engines [9][10], should be taken into consideration and encourage current automotive research and development to focus further to internal combustion engine optimization.

Table 2.3 Reduction of Emissions Levels Attainable in LEVs Relative to a Basic Standard§ Passenger Car[11]

CARB Passenger Car Emissions Reductions			
Classification	**Reductions vs. Basic Standard in Percent**		
	Hydrocarbons (HC)	Carbon Monoxide (CO)	Oxides of Nitrogen (NOx)
Transitional Low Emissions Vehicle (TLEV)	50	=	=
Low Emissions Vehicle (LEV)	70	=	50
Ultra Low Emissions Vehicle (ULEV)	85	50	50
Super Ultra Low Emissions Vehicle (SULEV)	96	70	95
Zero Emissions Vehicle (ZEV)	100	100	100

§ - an average for passenger cars exceeding CARB's least-stringent, TLEVs standard

= Equivalent emissions to vehicles meeting the basic standard

A study by Weiss *et al*.,[12] attempted to quantify the total "energy cost" and recurring effects on the environment of different vehicle technologies using the "well-to-wheel efficiency" concept. In this work an assessment and comparison of the current and latest technologies that project their results by 2020 has been performed evaluating each case separately in terms of total cost including production cost, fuel processing and running costs. The results lead to the conclusion that when energy consumption per distance travelled unit is used as a measurement, diesel/electric and gasoline/electric hybrids provided the best results and they were recommended as the optimum solution. Fuel cell was also confirmed to be least energy efficient as they employ a fuel conversion mechanism from gasoline to hydrogen fuel. Following these reports, car manufacturers including Ford, General Motors, Honda, Mazda, Nissan and Toyota launched gasoline/electric hybrids worldwide. Governments in the USA, Canada and the UK have created incentives such as tax discounts, toll free use of motorways, free parking etc. to promote the widespread use of such vehicles and campaigns have been launched that would raise public awareness on the benefits these vehicles had to offer inherently

increasing sales in the US with 199,148 new registrations for hybrid vehicles in 2005 – a 139 percent increase from 2004 [13].

At the same time evolution in internal combustion engines research has provided with remarkable results. In terms of emissions reduction has been feasible via the adoption of the 3-way catalytic converter that allowed reduction of NOx, HC and CO emissions by over 90%. Their drawback however lies in the fact that this unit can be used only within a very narrow range of stoichiometric mixture composition.[14] With older engines using carburetors, this accurate level of control wouldn't be possible unless a sophisticated closed-loop fuel injection system was employed that would however add to the vehicle cost. These operation requirements prevent the engine from operating at lean AFR at part load resulting in a small but important increase in the overall fuel consumption.

Consequently an SI engine is essential to operate with a homogeneous charge at stoichiometric operation thus requiring simultaneous control of air and fuel flow in order to contribute to the load variation. Intake air is adjusted by throttling leading to an increase in pumping losses reducing engine efficiency by up to 20%. Lately however, and with the adoption of diesel and stratified charge gasoline direct injection (GDI) engines, fuel flow rate was varied independently of airflow permitting lean engine operation inherently reducing fuel consumption at part load. The problem though by lean operation is that traditional exhaust after-treatment systems for reducing NOx emission become less effective creating the need for a system that would provide with catalytic conversion of toxic emissions during lean operation. This technology even though it exists,[15] its high cost prohibits widespread use and is subject to durability problems.

Particulate matter (PM) produced in high rates from diesel engines, lead to the introduction by the Euro IV and Us Tier 2 regulations, of PM filters for the purpose of reducing PM levels. A diesel particulate matter filter (DPF) is defined by the US Environmental Protection Agency (EPA) [16] as a ceramic device that collects the particulate matter in the exhaust stream. The high temperature of the exhaust heats the ceramic structure and allows the particles inside to break down (or oxidise) into less harmful components. These filters should be maintained at about every 100,000 miles and require a periodical purging by injecting extra fuel after the injection effect in order to increase exhaust temperature to

around 500^{o}C so that the oxidization of carbon to CO_2 is facilitated. As a result the recurring fuel consumption increase of about 3-4% tends to counteract for the advantages yielded by lean combustion. According to a study by Salvat *et al.* [17] these aftertreatment systems are currently expensive and cannot yet last the life of the engine. It is clear that in the future a more efficient PM after treatment system is desired which would tackle with these important issues analysed earlier.

Furthermore according to Ogink [18], other innovative systems and approaches with a wide range of features have recently been introduced or are expected to be applied soon, including: flexible valve operation; cylinder de-activation; cycle-to-cycle, model-based engine control systems; and direct-injection of fuel. Bearing these advances in mind, together with the strict legislation on vehicle emissions that is to be applied in many countries, it seems reasonable to expect future reciprocating engines to be considerably cleaner and to have better fuel economy than current engines.

2.3 Controlled Auto Ignition Combustion

2.3.1 Introduction

So far with SI and CI engines continuous efforts have been made to optimise their operation and characteristics as it has been mentioned above. In addition, the potential for application of fuel cells seems to require a substantial amount of time and research efforts until it is implemented in production vehicles. It can therefore safely be claimed that in the near future internal combustion engines will dominate the research interest and optimization targets.

SI engines have so far exhibited the potential for low emissions and are a rather simple product with a low initial cost but with poor part load efficiency due to large losses during gas exchange. CI engines on the other hand are much more fuel efficient and hence the obvious choice in application where fuel cost is more important than the initial cost. However, CI engines powered vehicles produce high NOx emission and particulate matter

(PM) levels and aftertreatment as mentioned earlier is not really cost effective for widespread use [19].

These characteristics in recent years have been attempted to be incorporated into a combustion type that would offer benefits from SI and CI engines, resulting in the development of a new type of combustion known as Controlled Auto Ignition (CAI) and its popularity has been continuously growing amongst researchers' worldwide with a constantly increasing number of publications dedicated to it. According to Thirouard *et al.*, [20] CAI refers to auto-ignition combustion obtained with a high proportion of burned gases trapped in the fresh mixture.

2.3.2 Overview of CAI Combustion

Zhao et al.[21] provide an overview of the different names given to CAI by people who studied it. According to this report, CAI combustion during its development stages received different names assigned differently by each researcher. Active thermo atmosphere combustion (ATAC) [22], and Toyota-Soken compression [23], compression-ignited homogeneous charge combustion ignition [24], homogeneous charge compression ignition combustion [25], activated radicals' combustion [26], premixed charge compression ignition [27] and fluid dynamically controlled combustion process [28]. All these works have a common denominator of describing this emerging type of combustion as extremely smooth, demonstrating low cyclic variation of cylinder pressure histories offering high thermal efficiencies and low exhaust emissions; NOx in particular.

All these nomenclature stated above refers primarily to particular engine set-ups used during the course of the experiments. For example, the widely accepted term "Homogeneous Charge Compression Ignition" (HCCI), is insufficient to describe either the practical two-stroke or four-stroke combustion mechanism identified in work by Onishi *et al.* [22] and Lavy *et al*. [29], respectively where mixture is not homogeneously mixed. PCCI is used to describe fuel and air mixture formation in the inlet manifold, which isn't necessarily the case especially with direct injection (GDI) and diesel engines running CAI combustion. More importantly, this combustion process introduced can be achieved not

only by compression but normally intake air heating has to be used via either internal EGR or with external charge heating. For this study the term 'CAI combustion' is preferred as it describes more closely the generic process than the aforementioned terms simply because this new combustion process is initiated by autoignition of a combustible fuel/air mixture and also because the autoignition process needs to be controlled in order to avoid excessive knocking combustions. This term is also compatible with the conventional classification of internal combustion engines into Spark Ignited (SI) and Compression Ignited (CI) [30].

The principle behind CAI combustion traces back in the 1930's when Semenov first published his ignition theory [31]; however the first attempt to put this theory into action was performed in the late 1970's by Onishi et al., [32] and Noguchi et al., [23] with two stroke gasoline engines. In Onishi's experiments the necessary high temperature levels where achieved by increasing the amount of hot residual gases in the cylinder. As a result, increased fuel economy and reduced NOx and HC emissions were observed. With two-stroke gasoline engines the operating region was limited by insufficient combustion temperatures at low load (lean misfire) and by knocking combustion at high loads. Nevertheless, CAI combustion two stroke engines had reached production in a motorcycle engine that employed a throttle to increase the residual gas concentration in the cylinder. [26] Further investigation into the obvious potential of CAI to reduce emissions and improve fuel consumption in four-stroke engines, lead Najt and Foster in 1983 [24] to achieve combustion in a 4-stroke engine employing intake charge heating whereas a highly diluted charge was used to control the heat release rates. Their results showed that CAI ignition process is governed by low temperature hydrocarbon oxidation kinetics and that this type of combustion suffers from uncontrolled ignition timing and limited operating range.

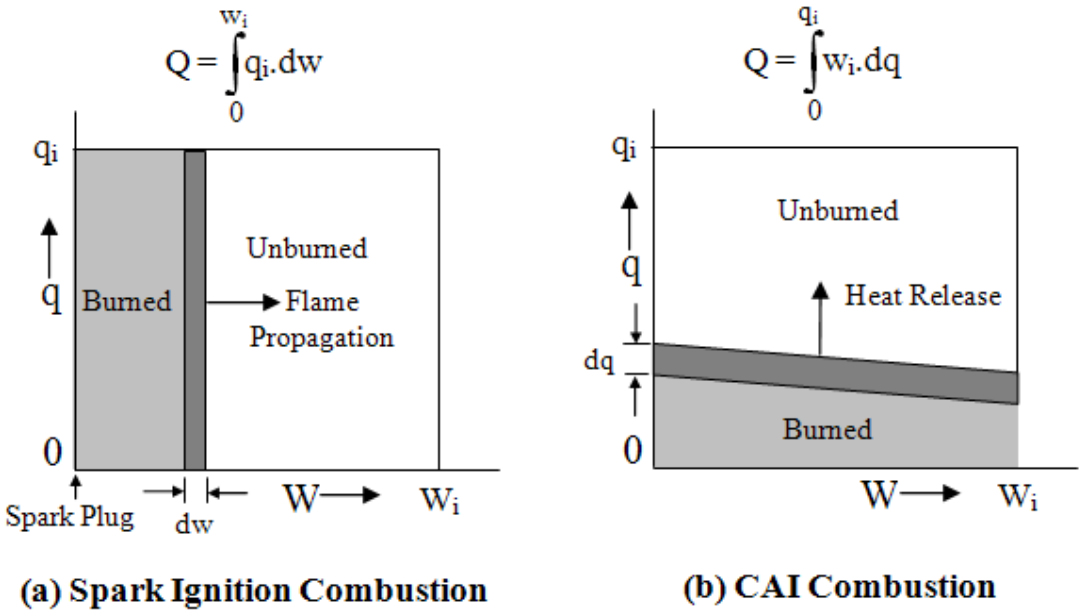

Figure 2.1 Ideal Models of Spark Ignition and CAI Combustion [74]
(Obtained from Ben Leach's PhD Thesis, Brunel University, 2001)

In figures 2.1 (a) and 2.1(b) the ideal model of SI and CAI combustion is demonstrated respectively. The x-axis represents the fraction of total mass and the y-axis the specific heating value of the fuel. During SI combustion, the grey area represents the percentage of fuel that burned completely; *dw* is essentially the flame region that propagates. With CAI combustion, combustion occurs almost simultaneously in every part of the charge where *dq* represents the heating value of the intermediate reactants that continue the chain branching reaction. It is safe therefore to conclude that the minimum duration CAI combustion is limited chemically by kinetic reaction rates, while minimum SI combustion duration is limited by the physics behind flame propagation.

The nature of CAI has been investigated ever since it begun drawing attention. In a study by Thirouard *et al.,* [20] the structure of CAI combustion was investigated using an optically-accessible engine and cycle-resolved direct visualization of the combustion chemiluminescence with the results summarised below:

- Local ignition of the fresh mixture. Auto-ignition may occur simultaneously in several locations in the cylinder.

- Fast extension of the combustion through the combustion chamber. The extension mechanism is characterised by successive auto-ignitions in the areas bordering the initial combustion zones. The continuous initiation of oxidation reactions in neighboring regions results from the global temperature increase caused by the pressure rise, which itself is induced by the on-going heat release.

- "Mass-combustion" phase. During this phase oxidation reactions occur simultaneously in the whole volume of the combustion chamber. Excessively high heat release rate may be expected.

- End of combustion characterised by isolated reaction zones preferably located close to the cylinder walls.

CAI combustion is characterised by spontaneous ignition and burning of a large volume of fuel/air mixture within the cylinder in a short time. In CAI combustion the self-ignition of fuels depends on the charge temperature. The combustion phase is controlled by chemical reaction rather than by turbulent flame preparation as in spark ignition gasoline engines or by mixing of the fuel spray and air as in Diesel engines. Compared with the charge stratification technology, the application of CAI combustion to direct injection gasoline engines has the following advantages:

- It does not require complex combustion chamber geometry and intake port design, since the auto-ignition process is controlled by the charge temperature.

- There is no need for the use of bulky and expensive lean NOx catalytic converter to meet stringent emission regulations as CAI combustion demonstrates ultra-low NOx emissions.

From a thermodynamic point of view CAI combustion cycles approach ideal constant-volume conditions resulting in the improvement of thermal efficiency especially at part load.

Some researchers believe however, that the ultra low NOx emissions cannot be solely attributed to reductions in peak temperatures resulting from mixture dilution, but also because of the lack of flame propagation. Flynn *et al.* [33], for instance, was lead to the conclusion that NOx emissions are inevitable for conventional SI and Diesel engines, since combustion in these engines is based on flame propagation and diffusion flames, respectively. It was found that there is a minimum combustion temperature below which flame propagation cannot occur. For typical engine conditions, a critical temperature of approximately 1900 K was identified, which is in the range where NOx formation chemistry becomes rapid. This may suggest that complete combustion in conventional engines can only take place in temperature intervals where NOx formation is inevitable. It should be understood however, that the reduced combustion temperatures in CAI conditions may lead to incomplete combustion, as proven by, typically lower than for conventional engines, HCCI combustion efficiency values.

Even though CAI applies for both diesel and gasoline fuels, there appears to be a difference in the processes involved in combustion owing to the different nature of each fuel. Diesel fuel for example evaporates at higher temperatures at atmospheric pressure than gasoline and show less resistance to auto-ignition. Therefore diesel cannot autoignite in conditions such as port-injection or direct injection during intake as they cannot provide the thermal environment for autoignition. For this reason the challenge emerges to choose the right injection timing so that the mixture of air and diesel at the end of the compression stroke not only evaporates sufficiently but also provides satisfactory mixing degree. With Diesel being a relatively easy self-ignitable fuel, reducing the effective compression ratio of regular CI engines and reintroducing preferably cooled combustion products into the cylinder, can be ways of facilitating autoignition.

On the other hand gasoline is less prone to autoignition and for that reason the thermal conditions at the end of the compression stroke need to be adequately high to ensure proper autoignition. In the existing literature a number of ways to accomplish these conditions are

proposed including increasing compression ratio, intake air heating, variable valve timing and residual gases trapping in the cylinder [34].

2.3.3 Approaches towards CAI Combustion in four-stroke gasoline engines

Even though the practice of heating intake air is very common amongst many research approaches, it hasn't provided with a satisfactory speed and load range where CAI combustion is attainable. The reasons behind the difficulty in implementing this approach lie mainly to the energy that has to be used to provide the intake heating. Large thermal inertia combined with the transient conditions met in modern automotive application result in making this CAI control method very unpopular and impractical. Unless the heat released from the engine coolant media or from the exhaust pipes is used to heat the intake air, a huge amount of energy is required leading to increased fuel consumption and reduced energy efficiency rates.

In further attempts to establish autoignition conditions before TDC, increasing compression ratio has been successfully employed [35] as a way to increase in cylinder temperature and pressure levels via mixture compression. The results however, demonstrated the need for operation under lean conditions so that increased heat release rates are prevented thus preventing the method to be applied on a wide load range as it happened with intake charge heating. A solution to the narrow operating region problem was demonstrated in work by Lavy et al. [29], the solution was based on the use of a CAI / SI hybrid strategy that would employ SI combustion when the engine needed to operate at high loads and CAI at low loads resulting in a lower fuel consumption and emission levels than when SI was only present. This approach however could not be realised with increased compression ratio levels since SI operation requires lower compression ratio configuration to prevent from excessive knocking combustion that would be hazardous for the engine; however the introduction of variable compression ratio systems could compromise the above to make CAI / SI operation a reality. The use of fully variable valve timing enables the engine to operate without the presence of the throttle even at part load

conditions of SI operation [36, 37] thus contributing to the relatively high efficiency of CAI combustion at the same load range.

Researchers such as Olsson and Johnson [38], investigated the possibility of using various fuel compositions to achieve CAI combustion but also to control the heat release rate employing supercharging and intake air heating. Iso-octane and n-heptane were tested in various proportions to achieve CAI combustion over a large speed and load range. Results were found to be quite satisfying however, the presence of intake heating as well as the lack of appropriate means of feeding each of the fuel blend into the engine, proved to be constraints in the potential application of such a system into production engine. According to Ogink [18], even though the use of fuels such as n-heptane, iso-octane, gasoline and Diesel on the one hand [39] and ethanol and natural gas on the other [40], are interesting to investigate into from a scientific point of view, only fuel that are currently widely available on the global market, such as gasoline, can be considered as a viable solution. Another reason for that is the practicality offered by gasoline-fuelled engines that are able to operate in CAI / SI hybrid mode, while using the same engine geometry.

One of the methods applied in work performed so far to establish CAI conditions by a growing number of researchers around the world, was the retention of large quantities of exhaust gases in the cylinder, also known as Internal exhaust gas recirculation (IEGR), so that they remain in the cylinder as soon the next cycles begins. The internal EGR can be realized by either gas rebreathing or trapping. In the exhaust gas rebreathing method the exhaust valve is first opened (Burned gas rebreathing) during the exhaust stroke and then re-opened during the intake stroke. During the second opening, burned gases that have been previously expelled from the combustion chamber are re-admitted simultaneously with the fresh gases. In this operating mode, one intake and one exhaust valves located along the diagonal of the combustion chamber were deactivated. With residual gas trapping the exhaust valves are closed early and trapping a large amount of residuals in the combustion chamber. In parallel, a late intake valve opening is used to limit the back flow of burned gases into the intake ports. During the negative valve overlap, residual gases are compressed up to Top Dead Center (TDC) and some heat loss to the walls occurs [20].

The hot residual gases provide the energy to heat the incoming fresh charge up to the autoignition point around TDC [41, 42].

- Dilution offered by the introduction of residuals in the cylinder, acts as a heat absorption factor that during combustion lowers maximum combustion temperature and temperature dependant NOx formation is slowed down at rates two orders of magnitude lower than those from conventional engines [34, 43].

- Slower burn rates appearing in diluted mixtures produce a less rapid heat release process thus minimizing the risk for knocking combustion.

- As soon as air/fuel mixture is heated up using internal EGR, it becomes easier for the mixture temperature to increase at the beginning of the compression stroke. In addition, intermediate and radical species present in the residuals at IVC may accelerate the chemical processes preceding the main heat release event [34, 44].

In the residual gas trapping method, the amount of trapped burned gases can be altered by the exhaust valve closure (EVC) timing. The earlier the exhaust valve closes, the more burned gases remain in the cylinder.

However, unlike the conventional SI combustion where the combustion timing is controlled by the spark timing, the start of autoignition combustion is mainly affected by the temperature history experienced by the fuel/air mixture. In order though to further optimise the start of combustion and the yield maximum benefits from CAI combustion, accurate control of the onset of autoignition would be considered an advantage.

With the proficiency of direct injection technology, it is possible to control the start of the autoignition combustion by altering the autoignition process leading to the main heat release event. With homogenous CAI combustion operation, start of main combustion can be altered by the fuel injection event. If the fuel is injected into hot charge, fuel oxidation accelerates; otherwise, fuel injection into a cooler charge may delay the auto-ignition process initiation. Therefore, by selecting the charge temperature under which the fuel

injection takes place the initiation of the autoignition process, and hence the start of combustion, may be accurately controlled. Lower valve lift, will force the hot exhaust gases to be re-compressed to an even higher temperature; as soon as fuel is injected directly into the exhaust gas retained in the cylinder immediately after the exhaust valve is closed, the oxygen contained in the hot exhaust gas will start to oxidise the injected fuel. Fuel injected under such circumstances will experience intensified oxidation process and will accelerate the autoignition process. On the other hand, if the fuel injection is takes place during the intake stroke, the oxidation rates will be slowed down as the charge temperature drops due to charge expansion.

Zhao et al [45] studied the following five effects of recycled burned gases on four stroke CAI combustion:

1. **Charge heating effect:** Increased charge temperature due the presence of hot burned gases in the air/fuel mixture

2. **Dilution effect:** Reduction in oxygen content due to increased burned gas quantity

3. **Heat capacity effect:** Increase in charge heat capacity, primarily due to high quantities of H_2O and CO_2 present in burned gas.

4. **Chemical effect:** Chemical reactions involving H_2O and CO_2 present in burned gas.

5. **Stratification effect:** Burned gases, fresh charge and fuel are not fully mixed.

In this study isolating the different effects of EGR on CAI combustion were isolated and studied independently from each other through computer simulation and experimental methods; the conclusions are given below:

1. The heat capacity and the dilution effects of EGR were found to equally extend the combustion duration; on the contrary charge heating effect produced opposite results.

Large EGR amounts tend to increase combustion duration resulting in misfire at high concentration.

2. Intake charge temperature was the parameter that autoignition timing and maximum pressure rise rate were the most sensitive to of all the engine parameters investigated.

3. Start of combustion advanced with the introduction of hot EGR into the cylinder. The charge heating effect was responsible for the advanced autoignition timing; nonetheless the heat capacity of EGR was found to moderate combustion phasing. The dilution and chemical effects were predicted not to affect autoignition timing.

4. Stratification permits ignition to take place in the high temperature region at the fresh/charge residual gas interface. It is probable that complete mixing of the same gases would result in insufficient temperature to allow auto ignition.

All the above can explain the reasons that CAI combustion has become particularly attractive with researchers since it appears to offer the best potential for manufacturing a hybrid SI/ CAI engine within the foreseeable future as it has been exhibited in work by Koopmans *et al*., [46].

CAI combustion so far has been studied as an alternative to SI and CI combustion with certain benefits to the engine efficiency and emissions output. The merits have been summarised however there appears to be a number of issues rising as research proceed towards realizing a production CAI engine. These challenges can be summarised as follows:

i. In many cases, the CAI combustion starts well before the top dead center (TDC) of compression as soon as the charge temperature becomes higher than the autoignition temperature of fuel.

ii. The limited load range over which CAI process is applicable.

iii. CAI combustion is much faster than the normal SI combustion, leading to rather high pressure rise and hence engine noise, or even engine damage if it is too high.

iv. CAI operation range is limited by knocking at high load and by misfire at low loads and speeds.

v. uHC and CO emissions are somewhat higher than SI combustion due to incomplete combustion.

vi. Switching between CAI and SI combustion maybe more difficult to accomplish than between stratified lean-burn mode and homogeneous mode for direct injection SI engines.

Effects of Engine Operating Parameters on CAI Combustion

In a study by Oakley, [48] CAI combustion was investigated within a wide range of lambda and EGR percentages with results revealing that for most operation conditions AFR had little effect on ignition timing, except at EGR rates above 40% where AFR reduction tends to significantly retard ignition timing. In work by Christensen and Johansson [39], the effect of compression ratio, inlet air temperature and fuel octane number (ON) was studied. Inlet air temperature and compression ratio was adjusted accordingly so that ignition occurs at TDC. The results demonstrated a dependency between ON and compression ratio; more specifically as ON increased, compression ratio had to further increase so that ignition timing advances to reach TDC. As intake air temperature was increased though, a lower compression ratio was required to achieve ignition timing at TDC.

Particular interest has been paid towards solutions for controlling burn duration with focus on speeding up combustion so that the knock limit increases and maximum output improves respectively. [50] Under ideal homogeneous conditions, the mixture containing fuel and air would release all the heat created by combustion simultaneously, since auto-ignition would occur simultaneously and evenly throughout the combustion chamber. This

may results in small cycle-to-cycle variations through a significant number of consecutive cycles unlike SI engines where the early flame development varies significantly. [51]

In real conditions, however, the mixture is not entirely homogeneous right before auto-ignition due to the presence in the combustion chamber of stratification in the mixture temperature, equivalence ratio and/or residual gas percentage. This inhomogeneity is likely to occur due to heat losses towards the combustion chamber walls, inadequate mixing of the fresh charge and residuals, as well as incomplete mixing following fuel injection. Stratification therefore plays an important role in determining the overall burn duration.

A likely explanation for that is the fact that the overall burn duration is dictated by the timing range of all of the local heat release events throughout the combustion chamber, and the dependence of the ignition events occurrence on the local mixture characteristics near TDC [52]. The overall burn duration can in turn, limit the load range where stable CAI combustion is feasible; too fast heat release rate increase the chances for knocking combustion phenomena to take place, whereas long burn durations result in incomplete combustion, or even misfiring, as the mixture temperature falls during the expansion stroke.

CAI Combustion in DI Gasoline Engines

In recent research studies, the potential of injection timing as a means of controlling CAI combustion phasing had been investigated. As already mentioned, homogeneous mixtures tend to improve the formation for CAI combustion conditions; however this may lead to rapid heat release and therefore serious combustion noise as a large volume of mixture is burned simultaneously. Charge stratification achieved by late GDI fuel injection was found to be very effective at improving combustion efficiency and reducing emissions for low fuel load. [53-54] Kontarakis *et al*., [55] in a study on a conventional PFI gasoline, demonstrated the capability injection timing provides in forming a homogeneous mixture. Cao *et al.,* [56] in a simulation study on the effects of fuel injection strategy on in-cylinder fuel distributions and CAI combustion, concluded the following:

1. Injection timing has a large effect on charge cooling and hence the volumetric efficiency and combustion phasing while at the same time it significantly affects fuel/air mixing in the cylinder.

2. Initial high residual gas temperature and subsequent recompression process lead to faster fuel vaporization and acceptable amounts of mixing with early fuel injection (-75^{o}CA ATDC). The air/fuel mixing in the mid-injection case (100^{o}CA ATDC) is greatly enhanced by the strong interaction of intake generated flow.

3. Insufficient mixing time and weak charge motion contribute to the most stratified fuel distribution in the late injection case (220^{o}CA ATDC).

4. Direct fuel injection into a stoichiometric burnt gas during the negative valve overlap period increases the pumping work due to the reduced re-expansion work after TDC of the overlap period whereas pumping work slightly increased during late fuel injection and exhaust gas temperature increases owing to delayed combustion.

5. With stoichiometric mixture conditions, direct injection leads to milder combustion than Port Fuel Injection (PFI) owing to stratification of fuel-rich and fuel-lean areas in the cylinder.

Overall, it can be concluded that the potential for air/fuel mixture quality management offered by multiple direct injections can be used to control the phasing of auto-ignition in CAI combustion. [53]

Further retarded fuel injection, during the compression stroke, is also expected to affect the autoignition combustion process by forming a stratified charge which in turn will further influence the start of autoignition and eventually combustion. According to Zhao *et al.,* [47] a stratified combustible charge will burn faster than a homogeneous charge of the same air/fuel ratio. Sjoberg *et al.,* [49] used a GDI injection system to conclude that, under some conditions, use of a late injection, stratified charge strategy could promote very

advanced ignition that can lead to knocking combustion, while employing a homogeneous charge under the same conditions lead to much later ignition.

According to Thirouard *et al.*, [20] CAI combustion phasing was found to be sensitive to the start of injection at the beginning of the recompression stroke. In this case, oxygen is available in the residual gases. Part of the fuel when injected at the beginning of the recompression phase, it's subject to a pre-decomposition and/or combustion of leading to an advanced combustion phasing in the following cycle. Furthermore delay in combustion start in the case of late injection can be attributed to the charge cooling effect caused by the injected fuel vaporization.

In the same study, split injection strategies involving two independently controlled injection events, were also investigated. The first fuel injection takes place at the beginning of each engine cycle, so that a homogeneously lean and/or diluted premixed mixture is created in the cylinder. The second fuel injection occurs during the later stage of the compression stroke to prepare a stratified charge that can be ignited eventually by the spark discharge. Fuel-rich zones are created locally with the two injection events in each cycle, promoting auto-ignition thus advancing the combustion. Similar results were reported by Wang *et al.*, [57] where the stratified charge compression ignition, caused by the second fuel injection during a double injection strategy, is described as a "two-zone" combustion; rich at the center and lean at the circumference. It is also mentioned that this two-zone combustion creates advanced ignition and stratified combustion thus enabling control of ignition timing and combustion rate.

As far as spark assisted CAI mode is concerned, a premixed flame, after ignition, will propagate in a small stratified charge whereas at the same time, the homogeneous lean/diluted premixed mixture will be compressed by the propagating flame front as well as by the ascending piston, leading to the autoignition combustion of the lean/diluted main mixture. Fuel quantity injected in the first injection can be adjusted to that extent that the premixed charge formed is adequately lean and/or highly diluted with burned gases, so that knocking combustion is avoided.

Extremely lean and/or highly diluted mixture, may lower NOx emissions levels while autoignition timing is controlled now via spark discharge event, mixture composition as well as the fuelling rate of in the stratified charge. Dec *et al.*, [65] however underline the possibility that high levels of stratification present in the cylinder with late fuel injection timing, may lead to an increase in the overall NOx emissions; a claim that is also confirmed by Wang *et al*, [57].

This method of creating the appropriate conditions for spark assisted CAI combustion seems able to offer satisfactory combustion timing control levels along with high load operation; it can be therefore considered as an excellent prospect for realising transient operation mode between the self-initiated CAI combustion at part-load and normal SI engine operation at full load.

2.4 Exhaust Emissions

Ever since the early CAI investigations, the prospect of reducing emission levels from this new and promising type of combustion always seemed attractive to researchers. Zhao *et al.*, [58] compared the performance of a CAI/SI hybrid engine to the equivalent SI one over the New Emission Drive Cycle (NEDC) with results showing reduced fuel consumption by 4.7%, NOx and CO emissions dropped by 12.7% and 3.7% respectively, while HC emissions increased by 16.9%. CAI combustion unthrottled operation, allow engine efficiency to approach that of conventional diesel engines.

Meanwhile CO and HC emission in published literature seem to vary according to the type of engines used in each study [60-62], and they don't demonstrate any significant reduction; on the contrary CO and HC levels are found to be as high or even higher when compared to those from SI engines. Emission levels also vary with operating conditions and with most of previous work claiming an increase in both CO and HC levels at low loads since exhaust temperatures in CAI conditions are so low, that the application of conventional aftertreatment equipment becomes even harder.

As the most likely source of these emissions, has been considered to be the incomplete combustion taking place in crevices and/or near cylinder walls where the mixture is cooler.

Christensen *et al.,* [63], varied the geometry of the piston top-land crevice and were lead to the conclusion that crevice was the source for most of the HC emissions for the engine configuration used (premixed HCCI, iso-octane and equivalence ratio (φ) of 0.22 and higher). Similar results were found by Aceves *et al.* [64], using a multi-zone modeling approach to analyse the experimental results of Christensen *et al*. [63]. The modeling results in Aceves *et al.* [8] also indicated that a substantial portion of the CO was due to the crevices and boundary layers at these conditions.

Results obtained by Dec [65] also indicated that the source for CO emissions was the crevice volume and boundary layers within the cylinder. In other studies published, the term bulk-gas is employed to describe another possible source of CO and HC emissions; this term describes the gases not in crevices or thin boundary-layer regions that when quenched, can become a source of emission production.

In order to better understand the changes in CAI emissions and combustion efficiency with changes in fueling rate, Dec and Sjoberg [53] recently conducted a comprehensive study involving both detailed experiments and single-zone chemical-kinetic modeling. In this study, the fueling rate was systematically varied from $\varphi = 0.26$ down to $\varphi = 0.04$ in steps of 0.02. These equivalence ratios cover the range from typical HCCI operating conditions to a well-below-idle fueling that is the near the limit for determining the heat release from the cylinder pressure trace. The data showed that at higher fueling rates, CO, HC, and OHC emissions were low and not strongly affected by changes in φ. However, as fueling was reduced, CO emissions begin to rise. The increase was gradual at first, then as φ dropped below 0.2 the CO level began to rise rapidly, and HC and OHC levels also increased. OHCs are toxic pollutants consisting of formaldehyde and other compounds [66]. This occurs because combustion temperatures become so low at these very dilute conditions (i.e., low equivalence ratios) that the reactions are not complete before they are quenched by expansion. The CO-to-CO_2 reactions are particularly sensitive to the combustion temperature. For operation at 1200 rpm with combustion phasing at TDC and using iso-octane as the fuel, a minimum peak temperature on the order of 1500 K is required to complete CO oxidation. A more recent detailed investigation has shown that this temperature is independent of both fuel type and combustion phasing [68], although it does vary somewhat with engine speed [67].

Aceves *et al.,* [69] examined twelve fueling rates with φ varying from 0.26 to 0.04 in steps of 0.02; idle fueling corresponds to φ = 0.10 - 0.12. The analysis is based on a segregated multi-zone methodology that makes it possible to solve the fluid mechanics separate from the chemical kinetics, thereby greatly reducing the computational time while providing accurate results. The results obtained from the simulation work were then compared with experimental results, and it was found that the engine produces substantial CO emissions at values of φ corresponding to idle-like fueling rates (63% of all carbon in the fuel goes into CO at φ=0.10). As the equivalence ratio is reduced further the emissions of CO drop and the emissions of HC and OHC increase. At high equivalence ratios (φ=0.26), the results correspond closely with those previously studied for typical CAI conditions, with HC and CO emissions originating at crevices and boundary layer, which are too cold to react to completion. As the equivalence ratio is reduced to φ=0.16, there is a broad boundary layer zone where the temperature is not hot enough for complete combustion in the available time. In the boundary layer, combustion stops early in the expansion stroke, resulting in a high concentration of CO. The mass distribution for φ=0.10 shows that the temperature is low enough that even the core is too cold to react to completion, and most of the gases in the cylinder react partially to form CO at the maximum rate observed in these experiments. Finally, at φ=0.04 combustion temperatures are extremely low, so that only the central core reacts into CO, while there is a wide boundary layer region that burns partially into intermediate hydrocarbons. This explains why the CO emissions drop and the HC emissions increase as the equivalence ratio is reduced below φ=0.10.

2.5 Summary

An overview on the automotive research field has been presented in this chapter. The plethora of methods and techniques available to the researchers' community to develop engines with primarily lower emissions levels and improved fuel consumption, were explained.

A number of combinations of alternative fuels and control systems have been investigated towards this direction with encouraging results. However, the results from recently

developed technologies would not be able to be implemented at least for the foreseeable future as further action needs to be taken so that that these technologies can be applied widely. Until then, the focus would be given to those methods and techniques that would optimise fossil fuel powered engines that are both popular in terms of cost and also offer potential for further improvement.

Within this context, CAI combustion brings an innovative idea about combustion that provides with the merits of increased engine efficiency and at the same time reduced emission levels. Potential use of CAI combustion in engines would enable vehicle manufacturers to spare the use of extra after treatment equipment for exhaust aftertreatment as it is the case with SI and CI engines currently.

Like any other technology that emerges, CAI combustion still has to overcome a significant number of challenges associated mostly with the necessary control level that needs to be applied so that it fuel economy and lower emissions levels are established. Introduction of the GDI engines in combination with the development of fully variable valvetrain and compression systems, has offered the capability to control, up to a reasonable extent, the timing and the level of autoignition within the cylinder. Single and double injection strategies aiming to provide autoignition timing and burn rate control, have been thoroughly explained with regard their prospect of enabling engine operation under both CAI and SI combustion mode with each mode activated according to the load levels.

In this review, it has been shown that under CAI combustion offers improved engine efficiency as well as low NOx emissions over current SI combustion operation. High carbon related emission levels such as HC and CO in CAI combustion engines, can be treated by the use of cheap and robust exhaust gas aftertreatment systems that are already available offering very good results.

Combining all the aforementioned fact, it is easily understood that investigation into CAI combustion has produced substantial amounts of information and insight on the mechanisms and dependencies of CAI engine operation. Therefore, transformation of the existing knowledge into practical applications can be considered to be the next target in

automotive researchers by means of optimizing the existing techniques and introducing new ideas into research that would contribute to this direction.

Chapter 3

Experimental Test Facility

Chapter 3 Engine Configuration and Testing Facility

3.1 Single Cylinder Research Engine

3.1.1 General description

The whole experimental work described took place in the University's testing facilities which involve a Ricardo Hydra research engine mounted on a Cusson's single cylinder engine test-bed. The test-bed is driven by a 30 kW DC dynamometer which allows operation for both motoring and firing conditions. The test-bed's water and oil conditioning systems are controlled by a separate control unit.

Work carried out during the experiments involved various compression ratios, camshafts and valve timing configurations. For the SI measurements a set of camshafts successfully employed in previous work was used whereas for CAI combustion two sets of camshafts with shorter duration and smaller valve lifts were employed. Details on the camshafts profiles are given in Chapter 4.

For test purposes compression ratio has two different values (9:1 and 11:1). These changes were made possible by installing a metal plate between the cylinder block and the crankcase. Removing the plate decreased the clearance volume, therefore increasing the compression ratio. Engine bore and stroke were 80 and 89mm respectively.

A wet sump type lubrication system, remotely fed by a gravity pump and powered by an AC motor was used. Oil from the sump is supplied to the camshafts and the crank providing lubrication on the bearing surfaces radially. Lubrication of the big and small end bearings takes place through a hole on the big end of the connecting rod, which squirts oil at the bottom of the piston and falls down lubricating the small end.

Inside the oil sump a pair of immersed electrical heaters ensures the engine warms up quickly and at the same time adjusts the oil temperature at low load conditions. Another

element of the lubrication system is a mains water heat exchanger equipped with a closed loop that automatically adjusts the oil temperature according to the operating requirements. Cooling of the engine is provided by a circuit with the following components: electric pump, immersion heater, mains water heat exchanger and closed loop control system.

The DC dynamometer, as mentioned above, offers motoring and firing operation providing an increase and decrease in the speed on demand. At the same time it uses a speedometer and a load cell to provide input and output indications for engine speed and torque respectively. Subsequently the dynamometer can maintain constant speed regardless of the operating conditions or speed can be increased or reduced accordingly.

3.1.2 Cylinder Head

A prototype GDI cylinder head supplied by Orbital Engine Corporation Ltd was used for the course of the experiments. It features a centrally mounted fuel injector, pent roof combustion chamber with four valves and double overhead camshafts. There is also a mounting hole in the cylinder head to accommodate a pressure transducer for in-cylinder pressure measurements. The camshafts can be turned freely with regard to their tooth pulleys after loosing fasten thread bolts so as to change the valve timing. A closely spaced spark plug enables the engine to run in SI mode as well as in spark assisted CAI mode. The following figure shows the combustion chamber layout and how the injector and spark plug are situated in it.

Figure 3.1 Combustion Chamber of Prototype Orbital Cylinder Head (Orbital Engine Corporation Ltd)

3.1.3 Crankshaft Position System

A shaft encoder mounted on one of the ends of the crankshaft was used to provide information regarding its angular position. The encoder generates reference signals through pulses for every engine revolution and a clock signal with a pulse corresponding to every degree of the rotation. Through these signals the fuel injection timing, the spark timing and data acquisition system could be triggered and monitored.

These signals alone could not provide adequate information regarding the engines exact position during every cycle. This is because the reference signals produced for each cycle provide information on both TDC points without identifying them. Therefore the following method was used so that only one (instead of two) reference signal is produced for each engine cycle. A hall-effect sensor was installed on the exhaust camshaft pulley allowing the generation of a pulse synchronised to the crankshaft encoder. This sensor generates a pulse per camshaft rotation so that the synchronisation signal occurs every other revolution. The two signals generated, one from the crankshaft encoder and one from the camshaft sensor, pass through an 'and logic gate' that filters out signals without pulses from both sources. The remaining signals are transferred to the rest of the system.

3.1.4 Air-Assisted Fuel Injection System

The fuel injection system is a spray guided, air assisted type consisting of a direct injector and a conventional (MPI) injector behind it. This type of injector requires pressurisation of both the fuel and the air reaching it. Air is supplied to the injector through an air cylinder which uses a pressure regulator to set and control the quantity of air supplied to the injector. Pressure in the air supply line was adjusted at 6.5 bar.

On the other hand fuel is first injected into a chamber behind the direct injector by the MPI injector with an absolute pressure of 8bar (1.5bar gauge relative to the compressed air in the injector chamber).

The direct injector then injects not only the fuel metered by the MPI injector but also a quantity of the compressed air already supplied into the cylinder with a pressure of 6.5 bar, giving excellent atomisation, significant reduction of the spray velocity and penetration into the cylinder. The fuel amount is determined by the pulse duration of the fuel metering pulse and the injection of mixture commences at the rise edge of the direct injection pulse. Figure 3.2 shows the event sequence and Figure 3.3 shows a schematic of the Air Assisted Fuel System.

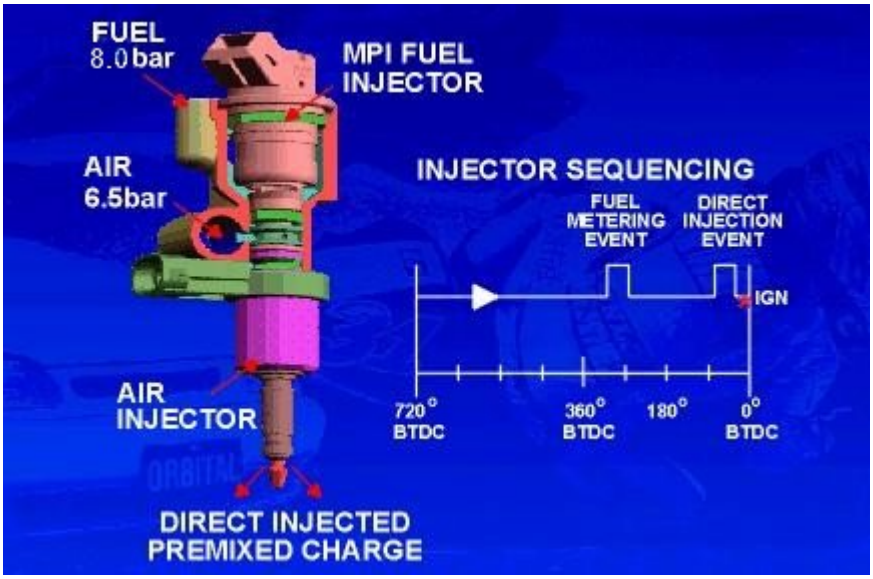

Figure 3.2 Orbital Air-assisted Injector with Typical Injection Sequence (Orbital Engine Corporation Ltd)

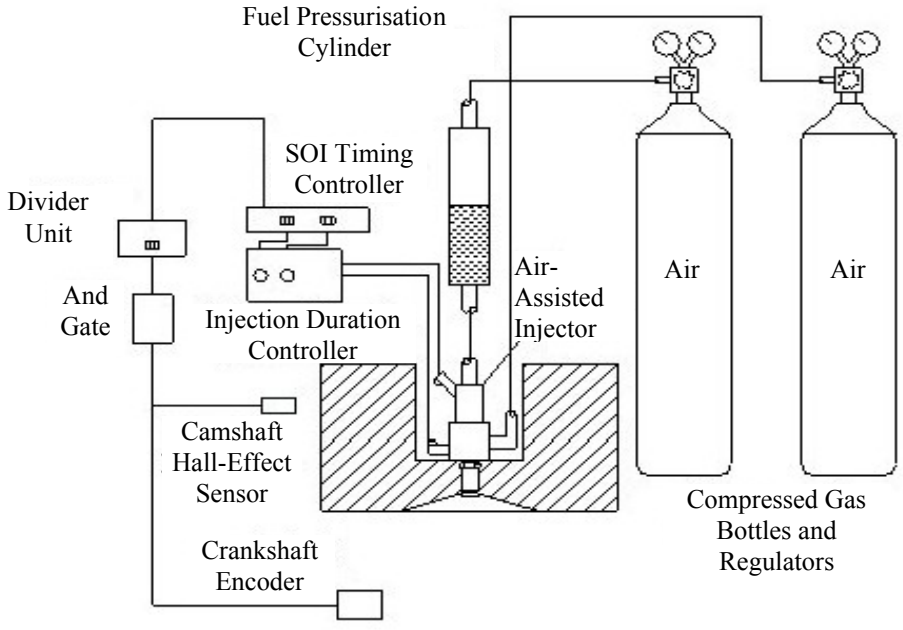

Figure 3.3 Schematic of the Air-assisted Injector Fuel System

Start of injection (SOI) was controlled by a custom made 2-channel delay unit allowing accurate control of the injection timing. An identical delay unit also controlled the air injection timing.

The TDC signal from the crankshaft encoder reached the delay units which allowed the signal to be delayed according to the desired SOI for each injector. After exiting the delay units, these delayed signals entered a 2-channel timer unit that allowed pulse width adjustment and thus the end of injection (EOI) for both air and fuel injectors.

For the split injection experiments an 'OR logic gate' was used to control fuel and air injection during each cycle. The signal for single injection leaving of the logic box was split through the two linked channel delay units. Then each unit's signal passed through the logic gate reaching the 2-channel timer unit which in turn adjusted the quantity of the fuel and air injected.

This configuration allowed equal splitting of the metered fuel and air quantities into the injector body enabling 50% of the fuel and air injected during the first injection and the rest during the second one.

Figure 3.4 shows the system connections in the double injection configuration.

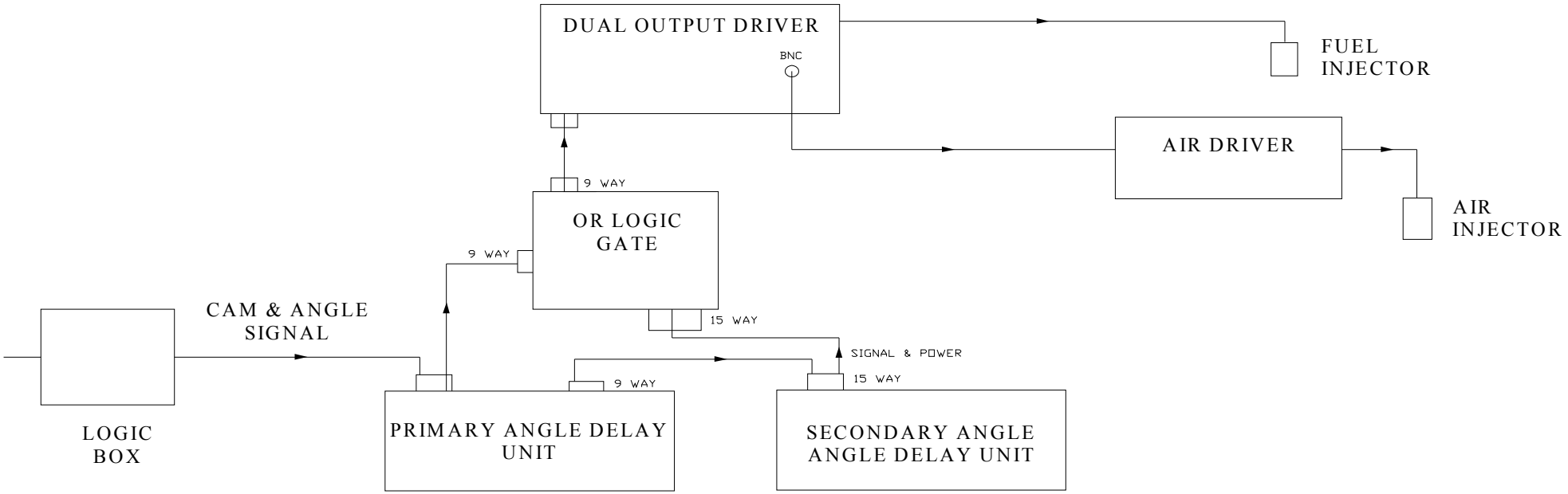

Figure 3.4 Connection and Double Injection system configuration

3.1.5 Ignition System

Figure 3.5 below shows an overview of the spark ignition system. Clock and reference signals coming from the camshaft Hall Effect sensor and the crankshaft encoder, reached the 'and gate logic' unit which output a modified signal, as mentioned earlier in section 3.1.3.

For ignition time delay purposes, the crankshaft encoder was set to supply a signal at 80° CA BTDC during compression stroke. The Lucas 'Dial-a-Time' unit took both signals and converted them into a single pulse with the ignition timing set through its dial as well as with the coil-on (dwell) time. Then the ignition driver amplified the signal and the output charged the ignition coil. This charging current, when removed, allows the spark ignition at the end of the spark plug electrodes. Ignition timing ranged from 79°CA BTDC to 45°CA ATDC in 0.5°CA increments.

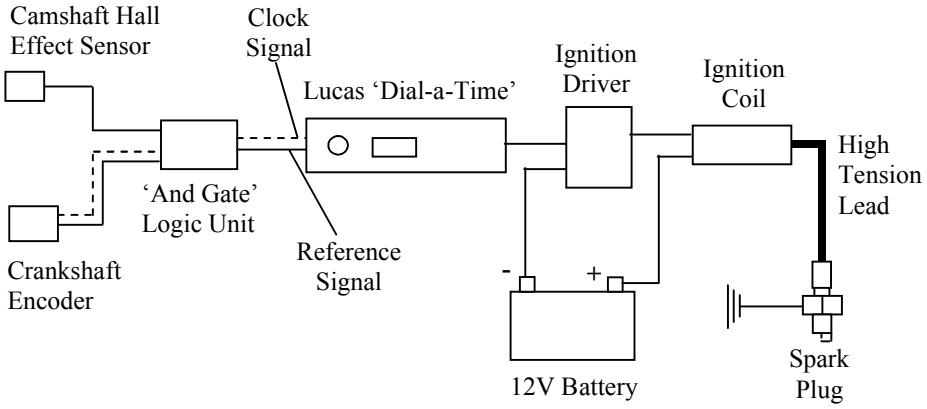

Figure 3.5 Schematic Diagram of Spark Ignition System

3.1.6 Sandwich adapter plate

A fundamental problem that had to be tackled was the way the Orbital cylinder head would be mounted upon the cylinder block. The whole issue had to do with the position of the mounting holes on each side. Mounting holes on the cylinder head didn't align with the

ones one the cylinder block. They also overlapped making drilling and tapping new holes onto the cylinder block impossible. A possible solution would be to plug the holes on the cylinder and re-drill and tap but it did not provide flexibility for the future use of another cylinder head or modification for optical access experiments.

A sandwich adapter plate was therefore designed and manufactured in order to provide a solution that would not damage the cylinder block significantly. Additionally, in case another cylinder head had to be used, the only thing required to fit it on the cylinder block would be to manufacture the appropriate sandwich plate. Figure 3.6 shows a sectional view of the assembly of the cylinder head; cylinder block and the sandwich adapter plate (see Appendix A for detailed drawings). The adapter plate consists of a 20 mm thick steel plate mounted on the cylinder block with counter-bored bolts. The holes for these bolts were drilled and tapped straight on the cylinder block at locations near its edges to prevent compatibility with potential use of another cylinder head in the future. On the cylinder head's side of the sandwich plate, holes were drilled and tapped to fit the cylinder head holes onto it.

The adapter plate is equipped with a water channel that allows sufficient cooling of the cylinder liner during firing conditions. Water flows from the cylinder head into the sandwich plate and returns to the cooling system through an outlet located on one side of the edge.

3.1.7 Cylinder Liner and Piston

Adding a sandwich adapter plate above the cylinder block automatically meant that the piston and cylinder liner could not reach the top deck surface of the cylinder head. Therefore a new extended cylinder liner along with a new piston were designed and manufactured. The assembly is showed on Figure 3.6.

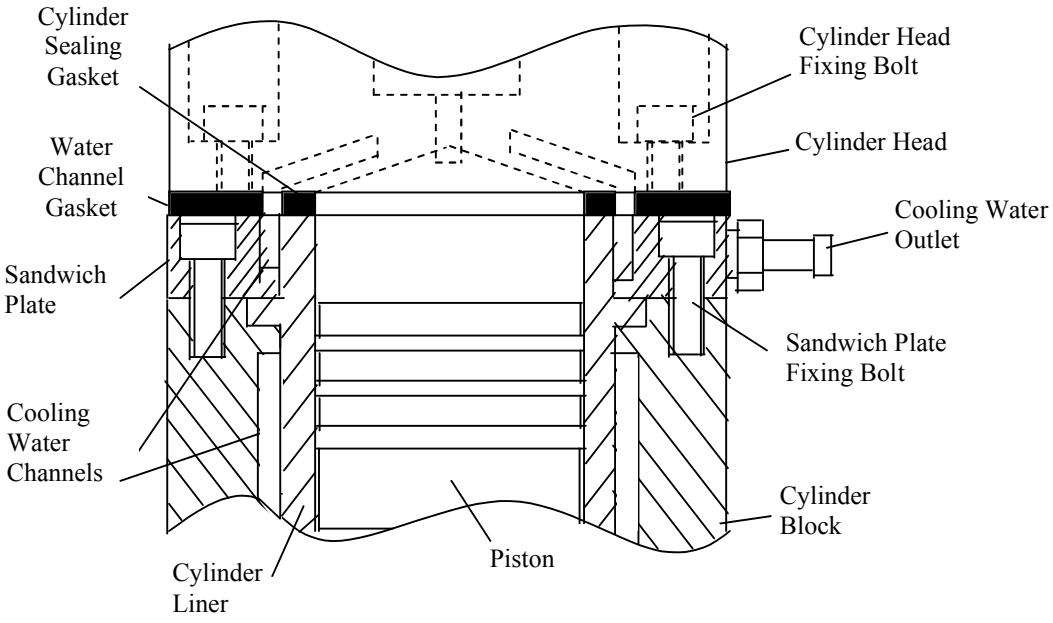

Figure 3.6 Cylinder head and cylinder block assembly using the sandwich adapter plate

A step section in a recess at the top of the cylinder block allowed not only the original cylinder liner to be positioned and fixed at its upper end but also made sure that the top surfaces of both were completely level. The cylinder head bolts, in turn, applied enough clamping force and maintained the cylinder liner in a vertical position. For the new extended liner the same mounting and location technique was employed. However another section on top of the cylinder liner was required to allow alignment with the upper surface of the sandwich adapter plate. The new cylinder liner remained positioned vertically by means of the clamping force of the sandwich plate bolts rather than those of the cylinder

head. The boring of the liner took place in the university's workshops from a cast iron billet. For the honing of the liner's running surface a 3-legged honing tool called 'glase buster' was used. Ridges left by the boring tool were removed with a tool which also left a cross hatched pattern on the liner walls to retain oil with the least amount of leaking possible and to reduce wear.

For the purpose of retaining the compression ratio, a piston that could reach the top of the liner was provided by Ricardo Engineering Consultants. After installing the new liner the cylinder bore was reduced from 86 mm to 80 mm; thus the new piston's bore was also 80mm. The only modification on the new piston was to remove 3mm from the skirt to avoid contact with the engine block around BDC. However during the new piston installation it appeared that the gudgeon pin diameter was smaller than the existing one. Increasing the bore to accommodate the existing gudgeon pin and thus the connecting rod would cause further problems as a high level had to be maintained between the piston and the connecting rod. To provide a solution to this problem, a new connecting rod bearing was manufactured and installed into the connecting rod allowing the use of the new gudgeon pin.

3.1.8 Gasketing

After the new engine configuration was completed, a viable solution had to be found for engine sealing. In particular sealing of the cylinder head and sandwich plate joint was the most challenging problem to overcome. Conventional head gasketing from a multi-cylinder automotive engine did not provide sufficient sealing of the water channel due to the engine's bore centres being relatively close to each other. Therefore alternative gasketing materials were used in practice to choose the one that would provide adequate sealing as well as sufficient resistance to high temperature and pressure. A high temperature resistant material name Klingersil was first used to create gaskets of the same bore as the liner but the results were disappointing as it only lasted a few firing cycles before being destroyed. Another suggestion was to use copper gaskets of different thicknesses but after they had been manufactured and tested, they were discarded as they did not provide sufficient compressibility. After careful consideration of the parameters and the solutions available,

the problem had to be divided into two different stages. The idea was to seal the water channel and the cylinder head/sandwich plate joint separately. For the latter a highly compressible material called Gasketoid was used and modified to fit the pattern on the sandwich plate top surface while for the former a central part was cut from an automotive engine cylinder sealing gasket with the same bore to fit the water channel.

Sealing between the sandwich plate and the cylinder block was successfully dealt with by applying Hermatite Instant Gasket sealing paste on the touching surfaces. This material was preferred to a conventional one as it offered satisfactory sealing and most importantly because it did not affect the distance between the cylinder liner and the sandwich plate.

3.1.9 Fuel Supply System

Engine fuelling was provided by a relatively simple fuel system shown in Figure 3.7.

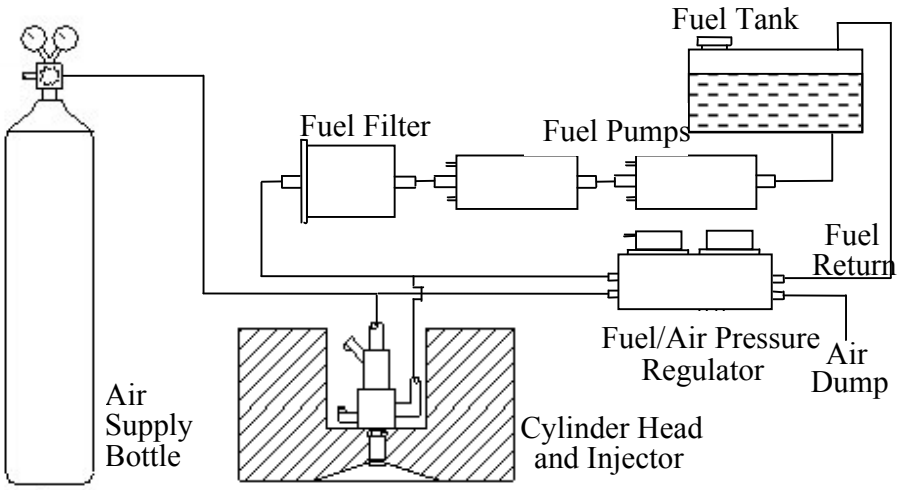

Figure 3.7 Schematic Diagram of the Fuel Supply System

Fuel leaving the fuel tank goes through two pumps and after the filter it reaches a fuel/air pressure regulator which ensured that air and fuel pressure remained constant. At the same time compressed air was supplied to the air injector at a pressure higher than the regulator's rated value so that the air returning from the injector was dumped through the regulator

back to the atmosphere. Fuel return was also connected to the regulator body and then back to the fuel tank.

To be certain that the fuel and air supply was regulated without any disruptions, specific attention was paid to the correct setting of the air pressure reaching the injector. A wrong supply pressure value would endanger the normal operation of the air injector and would also fail to establish sufficient flow for the air to return to the atmosphere. Orbital equipment allowed changes in the regulator's dumping air flow rate but because the latter was too low it couldn't be measured by any instrument.

Air supply pressure was set to the same value successfully used in previous experimental work, 6.5 bar. Fuel supply was in turn set 1.5 bar higher than the air pressure thus leading to a total pressure supply requirement of 8 bar. Therefore a fuel supply system had to be developed to ensure the desired pressure was present throughout the supply line. Initial use of a conventional PFI fuel pump didn't provide high enough injection pressure, subsequently only a high pressure pump could supply the desired value of 8 bar. However a high pressure pump was not immediately available, therefore a second identical PFI fuel pump was connected in series to increase pressure to the value of 8 bar.

An important factor of the fuel supply system development was the way fuel and air pressures were related to each other. Air supply pressure, as expected, was directly related to the atmospheric pressure. The fuel pressure supply, in turn, was referenced to the air supply pressure. This setting offers direct and constant control of the fuel supply in relation to the air pressure. Another advantage is that fuel pressure across the fuel injector remains constant allowing easy and accurate calibration.

3.1.10 Injector Calibration

For the purposes of accurately measuring and calculating fuel consumption, the fuel injector had to be calibrated using a method both precise and easy.

The first step was to remove the fuel injector from the injector body leaving the air supply intact. The second step was to turn on the pressure along the fuel line to ensure fuel pressure would be the same as with normal engine operation regime. Then the fuel injector, which in the mean time was connected to its electrical driver, had its nozzle pushed through a hole made on a lid of a glass jar. In this way eventual losses from fuel evaporation or accidental fuel spill were kept to a minimum. The glass jar had previously been weighed and the scale had been tarred to this weight.

The measuring procedure had as follows: Fuel injection duration was set to minimum so that fuel coming out of the injector was visible. This minimum value was then recorded and engine speed was set to 1200 rpm with the injector turned off. Then the injector was turned on and the fuel filled the glass jar and the quantity collected after 1 minute of injection was weighed. In order to calculate the amount of fuel injected per cycle the following calculation was performed:

$$\text{Mass of fuel injected per engine cycle} = \frac{\text{Total mass of fuel collected}}{\text{20RPSx60 seconds}}$$

After the fuel quantity in the jar was measured the procedure was repeated at the same engine speed with different injection duration intervals up to the point where a fuel calibration curve could be produced. This curve is located in Appendix B.

3.1.11 Engine modifications for CAI operation

As already mentioned, the engine CAI operation was achieved by replacing the existing camshafts for spark mode operation with new low lift/short duration intake and exhaust camshafts from a 1.8l Ford Zetec Engine. Both camshafts were further modified to fit on a single cylinder engine. More specifically as shown in Figure 3.8, each camshaft had 3 out of 4 pairs of cams removed thus leaving the first pair on the camshaft enabling it to be fitted on the engine and to operate all 4 of its valves.

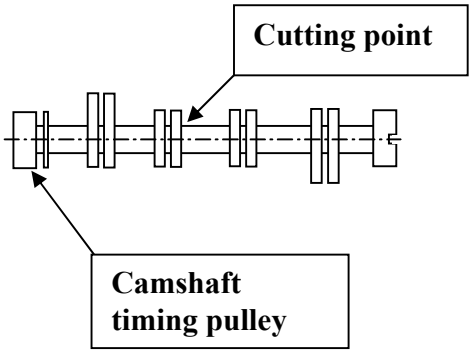

Figure 3.8 Camshaft cutting point schematic

Each cam was then further ground to modify the duration and valve lift for CAI operation. Intake valve duration was set at 130°CA and for the exhaust at 120°CA accordingly. After each one was fitted with a timing pulley on the one end, as shown on Figure 3.8, the camshafts were ready for use on the engine. During engine operation under the new camshafts regime, load was primarily controlled by valve timing without any need for throttling. However, the throttle body was not removed from the engine whereas all experiments were carried out with the throttle wide open.

3.2 Summary

The current chapter includes details of the devices and the general engine set-up used to perform the experiments for this research. A detailed description is given documenting the test bed the engine was mounted on, as well as the cylinder head. In addition the injection, ignition timing and crankshaft position systems have been explained. In the following chapter a description will be given on the use of these systems for our research.

Chapter 4

Experimental Set– up and Data Analysis for CAI and SI Engine Tests

Chapter 4 Experimental Set-up and Data Analysis for Spark assisted and Self-initiated CAI

4.1 Introduction

This chapter documents the strategy followed in the experiments on spark-assisted and self-initiated CAI operation modes. At the same time the various engine configurations and modifications are discussed as well as description of the measurement equipment used. Finally the various methods and techniques, upon which data processing was based upon, are explained. Engine speed varied from 1200 rpm to 2400 in increments of 150 rpm. Tests were completed with standard unleaded pump gasoline fuel of RON 95 (BS EN 228).

4.2 Engine variables and test parameters

4.2.1 Camshafts

In order to initiate CAI combustion, a sufficient amount of hot burned gases were trapped in the cylinder to increase the combustion chamber temperature. This could only be done by replacing the set of camshafts used for SI tests, with shorter valve duration and lower valve lift camshafts. Table 4.1 and figures 4.1.a and 4.1.b show the valve lift history for SI and CAI camshafts.

	SI original camshafts		**CAI original camshafts**		**CAI modified camshafts**	
	INTAKE	*EXHAUST*	*INTAKE*	*EXHAUST*	*INTAKE*	*EXHAUST*
Duration	180^{o} CA	180^{o} CA	110^{o} CA	100^{o} CA	130^{o} CA	120^{o} CA
Maximum valve lift	9.2 mm	9.2 mm	2.0 mm	1.96 mm	2.4 mm	2 mm

Table 4.1 Profiles for the SI and CAI camshafts employed in this research.

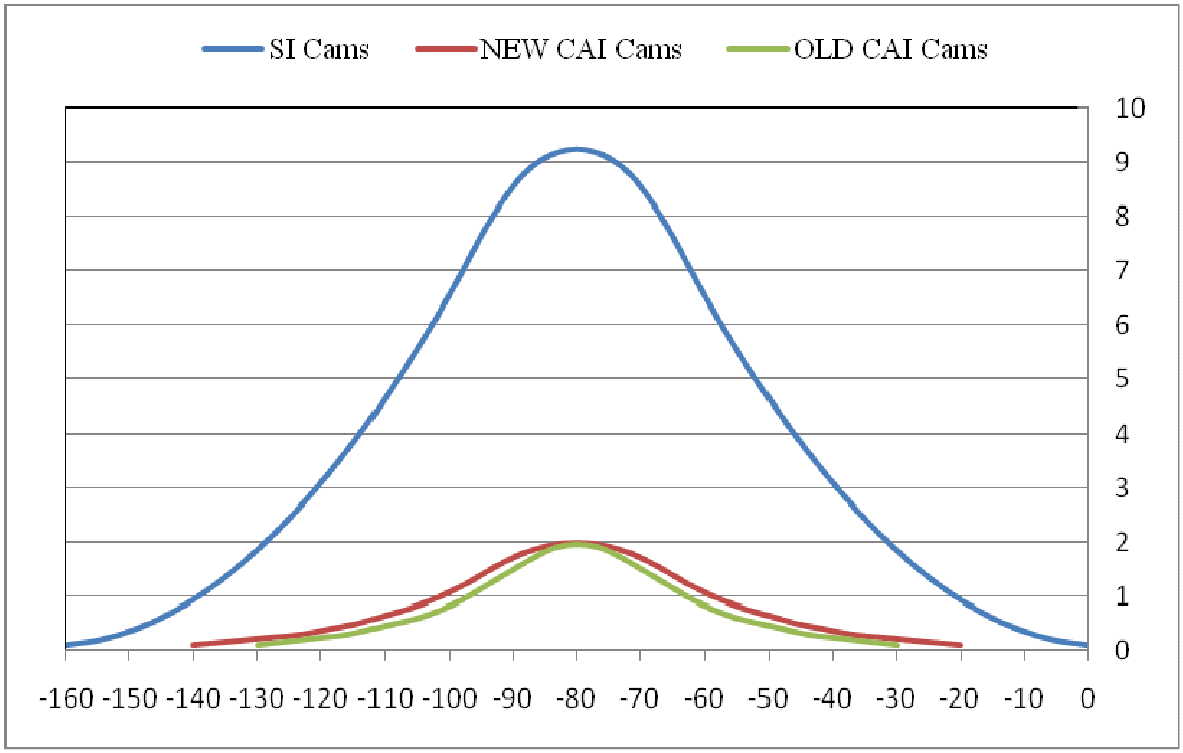

Figure 4.1.a Exhaust valve measured profiles and exhaust valve lift history for original SI cams, original and modified CAI camshafts

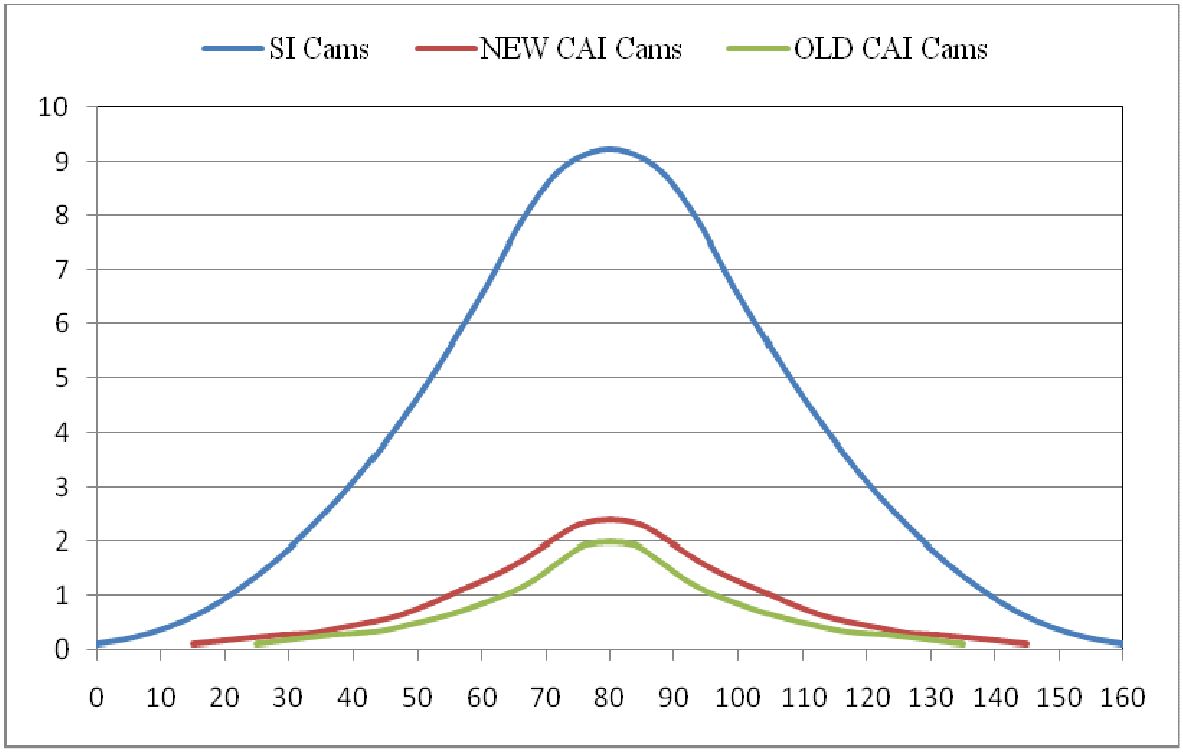

Figure 4.1.b Inlet valve lift history for original SI cams, original and modified CAI camshafts

The amount of burned gases trapped in the cylinder is determined from the in-cylinder pressure and exhaust gas temperature at EVC.

Because no intake throttle was used (this will be discussed further into this chapter) combustion phasing was mainly controlled by camshaft phasing. As mentioned above CAI operation dictates early EVC and thus delayed IVO in order to prevent excessive back flow of gases trapped in the intake manifold.

The way camshafts were installed on the engine permitted the change of valve timing to the desired value by loosing or tying thread bolts on the tooth pulley of each one. In order to proceed with the experiments a range of valve timings had to be used to determine the boundary values of valve timings for CAI operation. It was found that when EVC ranged between 60^{o}CA BTDC to 92^{o}CA BTDC, it provided satisfactory spark assisted and self initiated CAI operation. IVO was symmetrical to TDC (60^{o}CA ATDC to 92^{o}CA ATDC respectively).

4.2.2 Compression ratio

With the effect of compression ratio on combustion parameters being one of the investigation areas in our research, an effective way of changing its value had to be found. For the purposes of SI work previously done with this engine, compression ratio was set to 9:1 and in order to be directly comparable to past results, experiments started with the value mentioned.

As soon as the set of experiments required with this compression ratio had been completed, the desired metal plate thickness was calculated to provide an increased compression ratio to further proceed with testing. The calculation showed that removing the metal plate would give maximum clearance volume and a maximum compression ratio of 11:1 which in turn was used for the next stage of the tests. Details on the calculation are featured in the Appendix A.

4.2.3 Injection timing

Spark-assisted and self-initiated CAI tests were performed on the single cylinder engine with the properties discussed the Chapter 3. Two different engine tests were performed.

At first engine speed varied from 1200 rpm to 2400 in increments of 150 rpm and the relative air/fuel ratio λ varied from λ=1 to the limit where engine operation wasn't possible.

The other set of experiments was performed to provide basic knowledge on the effect of injection timing on combustion parameters and exhaust emissions. For this set, speed and relative air/fuel ratio were kept constant (1800 rpm, λ=1) whereas injection timing varied as shown in Figure 4.2.

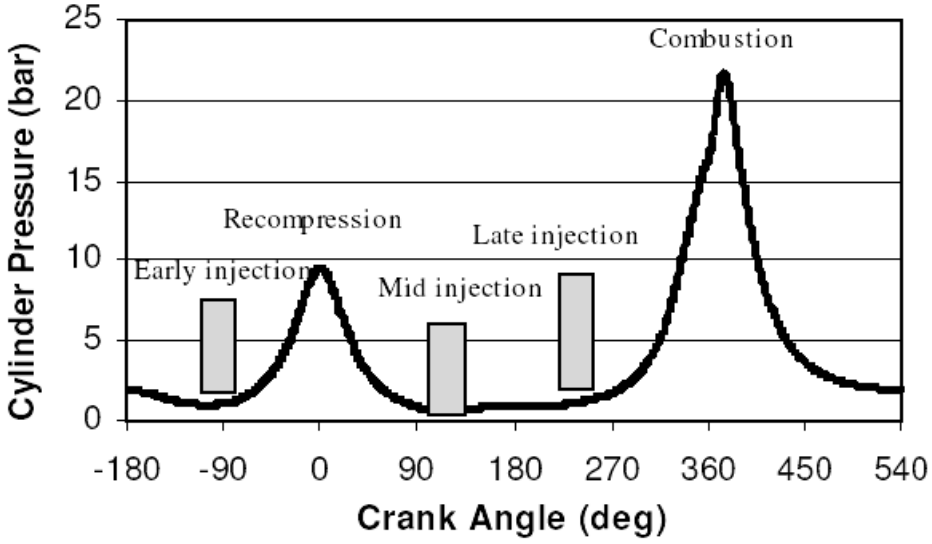

Figure 4.2 Cylinder pressure versus crank angle showing injection timing windows

Early injection refers to fuel being injected during the exhaust stroke whereas mid and late injection represent fuel injection during the intake stroke and injection during compression stroke respectively. Around TDC of intake and compression, the fuel could not be injected into the cylinder due to higher cylinder pressure than the injection pressure.

4.2.4 Spark timing

In order to initiate CAI combustion the engine had to run in spark assisted mode before it reached the condition where CAI is feasible without the need of presence of spark. This of course depends on the operating conditions (e.g. EVC, engine speed, injection timing).

For as long as the engine had to operate with the spark on to initiate and to maintain stable CAI operation, spark timing was adjusted accordingly so as to minimise the knocking phenomena occurring during spark assisted CAI, especially at low and middle range engine load. A typical value between 15-20^{o}CA BTDC provided best results and minimum knocking.

4.3 Engine Testing and Measurement Equipment

4.3.1 Introduction

During the course of experiments a number of appliances were connected to the engine providing necessary data on important engine operation parameters such as speed, load, fuel consumption, exhaust emissions, air/fuel ratio, exhaust gas temperature as well as other essential combustion characteristics.

To provide real time in-cylinder pressure measurement, a pressure transducer was installed on the cylinder head and the pressure signals were then transferred to a PC where necessary software was used to save the data. Exhaust emissions were measured using three exhaust gas analysers and exhaust temperature was measured by a thermocouple located on the exhaust pipe. Furthermore, the load cell was connected to a dynamometer which allowed direct reading of the engine brake torque.

4.3.2 In-Cylinder Pressure Data Acquisition System

In-cylinder pressure measurement is an effective diagnostic tool widely used amongst engine researchers. Its popularity lies primarily within its capability of accurately determining vital combustion operational parameters such as combustion phasing, burn duration and burn rates. It also allows knocking combustion, misfiring conditions and CAI combustion to be defined with accuracy under all operating conditions. Further analysis of the pressure data can be very useful in terms of defining engine load as well as cycle to cycle variation.

For experiment purposes, in-cylinder pressure measurements were extremely important in determining CAI operation points and distinguishing misfire and knocking phenomena from normal combustion.

4.3.2.1 Pressure Transducer

A piezoelectric pressure transducer was used to measure in-cylinder pressure directly. It was a Kistler type 6055 piezoelectric pressure transducer with a measurement range of 0-100 bars gauge and sensitivity of –6 PC/bar. The tapping subsequently, was made on the centreline on the pulley side of the cylinder head. One end of the transducer was located between the intake and exhaust valves whereas the other was connected by a high impedance cable that transferred electrical charge to a charge amplifier (Kistler Type 501). This, in turn, amplified the charge and converted it into voltage that would be used as input in the data acquisition system.

An important parameter that would ensure that the pressure output corresponded to the right output voltage was to calibrate the transducer to a predefined pressure and output voltage. The calibration method followed involved a dead weight machine, a machine that uses various masses of known value as load on a piston that pressurises a hydraulic circuit. Known mass, when applied, produces a known pressure that outputs a voltage, measured by an oscilloscope, on the charge amplifier. After a number of known masses were applied to ensure linearity of the transducer throughout the operating range, a calibration factor was set to the charge amplifier. The charge amplifier was finally set to correspond to 10 bars/V over a measurement range between 0-100 bars while the time constant was set to long during calibration.

Even though cylinder pressure values, in the most extreme conditions do not normally exceed 60 bars, the calibration made could be considered suitable for the purposes required. However in order to take the rapid change of pressure during engine operation into consideration, time constant was set to short while cylinder pressure measurements were taking place.

4.3.3 In-Cylinder Pressure and Heat Release Analysis

4.3.3.1 In-Cylinder Pressure Measurements

An in-cylinder pressure measurements system was developed based on a PC data acquisition system providing real time display and recordings of time resolved pressure data. The inputs of the data acquisition system are pressure signals from the charge amplifier as well as phasing signals (clock and reference) coming from the crankshaft encoder and camshaft position sensor. Both of the above are being used to send signals through the logic box and provide the reference signal for fuel injection timing as well as for spark timing. Clock signal is used to provide the data acquisition sampling interval (1° CA for the current configuration) while the reference signal determines the phasing of the data acquired based on the 4-cycle engine operation.

The interface used for transferring the pulses coming out of the above sources to the data acquisition system, was provided by the National Instruments (NI) BNC 2110 interface unit. The PC is a Pentium III at 400 MHz connected to the interface unit via a National Instruments PCIMIO16-1 PCI data acquisition card.

A custom made software written in NI Labview compatible format, was developed by John Williams, a former researcher of the Brunel University Engines Group, that enabled the user to visualise and record in-cylinder pressure data offering the capability to calculate and log various engine parametric variations such as IMEP, COV_{IMEP} and heat release rates. Another important feature of the software was to display real time p-CA as well as P-V diagrams. Because this software was developed for previous work carried out at the University's Labs on a different engine, its only use was to log in-cylinder pressure data which was at a later stage processed manually using a different software specifically developed by Dr Yufeng Li to calculate the necessary parameters for the experimental procedure (see Appendix D). Details of the fundamental calculations used by both pieces of software are given below.

Cylinder Volume Calculation

One of the basic calculations required to be performed by the software, was to calculate the cylinder volume during every crank angle in order to output a crank angle resolved in cylinder pressure measurement. An equation based on the engine's geometry is used so that it gives cylinder volume at any given crank angle value. This equation, given by the below formula, is loaded upon the program's initiation.

$$V = V_c + \frac{\pi B^2}{4}(l + a - 2s) \qquad \text{Equation 4.1}$$

V is cylinder volume, V_c is the clearance volume, B is the cylinder bore, l is the connecting rod length, a is the crank radius and s is the distance between the crank axis and the piston pin axis as defined as

$$s = a\cos\theta + \sqrt{(l^2 - a^2\sin^2\theta} \qquad \text{Equation 4.2}$$

where θ is the crank angle relative to the vertical.

Determination of Absolute In-Cylinder Pressure

The pressure signal that reaches the data acquisition system describes a relative pressure also known as gauge pressure. In other words, gauge pressure refers to a pressure value relative to an arbitrary value, differentiating it from the absolute pressure value that is required to obtain insight on the in-cylinder pressure conditions. Furthermore, gauge pressure at every crank angle, p(θ) (bar), needed, to be converted to absolute and subsequently was related to the voltage output from the charge amplifier for every crank angle, E(θ), via the following calculation formula.

$$E(\theta) = \frac{p(\theta)}{C} + E_b \qquad \text{Equation 4.3}$$

E_b is the bias voltage (V) with zero pressure and C (bar/V) is the gain (calibration) factor of the charge amplifier [70].

In order to quantify absolute pressures, the transducer output must be directly correlated with pressure at some point in the cycle in a procedure called 'pegging'. Randolph [71] describes nine of the methods used for pegging.

One of the most popular methods of pegging is to assume that cylinder pressure at intake bottom dead center p_{IBDC} equals to the manifold absolute pressure (MAP) i.e p_{IBDC}=MAP. MAP can be measured and therefore the system is pegged to pressure at IBDC. Absolute pressure at any crank angle θ (p(θ)), is given by equation 4.4.

$$p(\theta) = C.(E(\theta)-E_{IBDC}) + p_{IBDC} \qquad \text{Equation 4.4}$$

E_{IBDC} (V) is the charge amplifier voltage at IBDC where the absolute pressure is determined.

In order to minimise the interference of noise, an average of three or five points, namely the transducer output at IBDC, one and/or three CA degrees before IBDC, and one and/or three CA degrees after IBDC, should be used to reduce the potential for error associated with relying on a single point measurement [70].

This method was particularly straightforward to use for the CAI testing procedure as the engine was running without any throttling and load was controlled by valve timing. Therefore it was safe to assume that MAP was equal to ambient pressure measured by the barometer in the laboratory and in this way peg the system according to it.

4.3.3.2 Data Processing and Heat Release Analysis

Data analysis commenced as soon as in-cylinder pressure data was collected from the lab. It involved engine averaged output calculations, cycle to cycle variation analysis of each parameter calculated as well as heat release analysis. As already discussed the calculations were performed using custom made software written by Dr Yufeng Li that produced a data file containing all the calculated engine parameters for every testing condition. Calculation

methods are explained in this section. The source code of the software is further explained in the Appendix D.

Engine Output Calculation

In-cylinder pressure data recorded allow calculation of IMEP directly through numerical integration of the area bounded by the line in the pressure-volume diagram (P-V) over the entire engine cycle. Integration in this diagram uses a step interval of 1°CA that equals to the sampling rate of cylinder pressure. IMEP expresses the work delivered to the piston of the entire four stroke cycle over the cylinder volume V_d displaced during this cycle. Its calculation formula can be found in Equation 4.5.

$$\text{Net IMEP} = \frac{1}{V_d} \oint p.dV \qquad \text{Equation 4.5}$$

Figure 4.3 shows a P-V diagram of a spark ignition four stroke engine operating at part load condition

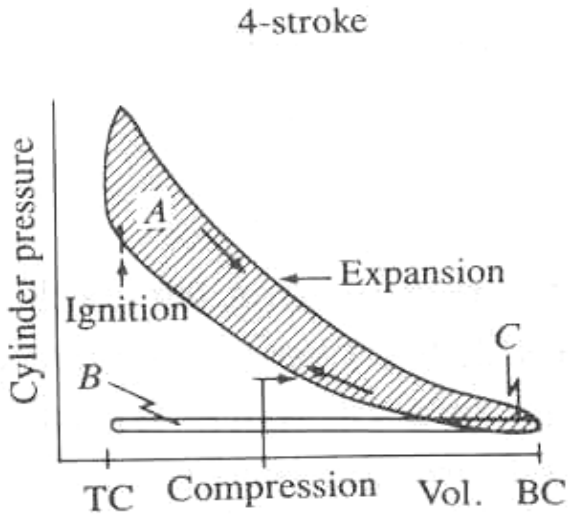

Figure 4.3 Example of a pressure versus volume diagram of four-stroke cycle engine [72]

The diagram is clearly divided into three main areas; area A, area B and area C. Area B and area C represent the work transfer between the piston and cylinder gases during inlet and exhaust strokes and is known as pumping work or as pumping mean effective pressure

(PMEP). Furthermore, the sum of area A + area C represent the work delivered to the piston over the compression and exhaust strokes and is often referred as gross IMEP. Consequently Net IMEP = Gross IMEP - PMEP [72].

Cyclic variation of IMEP

Variations in cylinder pressure due to flame development and propagation during engine operation differ significantly from cycle to cycle, leading to IMEP variations [70]. An important measure of cyclic variability is the coefficient of variation of IMEP (COV_{IMEP}) and is defined as the ratio of standard deviation in IMEP and the mean IMEP as it can be seen in Equation 4.6.

$$COV_{IMEP} = \frac{\sqrt{\sum_{1}^{n} (IMEP - \overline{IMEP})^2 / (n-1)}}{\overline{IMEP}} \qquad \text{Equation 4.6}$$

n is the number of cycles IMEP is recorded. At every test point 300 cycles were recorded. The particular importance of this calculation lies in that it allows evaluation of the stability of combustion, torque variation and eventually CAI combustion conditions.

Heat release analysis

With heat release analysis being a very useful method of analysing combustion phenomena, it was of particular importance to calculate heat release over the entire cycle to determine the parameters affecting combustion phasing and initiation. The most important approaches for the calculation of heat release are the Rassweiler and Withrow method and the One-Zone Net Heat-Release Analysis model.

The Rassweiler and Withrow method can estimate the mass fraction burned profile using cylinder pressure and volume data assuming that any pressure rise, Δp, during any crank angle interval is considered to be cause by the pressure rise due to volume change, Δp_v, and the pressure increase due to combustion, Δp_c,.

$\Delta p = \Delta p_v + \Delta p_c$ Equation 4.7

However, simple calculations based on this method might be that it is not preferred as it is contains several approximations. Most importantly the effect of heat transfer is not taken into account and the pressure rise due to combustion is proportional to the amount of fuel chemical energy released rather than the mass of fuel burned. Therefore, the calculations provided by this model are considered inaccurate as it provides a mass fraction burned profile that goes from zero at ignition to unity at the end of combustion, leaving aside the fact that combustion may be incomplete or the cylinder pressure data and the mass flow rate data are incorrect.

The method used in this work is the one-zone net heat release analysis model. It is based on the hypothesis that cylinder contents' state is defined in terms of average properties without distinguishing between burned and unburned gases; thus cylinder charge is effectively modelled as homogeneous and temperature as uniform. This model also calculates heat release as the amount of heat required to be added into the cylinder in order to produce the recorded pressure change. Therefore the first law of thermodynamics is applied on the cylinder contents that can be considered as an open system. In addition, reactants and products properties are considered to be identical.

$\delta Q_{ch} = \delta U_s + \delta W + \delta Q_{ht}$ Equation 4.7

δQ_{ch} is the chemical energy released by combustion, δU_s is the change in sensible energy. The term sensible is used since only changes in *u* or *h* that result from variation in temperature are included. Variation in *h* or *u* due to chemical reaction or phase change is excluded. δQ_{ht} represents the heat transfer to the cylinder wall and δW is the work done on the piston by the system and is equal to *pd*V.

It can be assumed that

$$U_s = m.u(T) \qquad \text{Equation 4.8}$$

T is the charge temperature and m is the mass within the system. Therefore any crevice volume effects are ignored.

$$\delta U_s = mc_v(T)dT \qquad \text{Equation 4.9}$$

By substitution into Equation 4.7 and writing on an angle incremental basis $d\theta$

$$\frac{dQ_{ch}}{d\theta} = \frac{mc_v(T)dT}{d\theta} + \frac{pdV}{d\theta} + \frac{dQ_{ht}}{d\theta} \qquad \text{Equation 4.10}$$

The first term, $dQ_{ch}/d\theta$ is the apparent heat release rate. Combined with the heat transfer term $dQ_{ht}/d\theta$ to give $dQ_{ch}/d\theta - dQ_{ht}/d\theta$ it describes the net heat release rate, termed $dQ_n/d\theta$. This is the energy release rate due to combustion, minus the heat lost to the walls.

Introduction of the ideal gas law, $pV = mRT$, with R assumed constant, allows further simplification of Equation 4.9. The use of

$$\frac{dp}{p} + \frac{dV}{V} - \frac{dm}{m} = \frac{dT}{T} \qquad \text{Equation 4.11}$$

allows the elimination of T from Equation 4.9 to give

$$\frac{dQ_n}{d\theta} = \frac{\gamma}{\gamma-1} p\frac{dV}{d\theta} + \frac{1}{\gamma-1} V\frac{dp}{d\theta} \qquad \text{Equation 4.12}$$

γ is the ratio of specific heats, C_p/C_v. In this way the net heat release rate can be calculated from the measured changes in cylinder volume and pressure by ignoring crevice flow. The

value of γ is almost always assumed to be constant with a value in the range 1.3 to 1.35. In fact, values of γ for both burned and unburned gases decreases with increasing temperature and varies with composition.

The net heat release profile obtained from integrating the two terms on the right hand side of equation 4.12 is normalised to give unity for maximum value. A mass fraction burned versus crank angle curve can be drawn after integration as shown in figure 4.4 and through this curve a number of useful combustion parameters can be quantified.

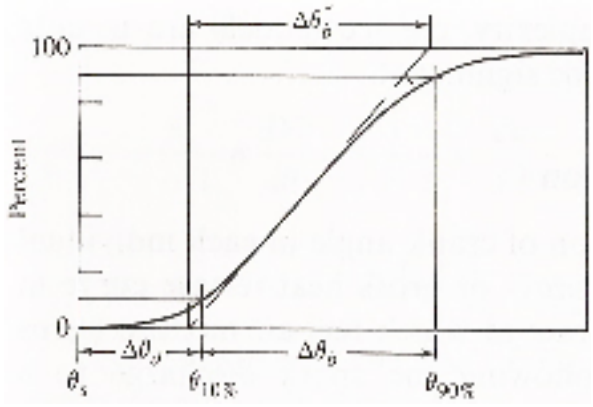

Figure 4.4: Definition of flame-development angle, $\Delta\theta_d$, and rapid-burning angle, $\Delta\theta_b$, on mass fraction burned versus crank angle curve [72].

Table 4.2 lists definitions commonly used to describe the various energy release stages in SI and CAI combustion in relation to MFB.

Mass Fraction Burned	*Combustion stage*	
	SI	**CAI**
0-10%	Flame development angle	-
10%	Start of rapid burn phase	Ignition
10-90%	Rapid-burning angle	Combustion duration
0-90%	Overall Burn Angle	-
90%	End of combustion	End of combustion

Table 4.2 Definitions of Energy Release Stages for SI and CAI Combustion [70]

4.3.4 Calculation of Trapped Mass of Exhaust Products

As already discussed CAI operation in this work was achieved by using short duration and short valve lift camshafts that allow the presence of high temperature exhaust gases in the cylinder during intake, the overall cylinder temperature is increased and autoignition of the fuel occurs. It is therefore useful to calculate and estimate the amount of trapped residual gases during each engine cycle to help gain better understanding on the relationship between exhaust gas mass and combustion characteristics.

A method employed by Zhao *et al*. [70] was used for the calculations. The calculation of the trapped exhaust gas rate was based on the ideal gas law at EVC as shown below.

$$pV = m_r R T \qquad \text{Equation 4.13}$$

Exhaust gas temperature T (K) at EVC was assumed to be equal to the one measured at the exhaust port by the thermocouple. In cylinder pressure P (bar) at EVC was measured by the in-cylinder pressure transducer and cylinder volume V (cm^3) was calculated from the engine geometry also at EVC. The exhaust gases retained in the cylinder at EVC timing can be considered as the amount of gases in the cylinder throughout the engine cycle regardless of the fact that a fraction could be lost, in the form of back flow, into the intake port under certain conditions. This fraction is eventually sucked back into the cylinder under steady state operating conditions. Equation 4.14 shows the calculation formula for the exhaust gases mass expressed as a percentage of the total charge in the cylinder at IVC

$$\text{Trapped residuals (\%)} = \frac{m_r}{m_{fc} + m_r} * 100 \qquad \text{Equation 4.14}$$

the mass of the fresh charge, m_{fc} derives from the mass of fuel injected per cycle, m_f, and the AFR as follows.

$$m_{fc} = (m_f * AFR) + m_f \qquad \text{Equation 4.15}$$

Calculations based upon the ideal gas law were found to correlate better with other experimental data and hence it was chosen as the preferred method.

4.3.5 Exhaust Emissions

4.3.5.1 CO_2, CO, O_2 and Air/Fuel Ratio Measurements

CO_2, CO, O_2 and A/F ratio were measured by a Horiba MEXA 554JE analyser. Exhaust gases after cooling enter the analyser via an integral vacuum pump and pass through a water trap and a particulate removal filter. The analyser consists of two cells; an infrared absorption cell and a galvanic cell. Gas is then divided into two parts and each part enters each cell to be further analysed. Measurements of CO and CO_2 are performed inside the nondispersive infrared (NDIR) absorption cell by measuring the level of absorption of infrared radiation by these gases. This analyser can be characterised as nondispersive as no light diffraction takes place and measurement of the emissions levels is based on total absorption over a given wavelength. The absorption rate A_λ is shown in Beer's law (Equation 4.16)

$$A_\lambda = 12\exp(2C_i Q_\lambda L) \qquad \text{Equation 4.16}$$

Where C_I = the concentration of the species i

Q_λ = the absorption efficiency

L = the optical path length

Details of an NIDR analyser are shown in Figure 4.5. Infrared light emitted by a heated filament that delivers black body radiation over a wide range of wavelengths, is filtered by a filter removing any non absorbable radiation by the gas to be measured. The remaining wavelengths then pass through the sample cell that is already filled with the dried sample gas and on to the detector cell. Both the detector cells are filled with the gas to be measured in order to absorb the radiation in the absorption band of the gas. The detector cells are separated by a diaphragm moving between the two plates of a capacitor.

Radiation passing through the sample cell is absorbed by the gas to be measured and its energy is thus reduced. The proportion of the radiation's initial energy reaching the upper detector cell is compared with the energy level of the radiation reaching the bottom half of

the cell that goes through a reference cell containing reference gas (nitrogen). Energy absorbed on either side of the detector cell subsequently causes pressure rise on this side.

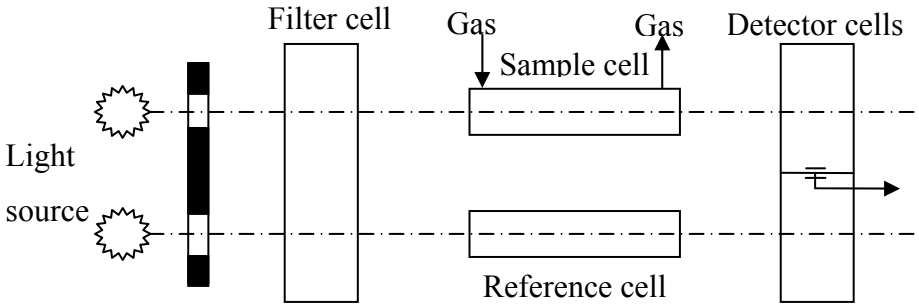

Figure 4.5: NDIR Analysers with Differential Detectors

Energy absorption and at the same time radiation levels variation causes the diaphragm in the detector cell to deflect according to the difference in energy absorption rates in both sides of the cell. The occurring deflection can be directly related to the gas concentration in the sample cell allowing the capacitor to be calibrated for gas concentration units' measurement.

An important issue that prevents accurate reading of CO and CO_2 concentrations is the absorption wavelengths overlap as no direct measurement of concentration of one gas into the other is possible. The issue was tackled by the use of band pass filters that switched position in front of the light source every time each gas species is to be measured. For example, if CO is to be measured, a filter removing wavelengths absorbed by CO_2 was employed and vice versa.

Band pass filters could in theory provide the solution for unburned HC emissions concentration measurements. However, hydrocarbon species contained in exhaust gases feature absorption in various wavelengths thus making concentration measurements a difficult task. Determining HC species is based on the (FID) technique employed in another analyser device, explained below.

Another capability of the gas analyser is to provide measurements for the oxygen content of the exhaust gases and consequently the air/fuel ratio. The procedure takes place in the galvanic cell in the analyser. It consists of a gold plated PTFE diaphragm cathode and a silver plated anode across which a potential is applied. These are immersed in an

electrolyte of potassium chloride gel. Oxygen gradually diffusing from the membrane causes electrochemical reduction and a current that is proportionate to the partial pressure of the oxygen in the sample is created. The magnitude of the current can be calibrated to the oxygen content of the exhaust gases. The galvanic cell's response to other gases including CO_2 doesn't affect results in practice even though CO_2 concentration in the exhaust gases is minimal. This method is accurate at 60.1% however the error in measurements is caused mainly during the 'zeroing' procedure where atmospheric oxygen is used. Usually ambient air contains oxygen in concentrations of 20.7% and 20.9% depending on the pollution and the humidity. Nonetheless when dry measured values of CO, CO_2, O_2, HC and fuel of known composition are used, the analyser can provide with measurements of air/fuel ratio and lambda. For the purposes of the research described lambda, air/fuel ratio, CO, CO_2 and O_2 values were recorded.

4.3.5.2 NO_x Measurements

NO_x is a term used to express the total concentration of nitric oxide (NO) and nitrogen dioxide NO_2 present in the exhaust gas stream. For the measurement of NO_x emissions in the exhaust gases, a Signal 4000VM chemiluminescence analyser was used. An analyser of this type measures the amount of light emitted from electrically excited molecules of NO_2 and the light intensity is used to determine the concentration of NO_x in the exhaust gas. Exhaust gases enter the analyser via a separate vacuum pump through a heated sample line and a particulate filter. The heated line ensures that no water vapour condensates and enters the analyser.

As soon as the sample enters the analyser, any NO_2 present is catalytically converted to NO. Zero grade air at the same time passes through an electrical discharge and some of its oxygen molecules are converted into ozone (O_3). Then both the NO and the O_3 molecules are fed into a reaction chamber where the reaction described in Equation 4.17 below takes place.

$$NO + O_3 \Rightarrow NO_2^* + O_2 \Rightarrow NO_2 + O_2 + \text{photon} \qquad \text{Equation 4.17}$$

NO and O_3 react in the chamber to form NO_2 molecule in an excited state and O_2; the excited molecules of NO_2 return to their ground state by emitting a photon or by being quenched by a molecular collision. The emitted light is directly proportionate to the combined content of NO_2 and NO in exhaust gas stream. It is collected by a photomultiplier and then amplified before being converted into NO concentration values.

The analyser had to be warmed up and calibrated daily before every engine test to ensure accuracy of the measurements. For the calibration, zero grade nitrogen was used and the span was checked with a gas containing 500ppm of NO with a balance of nitrogen. A fast response rate of about 2s and accuracy of 61% of the span gas was maintained through the engine testing procedure.

4.3.5.3 Unburned Hydrocarbon Measurements

Unburned Hydrocarbons, as already discussed, were measured using the infrared technique. However, results from this technique best describe the quality of the species included in the unburned hydrocarbons mixture.

A 'Signal 3000HM' analyser was employed for measurements. This type of analyser uses the flame ionised detector (FID) technique which though expensive and more complex, it performs accurate to the extent required measurements. Detection of ions produced while carbon species are burnt is the principle this technique is based on. The quantity of ions produced is closely related to the carbon atom numbers present in the hydrocarbons mixture.

As with the NOx analyser, the sample is drawn into the cylinder by a vacuum pump via a heated sample line connected to the exhaust pipe for the reasons explained above. The sample, after being mixed with fuel, enters a chamber containing an electrode system and burns with air at stoichiometric quantity. A non carbohydrate type of fuel, which would cause ionisation and thus affect the results, had to be used; therefore a 40/60 hydrogen/helium mix was used. Likewise, the air used had to be free from any hydrocarbon species to ensure that no impurities would affect the results. Ions produce a current that flows between the high voltage electrode and a ground electrode and can relate

to the amount of carbon atoms present in the hydrocarbons mixture. The signal received from the current is amplified a then scaled to match concentration readings. Calibration was achieved in a similar manner to the NOx analyser with the only difference being the use of a known hydrocarbon concentration span gas with an inert balance; in this case 1500ppm propane in nitrogen was used.

In recent studies the theory has been developed concerning the slight effect of hydrocarbons molecule size and species on the detector's response. Table 4.3 lists the relative responses of various organic molecular structures therefore great care has to be taken in order to regulate the fuel and air flow rates entering the analyser since they affect the flame temperature and subsequently the detector's sensitivity.

Molecular structure	**Relative response**
Alkanes	0.97 – 1.05
Aromatics	0.97 – 1.12
Alkynes	0.99 – 1.03
Alkenes	1.07
Carbonyl radical (CO-)	0
Oxygen in primary alcohol	0.23 – 0.68

Table 4.3 Typical responses of a flame ionisation detector to different molecular structures, normalised with respect to propane [73]

A serious drawback of FID technique is its incapacity to define and distinguish between different hydrocarbon species. Therefore, the results of the analyser should be described as parts per million carbon ($ppmC_1$) or parts per million methane ($ppmCH_4$).

4.3.5.4. Calculation of Specific Exhaust Emissions

Emission levels measured by the equipment are always expressed on a volumetric basis usually ppm or percentage %. This data can be of little use as it is related to engine operating parameters (speed, load) and dimensions and thus cannot be directly compared with data from other engines. Consequently a way of expressing this data had to be

established on an absolute rather on a relative basis. This universal expression should rely on the principles that it should allow direct comparison between the data and at the same time would output the data on a normalised basis. The most frequent method employed for that purpose, is to normalise volumetric flow on a gravimetric basis linked to the indicated or brake engine output.

In the calculations' program, the following generic equation (Equation 4.18) was used to calculate specific emissions' output

$$IS(x) = \frac{n_P * vol(x) * m_{(x)}}{n_R\, a(m_c + bm_H + cm_O)} * ISFC \qquad \text{Equation 4.18}$$

x is the emission concerned, vol(x) is the mole fraction quantity of that emission and $m_{(x)}$ is its molecular mass. n_P and n_R are the number of moles of products and reactants respectively and a is the wet molar fraction of the fuel. b and c are the H/C and O/C ratios of the fuel respectively and m_C ,m_H and m_O are the relative atomic weights of carbon, hydrogen and oxygen.

4.3.6 Engine Efficiency Calculations

The engine efficiency (n_f) represents the efficiency of fuel energy converted into the indicated work. It was calculated using the equation 4.19.

$$\eta_f = P_i \Big/ \dot{m}_f Q_{HVf} \qquad \text{Equation 4.19}$$

where P_i is the indicated power, $\dot{m}_f$ is the fuel flow rate and Q_{HVf} is the low heating value of the fuel.

4.3.7 Combustion Efficiency Calculations

The combustion efficiency (n_c) was obtained by the percent of actual energy derived from fuel combustion (fuel energy minus energy waste from CO and HC emissions) and the fuel energy supplied to the engine. It was calculated via Equation 4.20 as shown below.

$$\eta_c = 1 - \frac{\sum_i x_i Q_{HVi}}{\dot{m}_f Q_{HVf} /(\dot{m}_a + \dot{m}_f)} \qquad \text{Equation 4.20}$$

where x_i are the mass fraction of CO and HC, respectively. Q_{HVf} represents the lower heating values of these species, $\dot{m}_a$ is the air mass flow rate.

4.3.8 Temperature Measurements

Thermocouples were installed to measure water, oil and exhaust gas temperatures. Oil and water thermocouples were already integrated in the engine test bed and were a part of the closed loop temperature control system explained in Chapter 3. Each oil and coolant thermocouple was located near the entrance of the respective heat exchangers.

Exhaust gas temperatures were measured by a 'K'-type thermocouple mounted on the exhaust pipe and located very close to the exhaust port. This thermocouple was connected directly to an LCD display and temperatures were recorded.

4.4 Summary

Details of the various equipment and engine measurement systems that were employed throughout this work are presented. A brief description is given on the parameters that were varied through the test involved in this study followed by details of the cylinder head components that had to be modified so that CAI combustion could be achieved. Finally, the data acquisition systems and post processing for the in-cylinder pressure and heat release analysis are described together with emission measurement equipment used.

Chapter 5

CAI Combustion Experimental Strategies, Results and Analysis Part I

Chapter 5 CAI Combustion Experimental Strategies, Results and Analysis Part I

5.1 Introduction

The advantages of CAI combustion have been discussed in Chapter 2 along with details of the methods used for achieving it. CAI initiation has been achieved during this research by means of exhaust gas retention of large amounts of burned gases into the cylinder. Exhaust Gas Recirculation provides sufficient cylinder temperature rise to cause fuel to auto-ignite but also with necessary mixture dilution for the control of the released heat. Short duration camshafts with low valve lift were employed to trap sufficient residual gases in the cylinder by early closing the exhaust valves and by allowing small amount of exhaust gases to escape the cylinder.

This work primarily describes an investigation into the effects of injection timing on mixture quality and CAI combustion targeting mainly to control and extend of CAI regime operation. Cylinder pressure data was recorded and processed offline providing calculations on various important combustion parameters such as ignition timing, burn duration, combustion stability and combustion temperature as well as heat release analysis results. Single and split injection timings with varying fuel quantities along with exhaust valve timing variation were investigated.

5.2 Experimental Strategies

5.2.1 Valve Timing Strategy for CAI Combustion

The valve timing strategy employed in this work aimed primarily on achieving CAI combustion through exhaust gas retention into the cylinder thus providing control over CAI initiation and subsequent heat release rate control. This method most commonly known as Residual Gas Trapping is based on the early closure of the exhaust valves.

Subsequently the intake valves have to be retarded accordingly in order to prevent unwanted flow of exhaust gases back into the intake port, a phenomenon known as backflow. In practical terms and with the default SI combustion camshafts, synchronising the two events by advancing exhaust valve closing and retarding inlet valve opening is often difficult to accomplish. A reasonable explanation for this is that when the default camshafts, with their default duration have to be rephrased, this leads to an abnormal sequencing of events as the exhaust valve would open too early and the intake valve too late thus causing unacceptable engine operation. This solution was overcome by employing new pairs of camshafts with shorter duration and lower valve lift. For that purpose two pairs of production camshafts were modified and re-profiled to match the requirements of the work explained in Chapter 4. Each of the default camshafts had the lobes ground initially to modify their duration and valve lift. Then the camshaft itself was cut at the point after the first pair of cams allowing the remaining part, from the cams to the pulleys, to be installed on the single cylinder engine and in this way operate the valves.

For this work two pairs of camshafts were employed, as already discussed in Chapter 4, with different duration between them in order to investigate the way valve duration could affect engine operation and subsequently CAI initiation as well as CAI control and mixture formation. The pair of camshafts successfully used in previous research by Li *et al.*, [50] at Brunel University, described by Lavy *et al*., [29] was used first. This pair of exhaust and intake camshafts had durations of 110°CA and 120°CA respectively, measured at 0.1mm lift. Upon completion of the measurements and data recording using the camshafts, these were replaced by another pair with duration 10°CA longer also measured at 0.1mm lift as shown in Figure 4.1.a. For common reference purposes amongst researchers, valve opening and closing points are commonly described using a small predefined valve lift. It is very difficult to define the valve lift during the first degrees of rotation as the valve lift rate is very small thus making its estimation complicated. In order to resolve this condition, reference points were used to describe the opening and closing points of the camshafts. It has been estimated for the camshafts used in this work, that it takes around 10°CA for 0.1mm lift for intake valve opening and exhaust valve closing.

During engine operation no throttle was used to control engine load. Instead the latter was primarily controlled by the camshaft phasing. Exhaust valve closing phasing affects inlet

valve opening accordingly to avoid backflow. In particular when exhaust valve timing is advanced the inlet valve opening should be delayed accordingly in order to prevent the trapped residual gases to flow into the inlet port. Work by Leach [74] however indicates that phasing of IVO relative to EVC can be used to control the mixing of fresh and residual gases and, to a certain extent, the final charge temperature and ignition timing. If the intake valves are opened early, when the cylinder pressure is higher than the intake manifold pressure, back flow of the trapped residual gases into the manifold will occur. However, as the piston moves downwards, the backflow gas, along with fresh charge air, will be pulled back into the cylinder. Some heat from the back flow gas will be lost to the manifold walls. This occurrence is termed early back flow. If the intake valves are opened late, when the cylinder pressure has fallen below the manifold pressure, there will be no back flow at IVO. However, the late IVO will result in a late IVC, causing some of the in-cylinder gas to be expelled into the intake manifold as the piston begins to rise. This gas will then dwell in the manifold until it is returned to the cylinder at IVO of the next cycle and is termed late back flow. Under such conditions, during intake and early compression stroke, stratification of the fresh charge and the hot residuals is very strong. In fact, the fresh charge is more likely to be on top especially in the area round the valves during the stratification process. This essentially means that the even during backflow conditions, the freshly induced charge will flow into the intake port thus minimising the heat lost from the fresh charge, resulting in a slight increase in the overall charge temperature upon its return into the cylinder. At this point it should be stressed that continuous retarding the inlet valve closing event results in change in the effective compression ratio.

5.2.2 Injection timing strategy

Considering the importance of injection timing on CAI combustion process, the primary concern was to identify the operation windows in which injection can actually occur. The effect of single injection at various timings as well as double injection on CAI combustion stability and initiation was investigated. Careful selection of injection timings had to be made so that on one hand the full effect of injection timing on CAI could be studied and on the other to avoid potential problems with abnormal combustion and increased fuel consumption. Theoretically the earliest injection timing can take place at EVC. Further advance of the injection timing could not operate the engine due to escape of the fuel

through the opening exhaust valve. The injection could not take place around the TDC of both intake and compression processes as the in-cylinder pressure was higher than the injection pressure of only 6.5 bar supplied by the Orbital air assisted fuel injection system. This second pressure rise in the cycle around TDC of the exhaust stroke is caused by the necessary for CAI early EVC and late IVO timings and is known as recompression. Peak recompression pressure values lie between 8 to 15 bar and the duration of this stage of the cycle is between 30°CA and 70°CA depending on the valve timings configuration applied. For the above reasons injection should occur within limits that allow smooth engine operation and potential for proper control of CAI combustion.

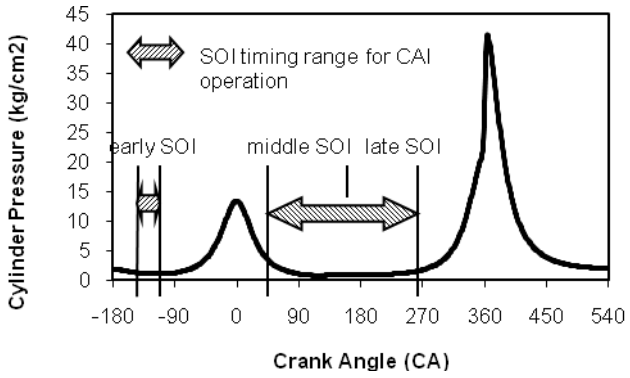

Figure.5.1 Cylinder pressure of CAI operation and injection timing windows

Figure 5.1 shows a plot of the in-cylinder pressure trace of the entire cycle using residual gas trapping. The plot offers a clear overview of the time windows in which injection is allowed, before the in-cylinder pressure reaches the injection pressure value of 6.5 bar. The earliest possible injection event can only take place at EVC. However as EVC timing changes throughout the course of the experiments, the earliest injection occurs at different crank angles accordingly. Timings used for this work allowed injection at EVC even during the 'worst case' condition at high engine speed operation with substantially higher recompression and larger amounts of trapped residuals.

The injection timing effect was investigated by means of varying injection and double injection over a range of timings. For single injection tests, the injection timing was varied from early to late injection for different EVC timings. As it can be seen in figure 5.1, early

injection refers to fuel being injected at a very narrow crank angle window around EVC. Middle and late injection describe injection taking place during intake and at the middle stage of the compression stroke accordingly. Split injection test on the other hand, involved fixed first injection at the crank angle of the EVC timing whereas the second injection event is delayed by 30°CA taking place in the intake stroke or it can be further delayed and take place during compression stroke.

Middle injection was chosen to take place after TDC of the intake stroke. Injection in this instance had to be treated the same way as early injection. However this time injection should be delayed in order to occur after the in-cylinder pressure was sufficiently low to allow injection at injection pressure of 6.5 bar.

5.2.3 Compression ratio

Another parameter investigated was the compression ratio. More specifically this prototype engine was built in a way that would enable future modification of the compression ratio. Initially tests involving valve timing and injection timing were carried out with a compression ratio of 9:1. As soon as all these tests were completed, the cylinder head was removed and the chamber volume was measured. In the mean time a 3mm thick plate lying in between the cylinder block and the crankshaft body was removed so that the deck volume was reduced and the compression ratio increased to 11:1.

After the increase of compression ratio the testing strategy employed at the lower compression ratio was repeated. However due to the increased compression ratio and thus the increased tendency for knocking combustion, all engine and lambda sweep tests involving injection earlier than 240°CA BTDC could not be performed. As far as the injection timing tests were concerned, injection timings varied from middle to late (120°CA to 270°CA) as with the lower compression ratio, however again because of high knocking occurrence the testing speed was reduced from 1800 rpm to 1500 rpm.

5.2.4 Engine coolant

Due to CAI combustion's dependency on the temperature of various parameters e.g charge and intake air, it was decided that the engine coolant fluid's temperature should be tested in order to gain a better insight into the effect it has upon CAI combustion. The engine employed for this study used water as a coolant media. The control panel used to provide speed and load adjustments also allowed the water temperature to be set to the desired value. After that the water pump was turned on and water temperature started increasing gradually up to the set value. This allowed for the control of the water temperature entering the engine and thus performs our tests.

5.3 Test Methodology

5.3.1 Introduction

Testing procedure was determined mainly by the parameters involved in the CAI operation initiation and control; exhaust valve closing (EVC) timing and injection timing. As already discussed in section 5.2, the approach towards realising CAI operation, was the trapping of large amounts of exhaust gases that would eventually raise the in-cylinder charge temperature, by means of early exhaust valve closure. The engine load was controlled by the EVC timing which ranged from -55°CA (i.e. 60°CA BTDC, the TDC of intake is taken as 0 in this study) and -95°CA. Later EVC timing would not allow the engine to operate smoothly as the amount of residual gases trapped in the cylinder that is not enough to initiate CAI combustion and too early EVC on the other hand causes too much burned gases to establish stable SI combustion. Furthermore very early EVC timing not only prevents stable engine operation, it also prevents initiation of any type of combustion due to the low exhaust gas temperatures.

Considering the importance of inlet valve opening (IVO) timing on mixture formation and composition on affecting the in cylinder contents backflow and the amount of fresh charge entering the cylinder, tests were performed with IVO timing varying from -20°CA to

20°CA around the symmetrical CA value. However, during the majority of the tests IVO was kept to a CA in the intake stroke symmetrical to the corresponding EVC in the exhaust process.

For each set of valve timing configuration, engine speed varied from 1200 rpm to 2400 rpm in steps of 150 rpm. When starting the tests, the engine was motored at a minimum speed of 1200 rpm referred to as critical speed here. The minimum speed depended on EVC timing and injection timing. Maximum speed was kept at 2400 rpm to maintain consistency with previous work conducted on the same engine.

Air fuel ratio (A/F) is an important operation parameter therefore its effect on CAI combustion needed to be investigated. For every valve timing, injection timing and speed, A/F ratio was varied from $\lambda=1$ to the limit determined by the presence of misfire cycles. Tests with varying speed and lambda are named sweep tests from now on.

5.3.2 Experimental practice

CAI combustion can only be established successfully after a number of consecutive cycles of SI operation that would allow in-cylinder temperature to increase sufficiently to assist auto ignition process. However CAI combustion at the same time needed not only to be initiated but also to be controlled especially by the controlling of heat release rate by means of trapping adequate amounts of residuals that would provide the high levels of dilution required. As it can be realised CAI operation of the engine with cold start was difficult to accomplish. At the same time, and for the purposes of the testing repeatability, measurements were taken only after the engine was fully warmed up. For this reason preliminary motored operation of the engine had to be performed to increase coolant and lubricant temperature to 85°C before starting the firing operation.

In the mean time the lab equipment necessary for the measurements, was warmed up and calibrated. As soon as the water and oil reached the desired levels, the engine was started and it was first motored to a certain speed, referred as critical speed here. It was about 1200rpm or more in this study depending on EVC timing and injection timing and then

turned on the fuel injection and spark ignition. As mentioned above, two main tests were carried out: the engine speed and lambda sweep tests and the injection timing effect tests. Further experiments involved investigating the effect of parameters such as coolant water temperature on combustion. Each engine test point was defined by the valve timing, the injection timing (early, middle or late injection) and by the type of test performed (engine and lambda sweep, injection timing effect etc).

EVC and IVO timings were set first. EVC was varied from 55°CA to 95°CA BTDC of the exhaust stroke and IVO to the exact symmetrical to the TDC crank angle value. The engine was motored and in-cylinder pressure traces were recorded. Then injection was set according to the schedule shown in Figure 5.1. It was found that the presence of the spark plug was necessary, in order to achieve the necessary temperature and pressure conditions that would allow CAI to be initiated and kept going at the same time. Due to the high cycle by cycle variation, it is necessary to keep the spark on, in order to fire those cycles that failed to auto-ignite and hence maintain the continuum of cycles successfully auto ignited, ensuring a stable CAI combustion operation. After some preliminary tests it was found that when ignition timing ranged between 20 and 25°CA of the compression stroke, engine operation remained stable and knocking phenomena were kept to a minimum.

With the engine being motored at 1200 rpm, fuel injection and ignition were turned on and subsequently the first CAI cycles were present. Lambda was adjusted to λ=1.0 by adjusting the fuel quantity entering the engine through the Orbital injection system and thus changing the air/fuel ratio. Then the engine would be going to CAI combustion automatically if its speed was higher than the critical speed. Otherwise, the engine would operate unsteadily. In these circumstances CAI combustion could be achieved by increasing engine speed to the critical speed which can eventually be observed as a very fast pressure rise during combustion on the real-time pressure/crank angle display on the DAQ PC monitor. The typical critical speed in this work was found to be 1200 rpm; however this value varied with EVC timing, injection timing, compression ratio and valve lift.

The presence of CAI combustion was verified by switching the spark plug off and the engine kept on running without any disruptions. In the mean time the measuring equipment

was allowed to settle before any measurements of exhaust gas temperatures and engine output were taken. As soon as the instrumentation was settled, readings of the above stated parameters were taken and DAQ was set to 'save' mode recording in-cylinder pressure data from 300 consecutive cycles and then stored on to the PC hard drive. During the time needed for the data acquisition system to record pressure data, the readings from the emissions analysers were taken, together with exhaust gas temperature and engine load readings.

For the speed and lambda sweep tests, lambda was set to 1.0 and then varied up to the leanest limit for every engine speed configuration. Upon completion of the procedure described in the previous paragraph and with the same engine speed, lambda was increased in increments of 0.05, reaching a maximum value that marked the end of the lambda variation and thus the testing procedure for the certain speed. The same procedure was repeated with the engine speed this time increasing in steps of 150 rpm up to 2400 rpm. For each speed setting, lambda was varied as described above and for every point emissions' readings, fuel quantity and pressure data were recorded.

Injection effect tests were followed by the speed and lambda sweep tests. These were performed with engine speed set at 1800 rpm and lambda at 1.0 with injection varying from early to late in steps of 30°CA. For every test point the same sets of data were recorded along with the speed and lambda sweep tests. Injection effect tests differed from previous tests on the basis that speed and lambda were kept constant and injection timing was the variable. Subsequently the amount of data was comparatively smaller to that collected during engine and lambda sweep tests. For the sake of time saving, injection timing tests were performed first followed by the speed and lambda ones. This also offered the advantage of investigating what injection timing would provide stable operation with minimum knocking at the same time.

After EVC was set to 65^{o}BTDC and IVO to 65^{o}ATDC the engine was started and speed was set at 1800 rpm. Then injection was set to occur during recompression stroke (early injection), fuel and spark were turned and on and data recording commenced. As soon as emissions, pressure data and fuel reading were recorded, injection was retarded by 30°CA and the same procedure was followed up until injection occurred during the compression

stroke (late injection). The next was to set speed at 1200 rpm and the injection to early and proceed with the speed and lambda sweep tests.

Upon completion of the above mentioned testing procedures, EVC was shifted 5°CA, IVO was set to the symmetrical to the TDC value and the tests were repeated to a similar manner. Table 5.1 describes the testing schedule of speed and lambda sweep tests.

Table 5.1 Selections of Valve and Injection timings used for engine speed and lambda sweep tests using different camshafts and compression ratios.

Default Camshafts (low lift 2 mm), CR=9

EVC (BTDC)	Injection
60	SI combustion
65	60ATDC, 120ATDC, BDC
75	120ATDC, BDC, 240ATDC
80	240ATDC
85	120ATDC, BDC, 240ATDC
90	240ATDC
95	95BTDC, 60ATDC, 120ATDC, BDC, 240ATDC
102	110BTDC, 60ATDC, BDC
105	Cannot start

Default Camshafts (low lift 2 mm), CR=11

EVC (BTDC)	Injection
60	240ATDC
65	240ATDC
75	BDC, 240ATDC
80	240ATDC
85	BDC, 240ATDC
90	240ATDC
95	BDC, 240ATDC
102	BDC
105	Cannot start

Modified Camshafts (high lift 2.4 mm), CR=9

EVC (BTDC)	Injection
65	--
70	SI at MBT, 90ATDC
75	BDC, 210ATDC, 240ATDC
85	90ATDC, BDC
90	100BTDC, 60ATDC, BDC
95	100BTDC, 90ATDC, BDC

Modified Camshafts (high lift 2.4 mm), CR=11

EVC (BTDC)	Injection
65	240ATDC
70	240ATDC
75	240ATDC
80	BDC, 240ATDC
90	BDC, 240ATDC
95	240ATDC
100	--

5.4 Discussion of Results

5.4.1 CAI Operation Performance

5.4.1.1 General / Overall Performance

Engine operation, as already mentioned, was influenced by the presence of various parameters that only allowed a certain attainable output range. Each operating point was defined mainly by the A/F ratio up to the extent that the engine would misfire for every possible combination of variables (compression ratio, different sets of camshafts). Subsequently both lower and upper misfire points would provide the limit at which engine operation was feasible. At low load limit, the engine's trapped residuals' rate is high enough but the overall charge temperature is not adequately high to initiate auto-ignition.

For high load misfire occurs for the reason that even though the temperature of the retained gas in the cylinder is sufficiently high, auto-ignition cannot be promoted because the ratio of fresh charge to trapped residuals is significantly low.

As experiments involved increased compression ratio effect on autoignition, the subsequent presence of knocking combustion was another parameter that could define maximum load. Research conducted on high rates of trapped residuals, has shown that under certain conditions involving high rates of cylinder pressure rise rates, maximum load is defined by knocking combustion rather than misfire [41]. Under such conditions, dilution rates are essentially low and although in-cylinder temperatures are high enough to initiate CAI, the mixture is not diluted sufficiently to prevent extremely high rates of pressure rise. As it can be further seen in Section 6.5, during the set of experiments with lower compression ratio, the presence of knocking was negligent and maximum and minimum load were defined by misfire. However, as compression ratio increased and knocking phenomena were strongly present, operation limits were still determined by the misfire occurrence. Knocking detected during combustion could be minimised mainly by retarding the ignition timing during the stage of operation were both spark ignition and CAI combustion occurred simultaneously and thus the presence of spark could affect the onset of combustion. Nevertheless, in full CAI combustion conditions knocking was present throughout the load range and the only parameter that proved to be effective in tackling it was retarding the injection timing.

5.4.2 CAI and SI Combustion Comparison and Analysis

In this study it was possible to make a direct comparison between spark ignition and CAI combustion under identical configurations of the same engine. The obvious benefit is that the results and the analysis following them, allow better understanding of the differences as well as providing direct evaluation of both types of combustion. Due to the fact that the engine was built for interchangeable camshafts, switching from one mode to the other was a matter of changing the intake and exhaust camshafts, one set for SI combustion, another one for CAI combustion with shorter valve lift and duration as shown (Fig 5.2). The above changes were themselves enough to “convert” a single-cylinder SI engine to an engine that

was able to operate under CAI combustion regime throughout a significant range of operation points.

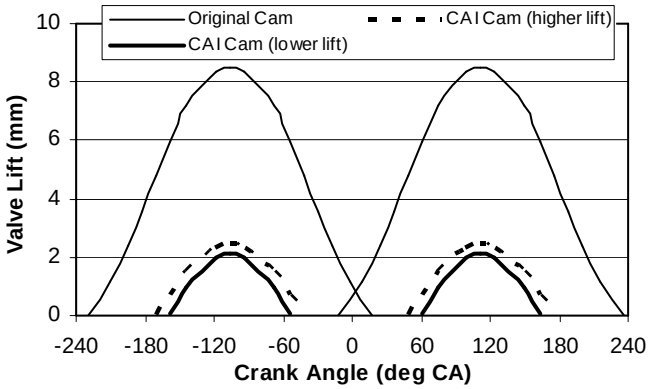

Figure 5.2 Valve lift history for SI and CAI camshafts

It was important that the parameters not associated with provoking CAI e.g. speed and lambda range as well as injection and ignition timing, remained unchanged during the course of experimentation with both combustion modes in order to ensure consistency and better understanding of the results.

As soon as CAI tests were performed, the camshafts were swapped for the ones to be used for SI combustion experiments. It should be noted that during CAI tests the engine was operated at Wide Open Throttle (WOT) due to the fact that engine load during CAI combustion with residual gas trapping is mainly controlled by EVC timing, while in SI combustion the throttle is responsible for the control of the load; therefore it was partly opened. The above configuration ensured that the load during SI combustion was maintained at the same levels as with CAI combustion. All the SI tests were carried out with the spark timing being manually adjusted to the maximum brake torque (MBT) timing and all engine and emissions data were recorded in the same manner as with CAI work. Due to time constraints, SI and CAI tests took place under the following configuration: Compression ratio was set to 9:1, EVC timing to -75°CA, SOI timing to 270°CA, and engine speed to 1800rpm while air/fuel mixture varied from stoichiometric up to the maximum attainable value of lambda. The residuals trapped during CAI operation were estimated to be 47% of the charge. The indicated mean effective pressure (IMEP) of 310kPa achieved during CAI tests was preserved, during SI combustion tests, by positioning the throttle as described in the previous paragraph.

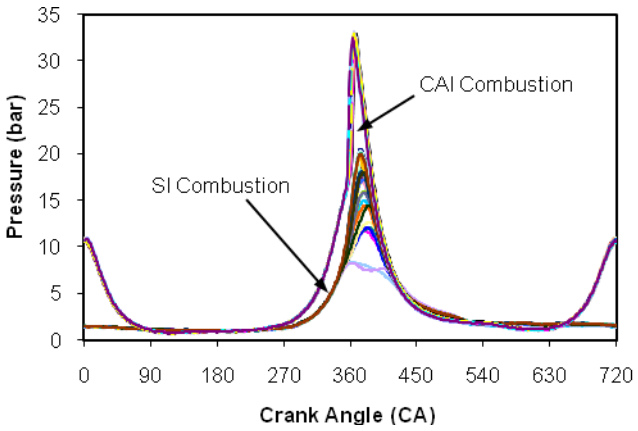

Figure 5.3 Cylinder pressure for SI and CAI combustion (IMEP=310kPa, 1800rpm, λ=1)

In Figure 5.3 the recorded pressure traces of 30 cycles of both CAI and SI combustion are being presented. This graph gives a clear idea of the different nature of each combustion type. As it can be observed, CAI provides higher peak cylinder pressure values than SI as combustion takes place simultaneously throughout the charge. On the other hand SI combustion relies on flame propagation. Consequently a closer look on the pressure traces in Figure 5.3 reveals how significantly smaller the cycle by cycle variation is during CAI than in SI combustion. This can be also attributed to the fact that SI combustion is based on flame propagation and turbulence within the cylinder leading to cylinder pressure fluctuation.

Additional experiments involved tests with λ values varying from 1 up to the leanest engine operation was feasible and allowed data reading both for SI and CAI combustion mode. Tests were performed under the above mentioned EVC, SOI timing values at the speed of 1800 rpm. Conclusions drawn from the results shown in figure 5.4 are summarised below.

IMEP *(Figure 5.4 (a))* CAI combustion's well known benefit of extending the range of λ values compared to the corresponding SI values is confirmed. The engine was able to operate under leaner mixture conditions under CAI regime while during SI combustion above λ=1.2 it operated unstably with significant amount of misfire to the extent that wouldn't allow further running. Furthermore IMEP deteriorated slightly at lean operation

compared to stoichiometric in CAI mode while at the same time in SI mode IMEP was reduced by almost 23% when the engine swung from λ=1 to lean limit.

COV_{IMEP} *(Figure 5.4 (b))* Autoignition occurring simultaneously in various sites into the cylinder and fast extension of the combustion throughout the chamber are considered to be the mechanism via which CAI combustion takes place into the cylinder [20]. In Figure 5.4 (b) this is depicted as very low (5%) COV_{IMEP} when the engine runs in CAI mode essentially revealing the capacity of CAI to make the engine run stably through the entire IMEP and lambda range. On the other hand SI is presented in the graph as a type of combustion that is only stable during a very narrow region around stoichiometric operation and which the leaner the mix becomes the more the engine tends to operate unstably mainly due to the fact that initialization and flame propagation are widely dependent on air/fuel ratio and thus keeping the engine unstable during lean conditions. An important conclusion that can be drawn out of this graph and provides a clear idea on how different both combustion modes are, is that around the region when SI combustion is stable and COV_{IMEP} is kept constant, the corresponding CAI value is not only constant but it's more than 50% lower compared to the one observed in SI mode.

CA of 10% burnt rate *(Figure 5.4 (c))* The mechanism and nature of CAI combustion development in the cylinder allows its early initiation as well as its rapid completion. This means that as soon as the mixture reaches the autoignition temperature, its oxidization begins in numerous locations simultaneously and promotes very rapidly without the need of a spark to initiate it and create a propagating flame front as is the case in SI combustion. In Figure 5.4 (c) CAI starts earlier than SI for every lambda value the engine was tested and with the lambda increase both combustion types start later. In the case of SI operation, MBT timings were used. Comparing the crank angles at stoichiometric and lean operation for SI and CAI combustion it is observed that in CAI there appears to be slight increase whereas in SI the increase is up to 5^{o} CA.

CA of 10%-90% burnt rate (burn duration) *(Figure 5.4 (d))* Shorter combustion duration is what can be immediately noted in this figure between the two combustion types. Combustion duration in CAI mode is almost 93% shorter than that of SI; a fact that enhances the view that CAI is a type of combustion that propagates very rapidly within the

cylinder producing high rates of heat release. Burn duration values remain more or less constant for the whole lambda range for both combustion types.

Maximum pressure rise rate *(Figure 5.4 (e))* As a result of the early commencement and the short duration of CAI, the maximum pressure rise rate is significantly higher in CAI than SI combustion by up to 94%. It is safe to assume that SI combustion appears less knocking tendency and less engine noise. This however can be also attributed to the low compression ratio (9:1) used in both SI and CAI operation experiments.

Pumping losses *(Figure 5.4 (f))* The main difference between the configuration under which experiments took place in order to compare SI and CAI combustion, was the use of a throttle body to control the load for SI experiments. This is main reason why pumping losses were higher by almost 60% in SI mode than in CAI. CAI involved large amounts of trapped residual gases and hence minimised pumping losses due to the closed throttle.

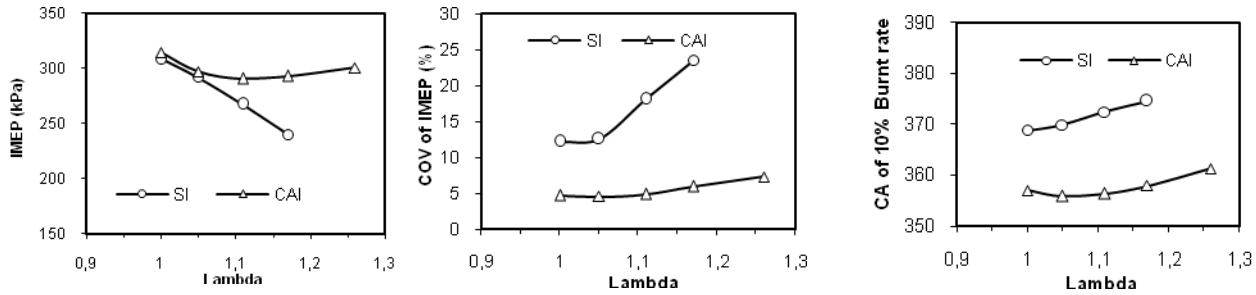

(a) IMEP (b) COV of IMEP (c) CA of 10%burnt rate

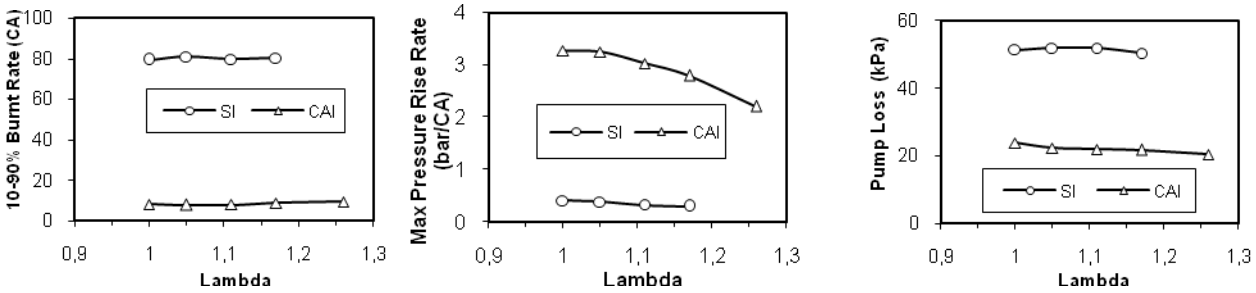

(d) CA of 10%-90% burnt rate (e) Max pressure rise rate (f) Pumping Losses

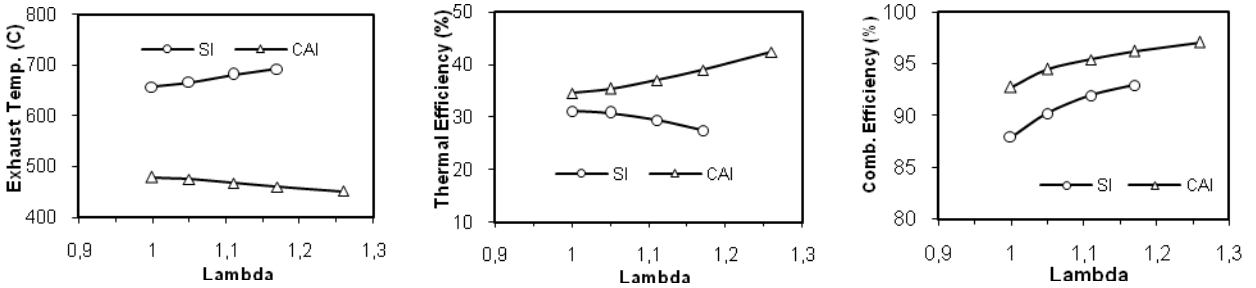

(g) Exhaust temperature (h) Indicated engine efficiency (i) Combustion efficiency

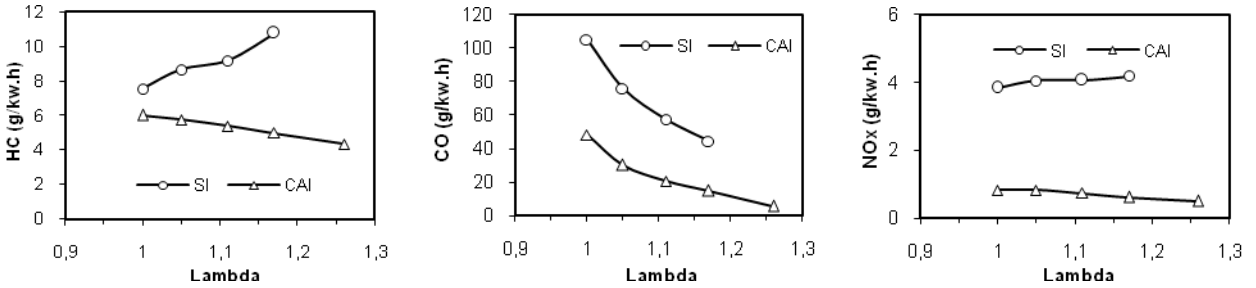

(j) HC emissions (k) CO emissions (l) NOx emissions

Figure 5.4 Combustion characteristics and emissions for CAI and SI combustions (EVC=75^{o}CA BTDC, IVO=75^{o}CA ATDC, CR=9:1, SOI=270^{o}CA ATDC, 1800rpm)

Exhaust gas temperature *(Figure 5.4 (g))* Owing to the fact that combustion occurs earlier and faster than SI, is the subsequent decrease of about 200^{o}C in the exhaust gas temperature in CAI mode. It can be also observed that in CAI mode there is a linear reduction in the exhaust temperature values as lambda increases whereas in SI mode leaner mixtures lead to a linear increase in the exhaust gas temperature. As more fresh charge enters the cylinder, in CAI mode, mixture temperature is reduced leading to further reduced temperature levels of the exhaust gases. With SI mode leaner mixtures means higher O_2 concentrations in the charge thus higher propagating flame temperatures and subsequently higher levels of exhaust gases temperatures.

Indicated engine efficiency *(Figure 5.4 (h))* During stoichiometric operation, indicated engine efficiency values were nearly the same for both types of combustion as it can be observed. However as the mixture gets leaner, it becomes more obvious that CAI is much more efficient than SI as it provides higher efficiency rates even at points where SI isn't feasible (λ>1.2). Additionally engine efficiency increases with mixture composition for CAI by 30% compared to stoichiometric conditions opposite to what happens with SI combustion where it decreases by 17%.

Combustion efficiency *(Figure 5.4 (i))* The characteristics and mechanisms that make CAI have a higher engine efficiency, are also responsible for the fact that it also appears to have significantly higher combustion efficiency rates than SI combustion. It should be taken into consideration that during CAI operation, exhaust gases from the previous cycle containing CO, CO_2 and unburned HC species are trapped and remain into the cylinder in order to burn together with the fresh charge during the following cycle. With lambda increasing and the mixture becoming leaner, combustion efficiency increases for both combustion types and during lean CAI operation it reaches very high levels close to 100%. SI also provides high combustion efficiency rates throughout the operating range achieved however, the curve of SI's combustion efficiency lies underneath the CAI one for every air/fuel ratio the engine was operated.

HC emissions *(Figure 5.4 (j))* The presence of low in-cylinder and exhaust gases temperatures during CAI operating regime resulted into an unexpected low unburned HC emissions output. The term 'unexpected' used because it has been described in scientific

literature [56] that HC emissions are equally or even higher in CAI mode than in SI mode mainly because of the high in-cylinder temperatures caused by the flame propagation. It should also be noted that during SI combustion, leaner conditions lead to higher HC emissions due to incomplete combustion or misfire in a fraction of the engine's operating cycles [76]. Nevertheless, in this study a reduction of 23% is observed between SI and CAI combustion for stoichiometric conditions and as the mixture progressively becomes leaner, this reduction reaches the maximum value of 55% in favour of CAI. Contrary to what happens with SI mode, CAI combustion's unburned hydrocarbon levels are progressively reduced as the mixture becomes leaner and a smaller fraction of residuals is contained in the cylinder. This reduction can be explained by the employment of late injection in the experiments that stratifies the mixture during both modes. In a DIG engine operating in SI mode, injection during the compression stroke increases HC emissions due to stratification leading to higher levels of unburned HC emissions [88, 89]. In the CAI mode however, use of exhaust gases trapping and short combustion duration, tend to reduce the HC emission levels measured.

CO emissions *(Figure 5.4 (k))* This figure shows the trend for reduced CO emissions for every load point and thus lambda value applied during the tests. The curves for both types of combustion follow a similar pattern of reduction with the CAI values curve lying underneath the SI one not only for stoichiometric but for lean operation. A percentage of approximately 55% represents the maximum reduction attainable when the engine was operated in CAI mode.

NOx emissions *(Figure 5.3 (l))* An important decrease in the amount of NOx produced during CAI combustion is being recorded. During SI operation NOx emissions are increased compared to CAI in a region between 75% and 83%. The appearance of low NOx emissions in CAI is mainly because of the low in-cylinder temperatures encountered. In SI, on the other hand, the burned gases region is subject to compression which increases its temperature thus exceeding the temperature threshold above which NOx emissions rise exponentially [74]. A more important reason is the extra dilution present in CAI combustion.

5.4.3 Spark Ignition Effect

A very interesting aspect of CAI that needed further investigation was the parallel occurrence of CAI operation supported by the presence of spark ignition under certain operating conditions. Understanding the phenomena involved during these conditions would provide very useful information on the way the initiation of auto ignition is triggered and controlled. The term spark assisted CAI, also known as partial CAI, is used in this section to describe the situation where the presence of spark is necessary to provide the spark discharge for igniting the mixture. In that way a flame propagation front around the spark plug is thus created and assists in igniting all the cycles that failed to reach the desired autoignition conditions, so that a continuum of auto-ignited cycles is not interrupted and engine operation remains unaffected. The unburned region of the mixture is further compressed by the expanding flame front and subsequently auto ignites. Clearly this process resembles the ignition of the end gas mixture in traditional spark ignition engines. However, in CAI conditions the mixture is highly diluted with residual gas, therefore the pressure rise is significantly reduced. Furthermore the spark ignition timing has to vary within a specific range to provide sufficient mixture burning. Advanced spark timing leads to misfire while retarded spark timing cannot promote autoignition, thus combustion develops in the same way as regular spark ignited combustion.[90]

For the purpose of studying the effect of spark ignition timing on CAI combustion, a number of experiments have been carried out involving spark timing swinging under different engine speed and lambda values. It was important to focus the study on the events and the change of operating parameters taking place during the transition between the point where CAI is established via the presence of the spark and the point where CAI was fully developed. Operating conditions were as follows:

EVC:	83^{o}CA BTDC
IVO:	77 ^{o}CA ATDC
Compression ratio:	9:1
Start Of Injection:	270 ^{o}CA ATDC
Lambda:	1.0-1.2
Engine speed:	1350-2100 rpm
Camshaft type:	Old Cams

During experiments, it was found that when the engine was run at speeds higher than 1650 rpm it operated under full CAI regime without the need of spark. At that speed or higher, when the spark plug was turned off, the engine continued to operate smoothly without any sign of misfire or unstable combustion. On the other hand, at lower speeds the engine was clearly dominated by spark assisted CAI mode. As soon as the spark plug was turned off, the engine started misfiring and only when the spark plug was turned back on, combustion was resumed. It should also be underlined that during spark assisted mode, auto-ignition timing is directly affected by the spark timing. Therefore it should be very interesting to investigate how the engine load and combustion stability varied with speed and mixture concentrations under such conditions.

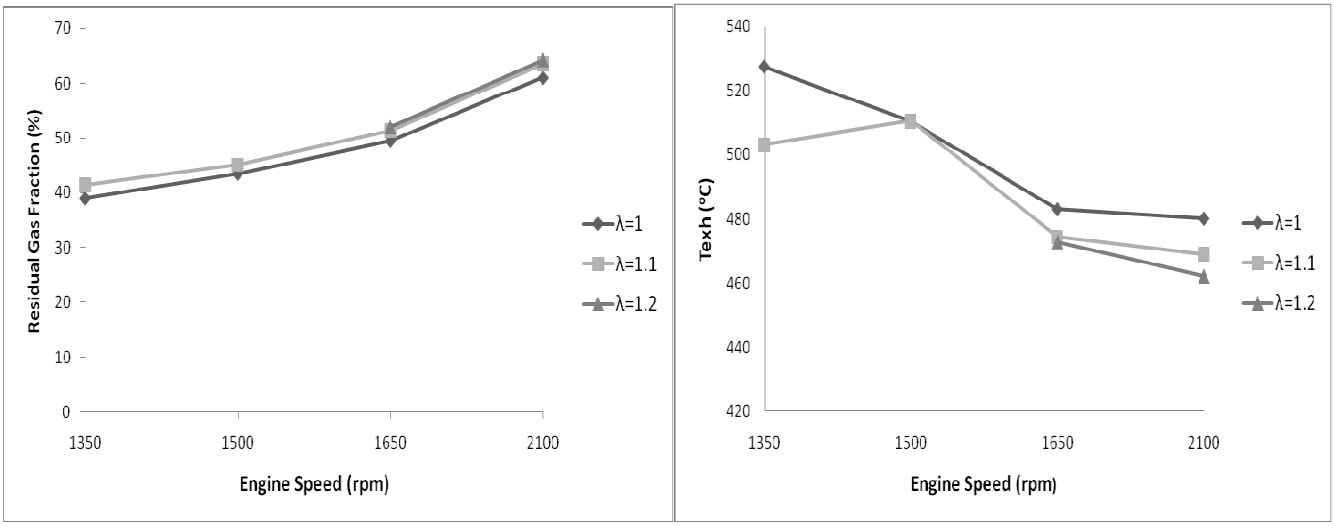

Figure 5.5 (a) Residual Gas Fraction and Exhaust Gas Temperature vs Engine Speed during Spark Ignition Effect Experiments. (EVC= -73°CA, IVO=65°CA, CR=9, SOI=270°CA)

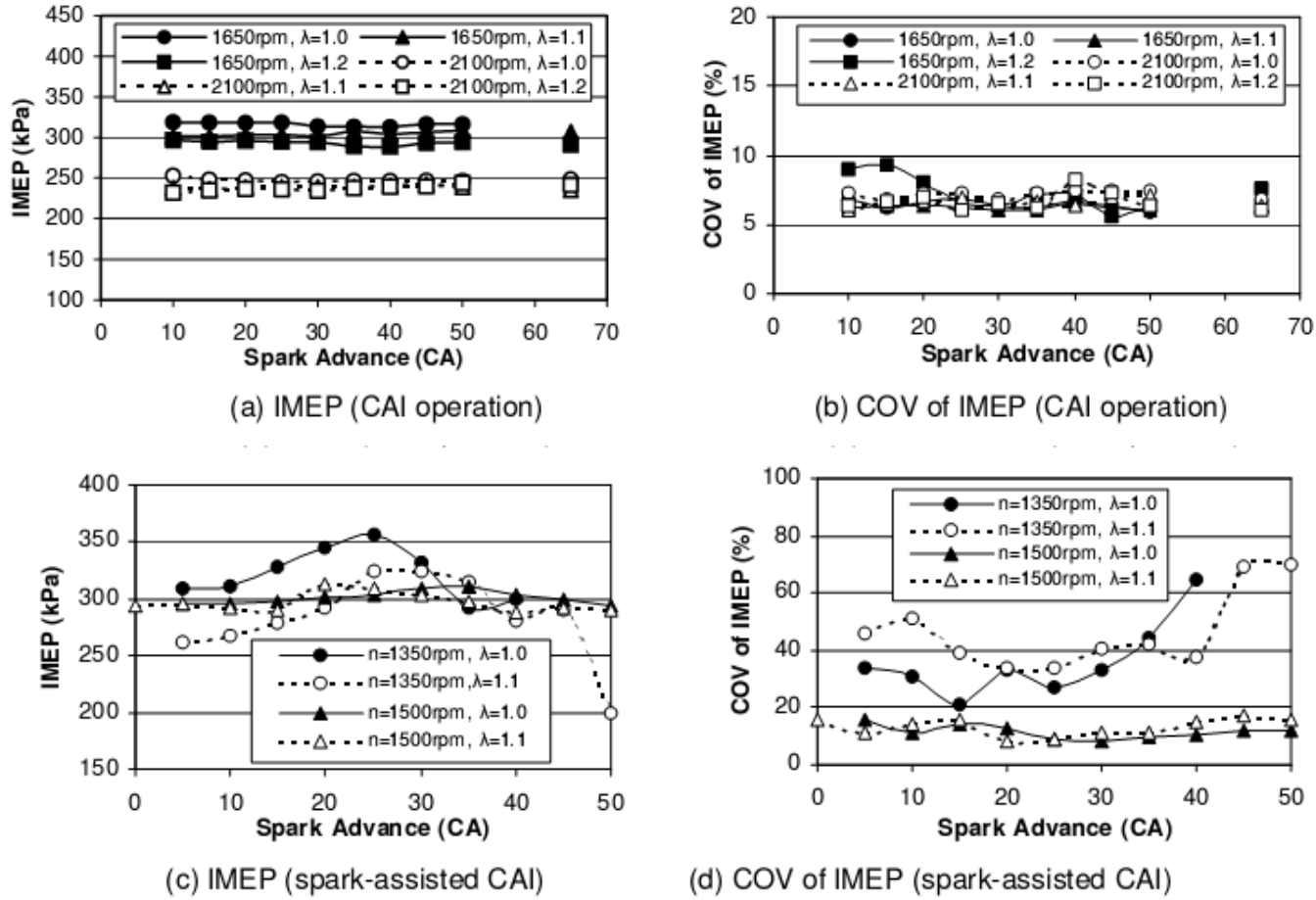

Figure 5.5 (b) Effect of spark timing on IMEP and COV of IMEP.
(EVC= -73°CA, IVO=65°CA, CR=9, SOI=270°CA)

Figure 5.5 (a), shows how Exhaust Gas Temperature and the percentage of Residual Gases in the cylinder vary during the spark timing effect experiments. Figure 5.5 (b) shows how spark timing affects IMEP and COV_{IMEP} under different engine speeds and lambda values. In the graphs (a) and (b) of Figure 5.5 (b), the points with the most advanced spark timing (at 65 °CA) were obtained during engine operation with the spark switched off. With the spark off it could be determined whether CAI combustion was assisted by the presence of the spark at a certain speed and load point. As mentioned earlier, in graphs (c) and (d) data could not be recorded with the spark turned off because the engine would stop firing. As it can be seen in Figure 5.5 for every engine configuration (speed, lambda, valve timings, injection timings, compression ratio etc), there appears to be a "critical" speed that determines the beginning of fully-developed CAI that is independent from the presence of spark. For the current configuration this speed was found to be 1650 rpm.

At speeds higher than the critical speed, the engine appears to operate without any sign of misfire and have little variation in IMEP values as spark timing advances and the mixture becomes leaner (Figure 5.5 (a) and (b)) even with the spark plug being turned off. When the engine speed drops below 1650 rpm, there appears to be a noticeable difference in the engine's performance and combustion stability. More specifically at 1500 rpm and at 1350 rpm the engine's output varies significantly with lambda and spark timing. The same effect is observed with COV_{IMEP}. The earlier the spark fires, the less stable is the engine operation. COV_{IMEP} increases by up to 70% as spark advance reaches 50°CA. It can be also seen that at 1500 rpm the fluctuation in IMEP and COV_{IMEP} isn't as big as those at of 1350 rpm. It is evident that in order for the engine to reach pure CAI conditions, it has to go through spark-assisted mode as the engine speed increases.

It can be therefore concluded that the existence of spark discharge in the spark-assisted CAI mode can be considered as a necessary means for igniting the cycles that are unable to do so for the reason that residual gases concentration in the cylinder is substantially low thus preventing ignition. High concentrations of exhaust residuals increase the possibility of a CAI cycle igniting by keeping the in-cylinder contents' temperature high enough at the beginning of the compression stroke. The presence of spark can be considered to play an important part in the onset of ignition as soon as the concentration levels of residuals are low. In this configuration lower engine speeds of 1350 rpm (Figure 5.5 (a)), means residual

gases levels of less than 40% in the cylinder aren't enough to ensure ignition under CAI regime and therefore the presence of the spark is considered necessary to ignite the cycle as well as for the engine to run into SI mode. This can be verified by the graphs in Figure 5.5 (b) where below 1650 rpm, the spark timing variation affects the moment combustion should begin within the cylinder. With the engine speed increasing to 1650 rpm, the percentage of residuals in the cylinder reaches 50% and the engine can operate in CAI mode without any further presence of the spark. This means that any variation in the spark ignition timing will have no effect on the onset of ignition.

5.4.4 IVO Timing Effect

Until now in the results demonstrated in this work, the engine was configured for each experiment so that the exhaust valve timing and more specifically the exhaust valve closing event would determine the timing of the inlet valve opening. This meant that the effect of varying the inlet valve opening timing had been not taken into consideration. Therefore it was important to perform a number of tests that would allow the comparison between the influence EVC and IVO timings have on CAI combustion.

EVC was set at -73^{o} CA and SOI at 270^{o} CA BTDC. Initially IVO was set symmetrically to TDC and as soon as data from this setup was collected, IVO was advanced in steps of 5^{o} CA until the value of the absolute difference between IVO and EVC timings was 12^{o} CA. The same procedure was repeated with IVO being retarded. In Figure 5.6 the effect of various inlet valve timing settings on IMEP is shown. On the X-axis the negative values represent advanced compared to 73^{o}CA and positive values the retarded IVO timings respectively.

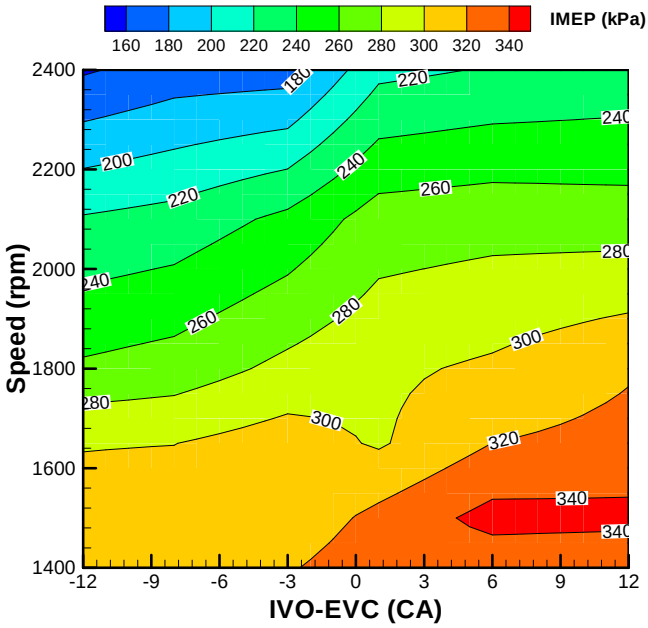

Figure 5.6 Effect of IVO timing on IMEP

(EVC= -73°CA, SOI= 270°CA, λ=1.0, Inlet Valve lift=2mm)

It can be easily perceived from Figure 5.6 that IMEP mainly varies with the engine speed rather with than with IVO timing at stoichiometric operation. There only appears to be a slight increase of IMEP with retarded IVO particularly below the limit of 1600 rpm. However as engine speed increases and the engine enters CAI, especially after 1650 rpm, it can be seen in Figure 5.6 that there is a slight drop in IMEP values for the same engine speed as IVO advances while with retarded IVO no significant change is observed. A possible explanation for this is that less air quantity enters the cylinder because of higher pressure in it than in the intake port at the moment when the intake valve opens.

5.4.5 Coolant temperature effect

One of the parameters that may not directly control CAI combustion but still play an important role towards that direction is the temperature of the means that provides cooling to the engine. Appropriate control of the temperature of the fluid, usually water, that is responsible for taking heat away from the engine, ensures that the required temperature for autoignition is reached. Experiments involving varying coolant temperatures were performed with an EVC set at 85^{o}CA BTDC of the exhaust stroke and SOI 120^{o}CA ATDC of intake stroke. Engine speed ranged from 1200 to 2400 rpm and lambda from

stoichiometric to 1.35. After data has been processed, the plots shown in Figure 5.7 have been drawn and they demonstrate the variation of COV_{IMEP} with engine speed and mixture composition at three different coolant temperatures.

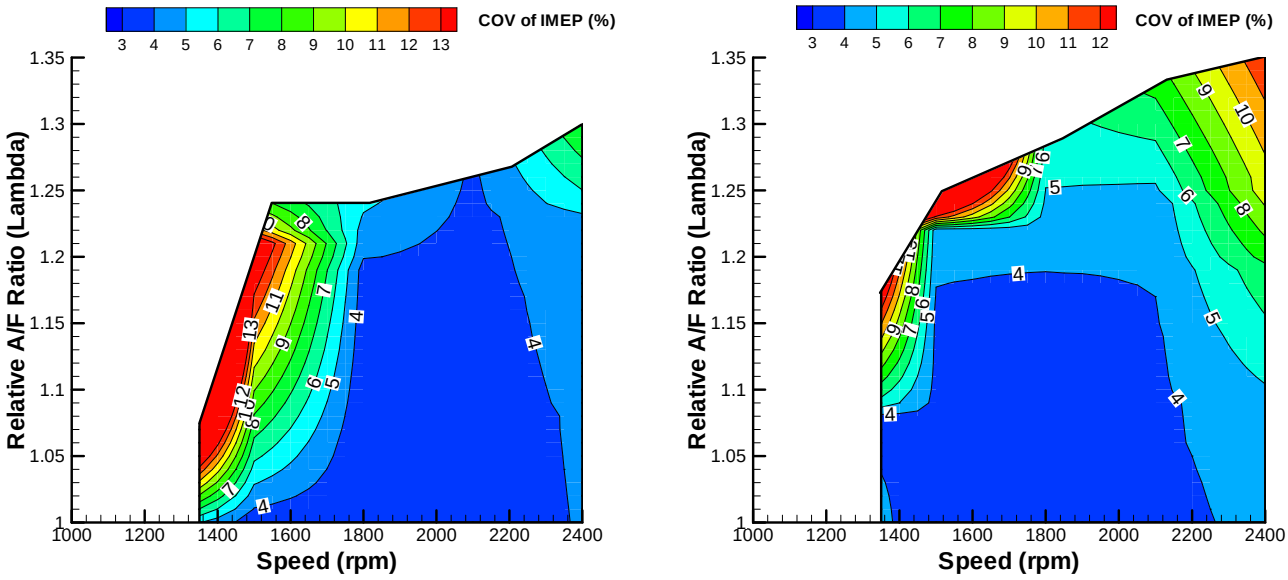

(a) 65°C

(b) 75°C

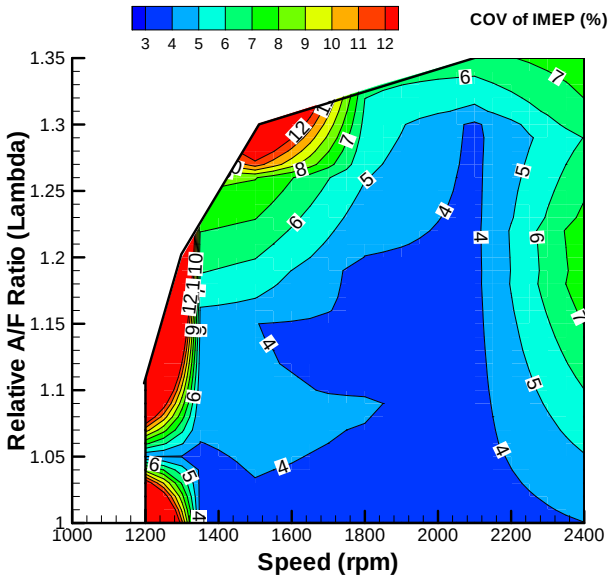

(c) 85°C

Figure 5.7 COV of IMEP at three different coolant temperatures (EVC= -85°CA, IVO=85°CA, SOI=120°CA)

It was found that by increasing coolant temperature, the critical speed to achieve CAI combustion was advanced from 1350rpm, for the coolant temperature of 65°C, to 1200 rpm when the coolant temperature increased up to 85°C. The increase in coolant temperature was also found to extend, the lean limit operation of CAI combustion, especially for the lower engine speed. If 5% of COV of IMEP is considered as the stable CAI combustion limit, the lean limit for CAI combustion increased from 1.25 to 1.31 when coolant temperature is elevated from 65°C to 85°C. Stable CAI combustion can be established as soon as the coolant temperature becomes higher than 75°C. For this study, coolant temperatures were set at 85°C unless otherwise stated.

Increasing coolant temperature will cause combustion phasing to be advanced, maximum heat release rates increase, combustion duration is shortened and peak cylinder pressure during combustion is significantly higher. Therefore changing this temperature directly controls the quality of CAI combustion, meaning that the coolant temperature effect is mainly focused on creating the necessary conditions rather than immediately affecting and controlling the onset of combustion.

5.5 Summary

An overview of the experimental strategies employed during the course of experiments, is given in this chapter. These strategies involved changes in valve and injection timings, changes in compression ratio and coolant media temperatures. This is followed by a detailed description of the testing methodology along with the experimental procedures. After a general description of CAI combustion, a comparison between SI and CAI is presented. Furthermore the effect of spark on CAI operation was studied. Finally the effects of IVO timing and coolant temperature on CAI operation were presented.

Results show the following:

- Comparing SI and CAI combustion at similar engine loads, it was shown that CAI combustion happens earlier, faster and it is more stable and is able to be extend its operation to very lean mixtures. CAI operation is also characterized with less cyclic

variations. However, these fast rates of CAI combustion lead to increased pressure gradients and eventually knock. CO, HC and NOx emissions with CAI combustion are dramatically reduced when compared to SI operation in the particular engine. Thermal and combustion efficiency in CAI combustion increase; in fact thermal efficiency can increase by up to 30% at lean operation. HC, CO and NOx levels are lower in CAI combustion with NOx reaching reduction levels of 75%.

- Spark discharge's effect on CAI combustion is only observed when the engine operates at low speed engine conditions where the spark discharge is required to fire cycles that weren't able to autoignite.

- IVO timing has a minor effect on CAI combustion. In contrast engine speed has a large effect on CAI combustion. At speeds above 1650rpm where fully-developed CAI combustion is present, IMEP values, for earlier IVO timing, tend to slightly decrease mainly due to less air mass inducted as in-cylinder pressure is higher than in the intake port by the time inlet valve opens.

- Coolant water temperatures can contribute to establishing the appropriate thermal regime for CAI initiation. Temperatures above 65^{o}C can help the engine enter CAI combustion at a lower critical speed. At the same time increasing temperatures, extend the lean limit CAI combustion; a 20^{o}C increase of coolant temperature leads to an increase in lambda of up to 0.06.

Chapter 6

CAI Combustion Experiments, Results and Analysis Part II

Chapter 6 CAI Combustion Experiments, Results and Analysis Part II

6.1 Introduction

So far in the previous chapter the effects of parameters such as spark timing, IVO timing and coolant temperature on CAI combustion were described and their importance and the way they can affect CAI was discussed. In this chapter, the other parameters were to be investigated so that a clear opinion can be shaped on how these can create the conditions under which CAI can be initiated and further controlled.

One of the aims of this work was to research on the effect of mixture formation and charge temperature (thermal control) on CAI combustion and therefore attention was given in experimenting on parameters that would influence the temperature and mixture conditions. Consequently it was of great importance to further investigate variables such as injection and EVC timing as well as compression ratio. Injection timing contributes towards the mixture formation whereas EVC timing, compression ratio and valve lift mostly take part in establishing the necessary thermal regime for CAI. This chapter contains the results obtained during experiments with the above mentioned parameters and their effects on CAI are analysed.

6.2 Effect of single injection on CAI operation

6.2.1 Overview

Facing the challenge of controlling the occurrence of auto-ignition was the next step as soon as the method for initiating it was selected. Successful employment of modified camshafts allowed the advanced closure of the exhaust valve thus increasing the amount of trapped exhaust gases which in turn increased the in-cylinder contents' temperature allowing the engine to operate in CAI conditions. However, it is important to control the

moment auto-ignition occurs for the reason that in CAI mode combustion can begin earlier than TDC of compression right after charge temperature exceeds auto-ignition temperature levels.

For the above reasons it is critical to apply a method of controlling the moment auto-ignition should occur under the best way possible so that engine output, combustion stability and efficiency, emissions and even engine noise can reach desired values. Researchers all over the world have proposed numerous methods for solving this issue. One of the proposed methods is controlling mixture quality by optimising the injection timing strategy [75-77] [20]. During this study much attention was given and efforts were focused on establishing a method that would enable accurate control of the auto-ignition timing via the control of the mixture process. Injection timing on a direct injection gasoline engine could be controlled with precision and by this way mixture composition could be adjusted.

Planar laser induced fluorescence (PLIF) measurements have provided with evidence that homogeneous distribution of fuel results from early injection timings while late fuel injection causes major mixture inhomogeneity [78]. Homogeneous mixture assists CAI combustion promotion but at the same time leads to faster heat release rates and great volumes of mixture burn simultaneously therefore increasing combustion noise. On the other hand, mixture stratification caused by late injection could be used to control CAI combustion by means of adjusting air/fuel concentration thus defining the total volume of self-igniting zones.

With the above taken into consideration the experiments were carried out. EVC was set at 85°CA BTDC, IVO at 85°CA ATDC during intake the engine was operated at speed between 1200 and 2400 rpm and lambda was set at λ=1. Higher speeds would cause the engine to operate under knocking conditions and experiments wouldn't have provided with reliable results. As soon as the engine reached the above conditions, fuel injection was turned on and experiments commenced. With the injection event set before the recompression process referred to as 'early SOI' in Figure 6.1 and pressure data were recorded. The next step was to further retard the start of injection (SOI) to a point after the expansion phase of the recompression stroke around 60^{o}CA. This SOI point is shown as

the left border of crank angle region marked 'middle SOI' in Figure 6.1. As soon as measurements were completed this point was shifted in steps of 30°CA up to the point when injection timing took place at 270°CA ATDC shown as the right border of the crank angle region marked 'late SOI'.

It is found that advancing the injection into the region before the early SOI timing window, didn't allow the engine to operate for the reason that fuel escaped through the opening exhaust valve as injection would effectively take place into the exhaust stroke. Another important observation is that fuel injection around the TDC's of intake and compression strokes is also impossible as the cylinder pressure is significantly higher than the injection pressure as it can be seen in Figure 6.1.

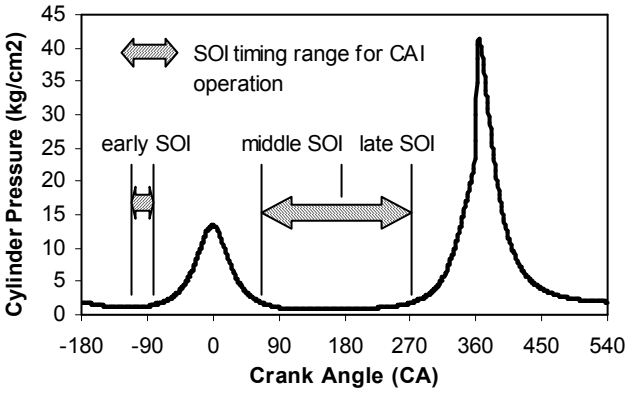

Figure 6.1: Cylinder pressure and injection timing window for CAI combustion (0°CA refers to the TDC of intake stroke)

6.2.2 Results and Analysis

6.2.2.1 Effects of Single Injection on CAI Operation Performance and emissions at λ=1

Previous work carried out by researchers [79], [20] worldwide has pointed out the direct effect of variation in SOI injection on the mixing process via mixture stratification. In particular early injection produced a more homogeneous distribution of air/fuel mixture than late injection, which increased the volume of auto-ignition and hence enhanced CAI combustion [80]. In Figure 6.2 one can notice the significant change in in-cylinder pressure

during variation of SOI timing from advanced to retarded. It is obvious that early, rather than late injection produced a higher charge pressure owing to the larger charge volumes that are able to auto-ignite.

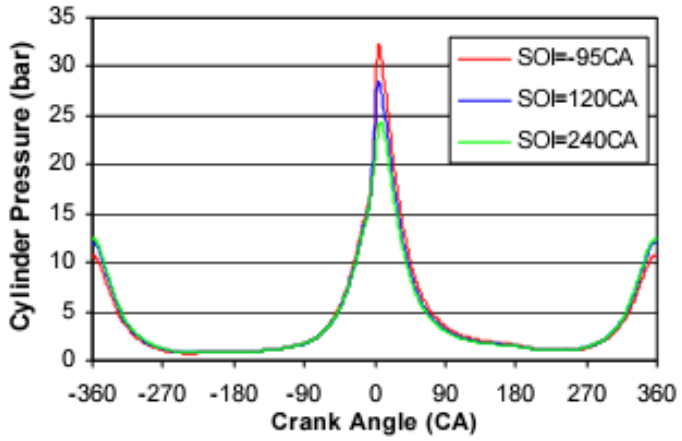

Figure 6.2 Cylinder pressure (1800rpm) recorded with early, middle and late injection timing (0°CA refers to the TDC of compression stroke)

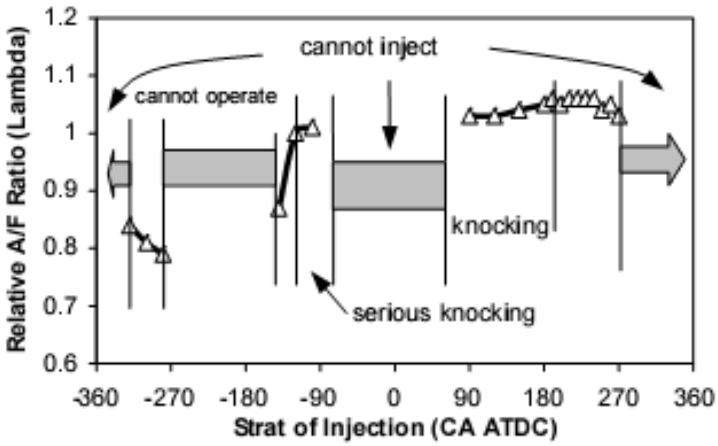

Figure 6.3 Effect of Injection Timing on Engine Operation (EVC 75°CA, IVO 70°CA, 1800rpm, λ=1) (0°CA refers to the TDC of intake stroke)

Furthermore Figure 6.3, shows the effect of injection timing on engine operation at the EVC timing of 75°CA BTDC, the IVO timing of 70°CA ATDC, the engine speed of 1800rpm and exhaust valve lift of 2mm. It is revealed that the injection timing has a very important effect on engine operation and CAI combustion as it can determine its onset, especially with middle (in the intake stroke) and late (in the compression stroke) fuel injection timings. Middle injection can produce very rapid combustion as it forms a homogeneous mixture within the cylinder and there is more time available for pre-flame chemical reactions to take place.

Meanwhile as injection timing is further delayed taking place at 240°CA (120°CA BTDC), CO emissions increase rapidly as it can be observed in Figure 6.4, suggesting that fuel oxidisation is incomplete due to mixture stratification leading to higher CO emission rates. CAI combustion mode, can be achieved when fuel is injected within a narrow crank angle window before EVC (Figure 6.3). However, serious knocking and very large pressure gradient is observed, as shown in Fig.6.5. With the early injection, fuel is injected into hot burned gases. As there is very little oxygen in the stoichiometric burned gases, fuel is subject to heating but with very limited oxidation reactions taking place. However, it has been shown that some form of fuel reforming could take place leading to advanced ignition. [90]

With advanced injection timing during the exhaust or even during the expansion stroke, the engine either is not able to operate or only operates at rather rich mixture conditions due to the escape of fuel through the opened exhaust valves, causing very high uHC emissions as shown in Figure 6.6.

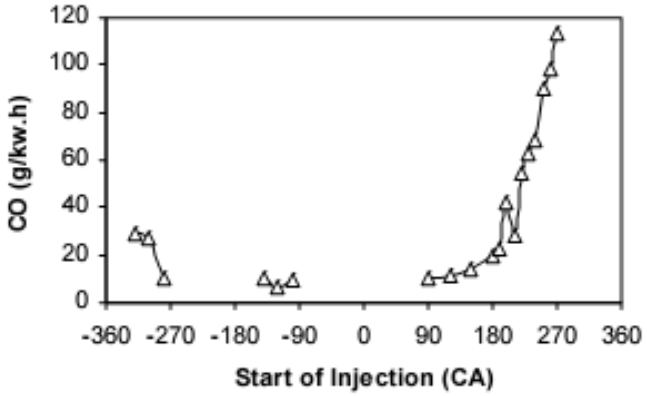

Figure 6.4 CO Emissions versus SOI Timing
(EVC 75°CA, IVO 70°CA, 1800rpm, λ=1.0, Exhaust Valve Lift = 1.96mm, Intake Valve Lift = 2mm)

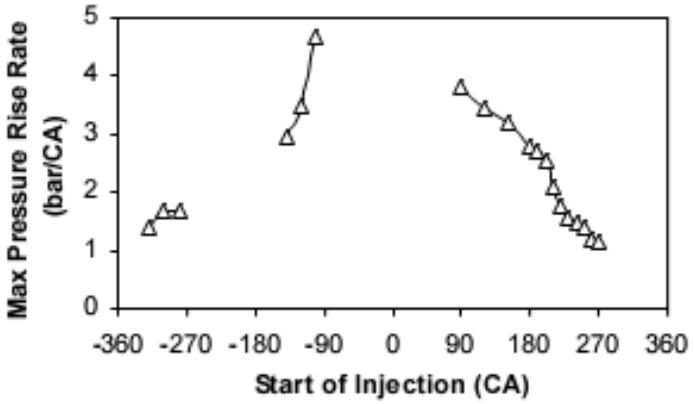

Figure 6.5 Maximum Pressure Gradients versus SOI Timing (EVC 75°CA, IVO 70°CA, 1800rpm, λ=1.0, Exhaust Valve Lift = 1.96mm, Intake Valve Lift = 2mm)

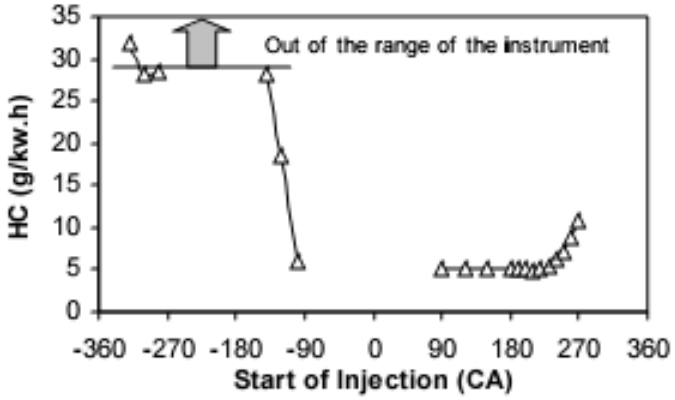

Figure 6.6 HC emissions versus SOI timing (EVC -75°CA, IVO 70°CA, 1800rpm, λ=1.0, Exhaust Valve Lift = 1.96mm, Intake Valve Lift = 2mm)

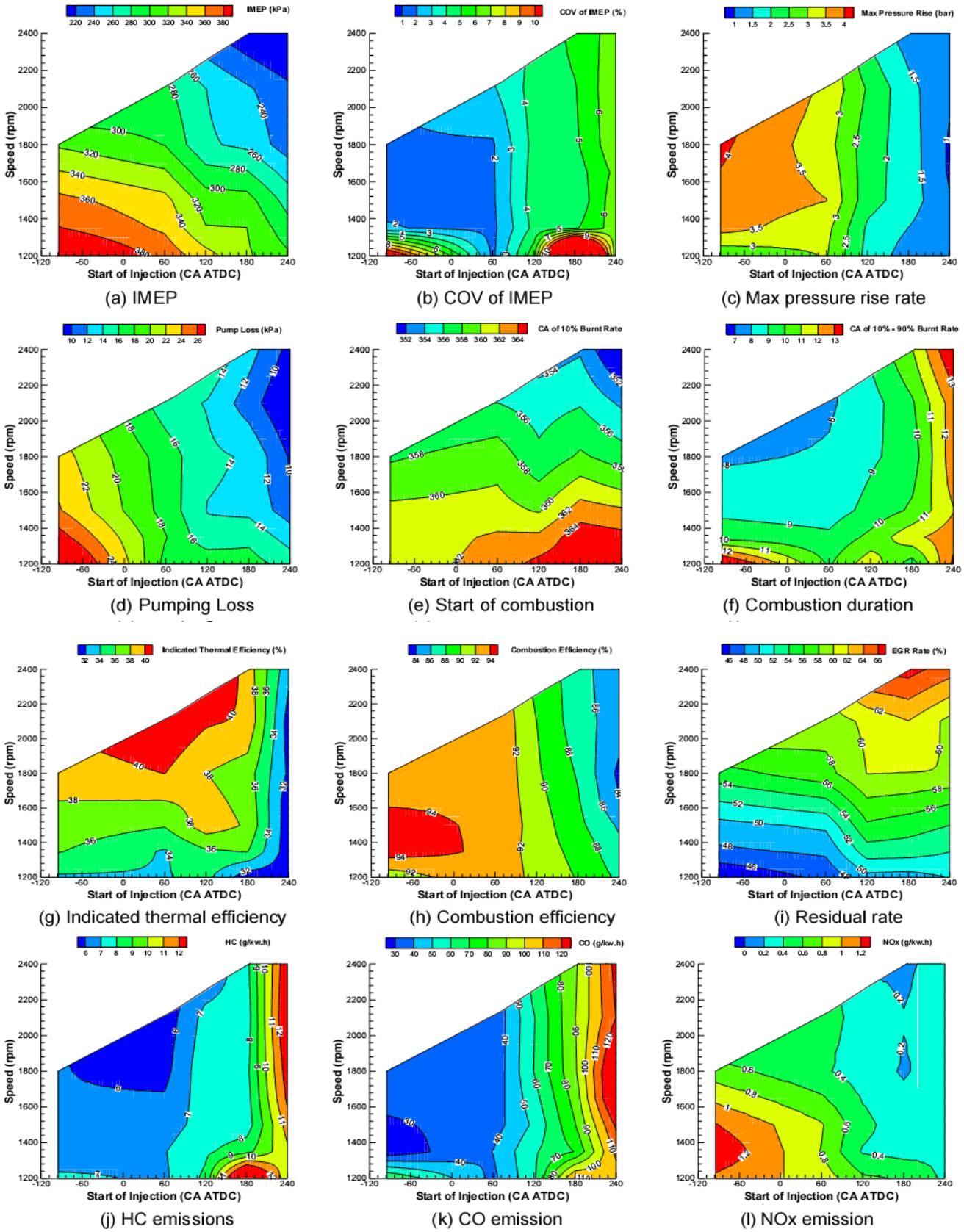

Figure 6.7 Effects of single fuel injection timing on CAI combustion at different engine speeds (EVC= -85°CA, IVO=85°CA, λ=1.0, CR=9:1, Exhaust Valve Lift = 1.96mm, Intake Valve Lift = 2mm)

6.2.2.2 Effect of Injection Timing on CAI Combustion at stoichiometric operation at λ=1

The variation of CAI combustion parameters with injection timing for a certain speed range under stoichiometric operation are illustrated in the plots contained in Figure 6.7.

IMEP – Results from Figure 6.7(a) reveal that engine output decreases as the engine speed increases as more residuals are trapped within the cylinder as shown in Figure 6.7 (i) hence less air and fuel mixture can be burned. Furthermore the engine output becomes lower as injection is retarded. This is caused by the lower combustion efficiency as indicated by the higher CO and HC emissions shown in Figure 6.7 (e) and (f).

COV_{IMEP} – COV_{IMEP} behaves differently from IMEP as it tends to vary with injection timing rather than engine speed as it can be seen in Figure 6.7(b). Advancing the injection timing produces a much more stable combustion while retarding the SOI results in an increase in the combustion variation. However, at speeds lower than 1350 rpm when the engine operates at partial CAI mode, COV_{IMEP} is much more dependant on engine speed change rather than injection timing. At this speed range as it is mentioned in the previous chapter, the engine operates at partial or spark-assisted CAI regime, where the spark discharge is necessary for firing the pressurised mixture and combustion is highly sensitive to the operating conditions like the coolant temperature, the fuel injection as well as the atmospheric temperature and humidity. Consequently combustion becomes very unstable and less repeatable within the aforementioned speed range, resulting in high COV_{IMEP} values and HC and CO emissions as it is explained further down.

Maximum pressure rise rate – At the same time gradient of maximum pressure rise, (Figure 6.7 (c)) varies according to injection timing with early injection timings leading to higher maximum pressure gradient and even cause knocking due to very short combustion duration (Figure 6.7 (f)). A likely explanation for this occurrence is the longer period that a homogeneous mixture has available to reside in the cylinder and provoke oxidisation reactions. If 3 bar/CA is considered as a safe threshold for allowable CAI operation, fuel injection needs to take place within intake and compression stroke.

Pumping Losses – In Figure 6.7 (d), positive pumping losses represent the magnitude of negative work on the piston. Pumping losses appear to vary more with injection timing rather than engine speed and they are minimised as fuel is injected during late injection conditions.

Start of combustion – In Figure 6.7 (e), it can be clearly observed that mixture temperature, rather than mixture composition, determines the onset of combustion. However, combustion takes place earlier when engine speed increases. More specifically, at speed of 2400 rpm combustion begins as early as 7^{o}CA BTDC which happens probably because of the higher charge temperature during compression at higher engine speeds as there would be less heat loss to the coolant and hotter exhaust gas temperature.

Combustion duration – Combustion duration (Figure 6.7 (f)) is overall much shorter in relation to SI combustion. As injection timing is retarded, it increases most likely due to the mixture stratification or/and less time available for the oxidation reaction to take place. At engine speeds lower than 1350 rpm, combustion duration increases because of the spark assisted mode the engine operates in.

Indicated thermal efficiency – The maximum indicated thermal efficiency is over 42% and it is achieved at speeds of over 2200 rpm with early and middle injections, while the minimum of 32% is observed with late injections (Figure 6.7 (g)). It can be seen during injection timing during intake and compression stroke, thermal efficiency is rather determined by injection timing values rather than engine speed while for the rest of injection timings the opposite can be said. In fact as injection takes place during compression stroke, thermal efficiency decreases with retarded injection timing due to mixture stratification.

Combustion efficiency – Combustion efficiency overall varies from 86% to 94% and it's mostly dependent on injection timing rather than engine speed. Late injection produces low combustion efficiencies due to high CO and HC emissions (Figure 6.7 (j) and (k)).

Residual gas rate – Figure 6.7 (i), illustrates that residual gas rates are hardly dependant on injection timing and are mainly affected by changes in engine speeds. In particular residual gas rates increased from 46% to 64% as engine speed increased from 1200 rpm to 2400 rpm as less time is available for the gas exchange process during intake and exhaust strokes.

HC, CO and NOx emissions (Figure 6.7 (j),(k),(l)) – CO and HC emissions appear to considerably increase as injection timing is delayed towards the late stages of compression stroke. The reason for this may be the mixture stratification occurring with late fuel injection. Stratification may result into incomplete combustion because of the presence of fuel rich areas or dense fuel vapour in the cylinder after injection takes place. In addition, it may lead to lower combustion temperatures due to reduced combustion rates and temperatures as well as low peak cylinder pressure (Figure 6.2). Inherently, NOx emissions are reduced as injection timing is delayed; even with early injection they are significantly lower (0.1 g/kWh) than SI combustion.

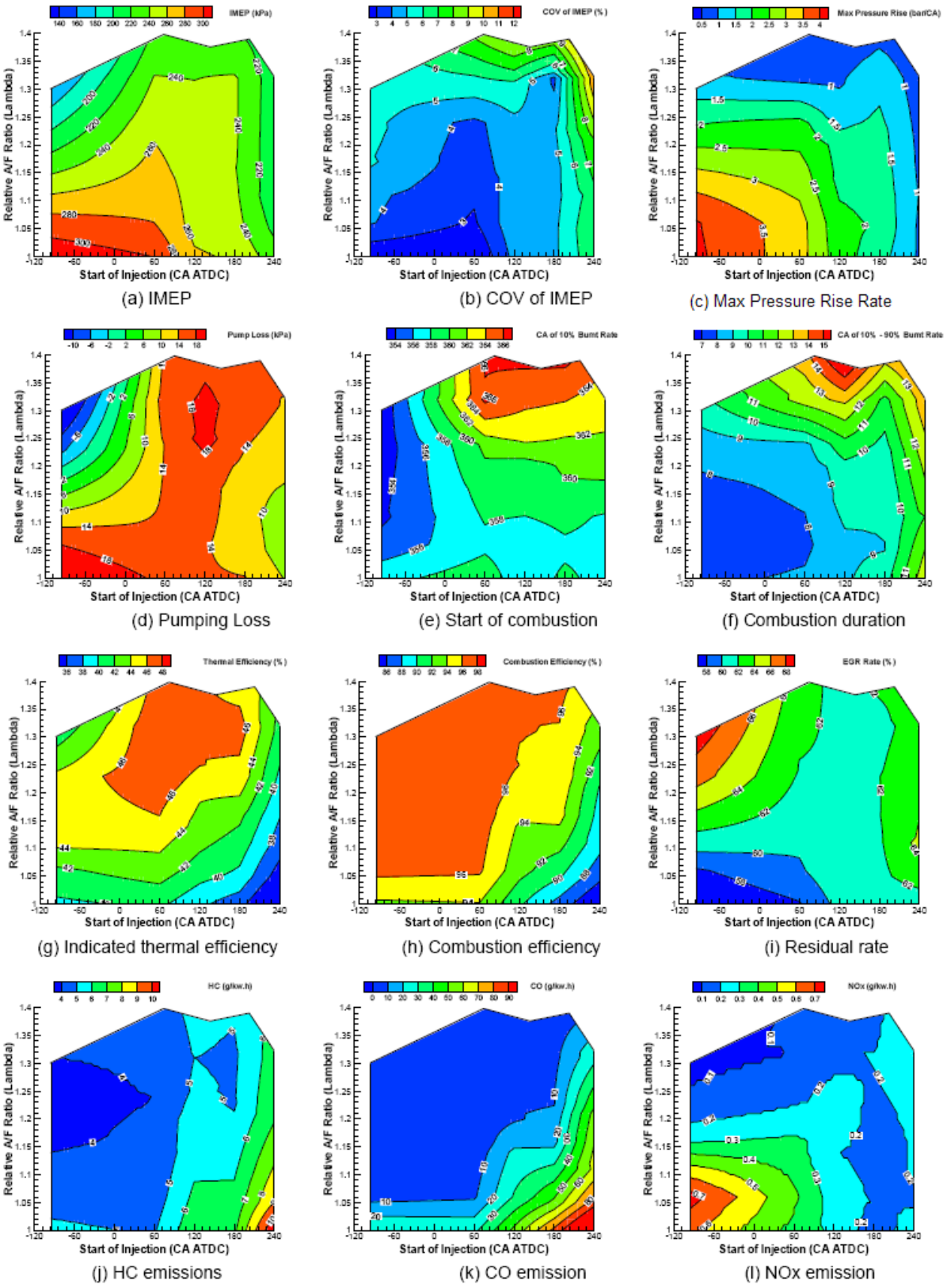

Figure 6.8 Variation of IMEP with injection timing and air/fuel ratio (EVC=-85°CA, IVO=85°CA n=1800rpm, CR=9:1, Exhaust Valve Lift = 1.96mm, Intake Valve Lift = 2mm)

6.2.2.3 Effect of Injection Timing on CAI Combustion at Various A/F Ratios

Figure 6.8 shows the effect of injection timing on CAI engine's performance and emissions at different air/fuel ratios under the same EVC timing and engine speed of 1800 rpm. In the graph the top boundary is determined by the air/fuel ratio where the engine misfires and it clearly varies according to the injection timing. With advanced injection timing this limit is reached sooner than when injection takes places during the intake and compression stroke.

IMEP – From Figure 6.8 (a) it can clearly be extracted that when fuel is injected before the recompression stroke, the engine output ranges from 320 kPa for λ=1 to 160 kPa for the leanest limit as expected. However, with injection after the end of the recompression phase IMEP hardly changes for the entire feasible lambda range. This maybe explained by the indicated thermal efficiency results in Figure 6.8 (g). As it shows, the engine efficiency increases with leaner mixtures and this effect is most obvious for the middle injections. Therefore, the decreasing fuelling is compensated by the higher engine efficiency as the mixture becomes leaner. Hence, the near constant engine output seen in Figure 6.8 (a).

COV_{IMEP} – Combustion variation seems to vary along with fuel concentration variations as well as injection timing (Figure 6.8 (b)). A closer look reveals a similarity to that of IMEP shown in Figure 6.8 (a). As injection occurs during recompression and lambda is less than 1.3, COV_{IMEP} values are rather low. On the contrary as the mixture becomes leaner and injection timing is retarded further into the compression stroke, variation in IMEP appears to increase mainly because of the mixture stratification present in the cylinder. If 10% of COV_{IMEP} can be considered as a safe index of acceptable combustion variation, then it can be stated that stable combustion is feasible over a wide load and injection timing area; this area offers lambda from stoichiometric up to 1.4 and injection timings ranging from early until 240^{o}CA during compression stroke.

Maximum pressure rise rate – As shown in Figure 6.8 (c) maximum pressure rise rates are attained with λ=1 with early fuel injection. As the mixture becomes leaner and injection timing is retarded towards the compresssion stroke, an overall decrease in the

pressure gradients is observed. Again if a 3bar/CA limit is imposed, injection timing should be positioned between intake and compression stroke. Otherwise a mixture leaner than 1.15, has to be used if injection is advanced towards the recompression process.

Pumping Losses - In Figure 6.8 (d) there appears to be an area where the highest amount of pump losses occurs regardless of the mixture composition. At the same time, within the lean mixture and early injection area, (top left corner), negative pumping losses values are observed (positive work output). This occurrence is mentioned in work published by numerous researchers ([20], [76], [85], [90]) and were attributed to the cooling effect of the injected liquid fuel evaporation or the heat release associated with minor combustion during fuel injection that can probably cause higher re-expansion than recompression pressure. Fuel reformation can take place as the fuel is compressed and mixed with the hot residuals during the recompression process. The fuel injected before or at the beginning of the re-compression process can mix with O_2 contained in the hot trapped exhaust gases from lean burn mixtures and cause minor combustion limited by the applicable O_2 which can result in higher pressure values during the re-expansion process than in the recompression process. Figure 6.9 illustrates a logP versus cylinder volume V diagram for two different A/F ratios and it can be clearly observed that the recompression pressure values are always higher than re-expansion pressure for the λ=1.0 case. In this case there is hardly any heat release reaction as little O2 is present in the stoichiometric burned mixtures. The heat loss from the residual gases and fuel evaporation during re-expansion causes the re-expansion pressure/temperature to be reduced from those that would otherwise be obtained. However, with λ=1.3 the pressure trace is crossed during the re-compression and re-expansion processes, demonstrating that the pressure in re-expansion process is higher than that in the re-compression process.

Figure 6.10 illustrates the variation of oxygen concentration in exhaust gases with the A/F ratio during early injection timing. It can be noted that oxygen concentration in the residuals increases with the mixture become leaner. When lambda becomes 1.3, oxygen concentration reaches 4.9%; a value that allows better possibilities for the fuel to partly oxidise and inherently increase re-expansion pressure as heat is released during the oxidisation. In Figure 6.11, the heat release rates for three different A/F ratios are illustrated and it can be observed that heat release rates emerge around TDC of intake as

the mixture becoming leaner. These results have confirmed that the negative pumping losses (or positive pumping work) occurrence during the recompression process is linked to the minor combustion taking place with lean mixtures.

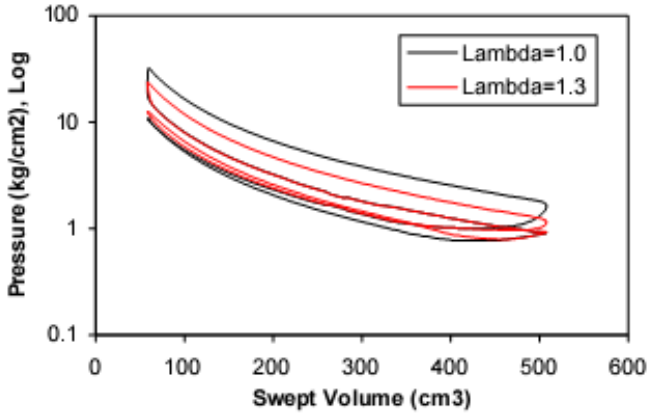

Figure 6.9 Log P versus cylinder Volume for two different lambda values (EVC=-85°CA, 1800rpm, SOI= -95°CA)

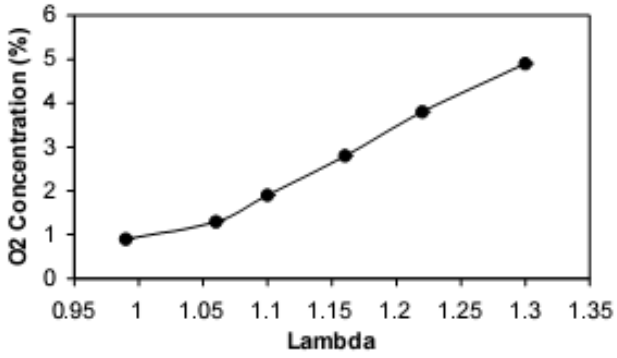

Figure 6.10 Oxygen concentrations in exhaust gases versus (EVC=85°CA BTDC, n=1800rpm, SOI= -95°CA)

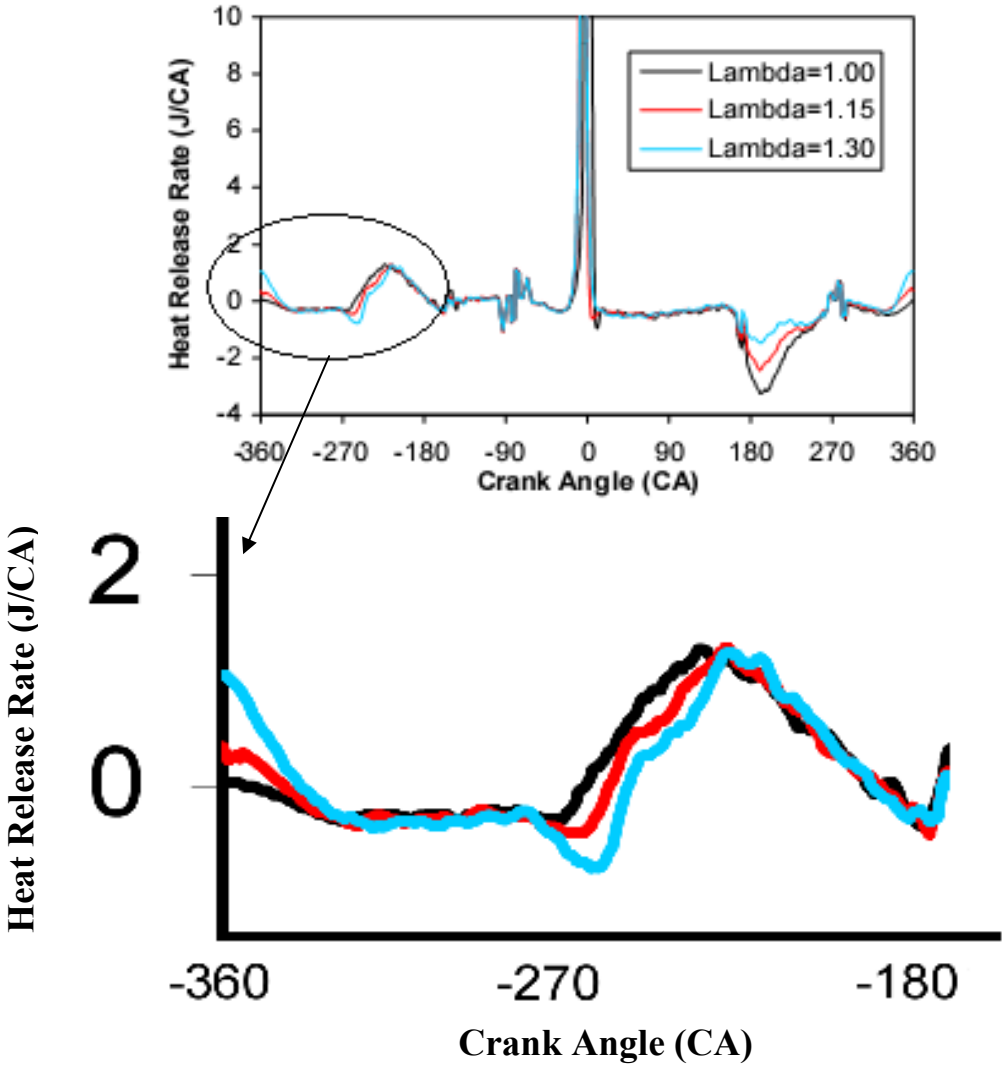

Figure 6.11 Comparison of the heat release rate profiles for stoichiometric and lean operation (EVC=85°CA BTDC, n=1800rpm, SOI= -95°CA)

Start of combustion – Figure 6.8 (e) provides with useful conclusion about the role of injection timing on the initiation of CAI combustion. Start of combustion seems to vary more with the timing fuel is injected in the cylinder rather than with A/F ratio. Inherently, early injection causes autoignition to occur as early as 354°CA. However, as injection timing is further retarded towards the intake and compression stroke, start of combustion seems to be regulated more by the mixture composition rather than the fuel injection probably because of the strong stratification throughout the cylinder.

Combustion duration – Burn duration contour lines in Figure 6.8 (f) tend to follow changes with both injection timing and mixture composition. Early injection and

stoichiometric mixture results in the fastest burn duration observed. As the mixture becomes leaner (up to λ=1.3) and injection timing is shifted towards the compression stroke, burn duration varies little between 8°CA to 10°CA. The slowest combustion is observed with the leanest and most retarded injection.

Indicated thermal efficiency – Like combustion duration, indicated thermal efficiency tends to be more dependant on the lambda than with injection timing (Figure 6.8 (g)). Maximum efficiency is observed as mixture is leaner and injection takes place during intake stroke. As the mixture approaches λ=1 or the fuel injection takes place earlier, combustion starts too early resulting in lower efficiency. On the other hand the reduced engine efficiency with retarded injection is caused by the lower combustion efficiency as CO and HC emissions are higher. It should be underlined at this point that the indicated thermal efficiency shown here is higher than expected because of the accuracy of the fuel consumption which was estimated to be low as the amount of fuel injected was controlled by the width of an electric pulse which was in turn calibrated with the fuel flow rate (See Appendix A).

Combustion efficiency – The plot shown in Figure 6.8 (h) illustrates the similarity and dependency relating CO emissions shown in Figure 6.8 (k) and combustion efficiency. Both injection timing variation and lambda swinging can affect the combustion efficiency. In particular, retarding the injection timing and keeping close to stoichiometric composition tends to reduce combustion efficiency and inevitably higher CO emissions. With injection ranging between early and middle timings and most of lambda values, combustion efficiency can be kept at percentages higher than 94%.

Residual gas rate (EGR) – A mixed effect is caused by injection timing and A/F ratio on the concentration of exhaust gases trapped into the cylinder. At early injection timings, leaner mixtures tend to increase the amount of exhaust gases trapped into the cylinder probably because of the lowered gas burned temperatures. In general, injection timing doesn't have an important overall effect on EGR rates present in the cylinder.

HC, CO and NOx emissions – Carbon related emissions (Figure 6.8 (j) and (k)), are closely related to the moment the fuel is injected in the cylinder rather than the mixture composition. HC and CO emission tend to increase with injection timing retarded towards the compression stroke injection. NOx emission levels are linked to changes in both parameters involved in the plots and with an overall rate lower than 0.3 g/kWh and a tend for reduction as mixture becomes leaner and injection timing is retarded, due to increased dilution and lower combustion temperature.

The same results shown in Figure 6.8 can also be presented as functions of injection timing and engine load so that the variation in CAI combustion characteristics can be linked to the engine's load points, as illustrated in Figure 6.12. The following observations are noted:

i. Early injection during negative valve overlap period allows wide range of CAI operations due to fuel reforming and minor heat release particularly to lower IMEP values (Figure 6.12 (a)).
ii. The rate of pressure rise increases with the load as the mixture becomes less diluted (Figure 6.12 (b)).
iii. Start of combustion occurs earlier and combustion process becomes faster as load increases due to higher exhaust temperatures (Figure 6.12 (c)).
iv. Pumping losses varies from negative (positive work output) to positive (negative work output) (Figure 6.12 (f)), as the load increases due to increased heat losses from the recompressed residual gases as their temperature becomes higher. And more importantly, the heat release due to minor combustion during the negative valve overlap period is reduced as the mixture approaches stoichiometry.
v. As expected NOx emissions increases with load (Figure 6.12 (g)) as the residual gases concentration decreases (Figure 6.12 (e)). The higher CO and HC at highest load conditions may be associated with the lower residual rate resulting into less CO and HC being burned in the subsequent cycle.

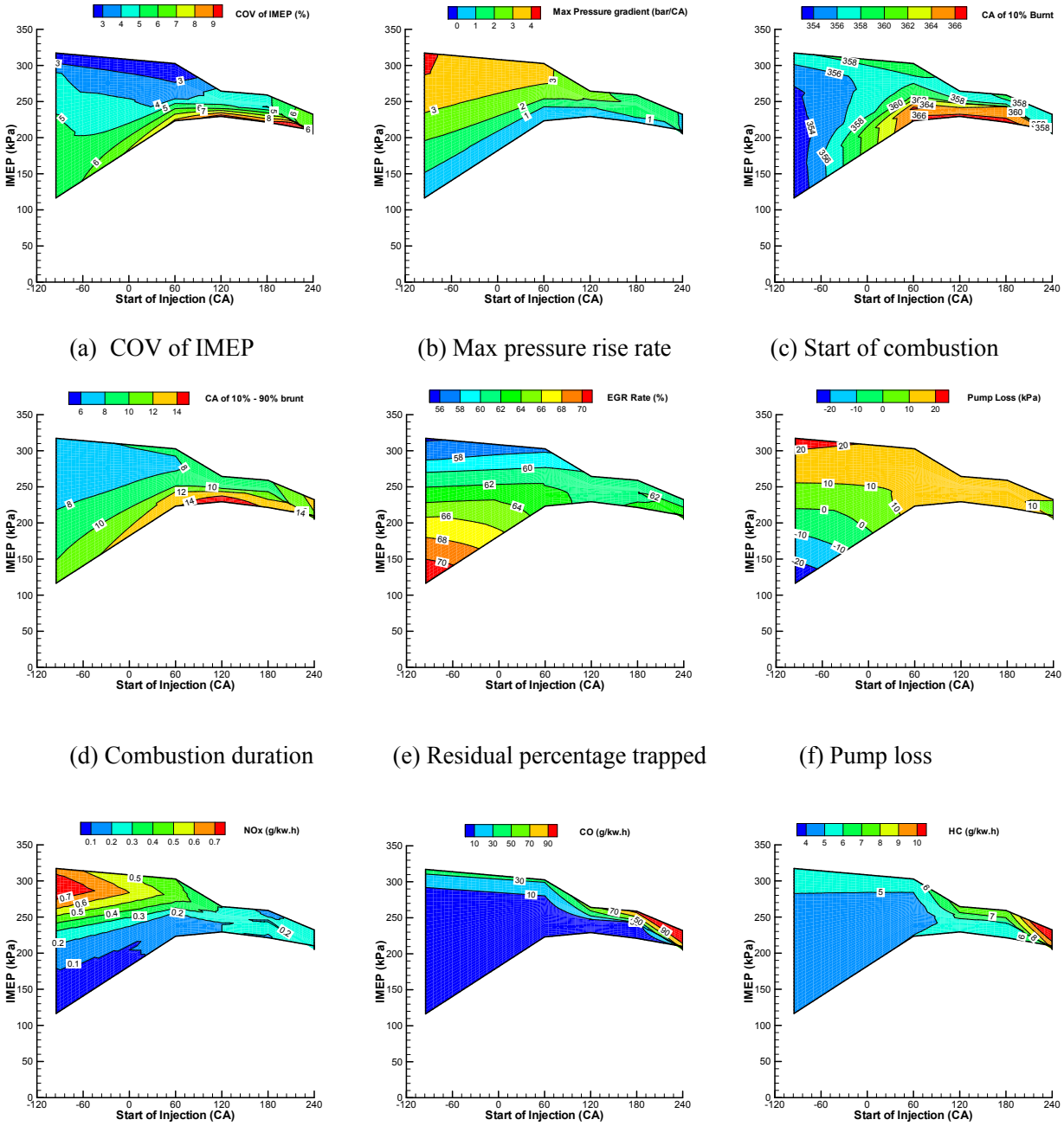

(a) COV of IMEP (b) Max pressure rise rate (c) Start of combustion

(d) Combustion duration (e) Residual percentage trapped (f) Pump loss

(g) NOx (h) CO (i) HC

Figure 6.12 Variation of combustion and emission parameters with IMEP and injection timing (EVC=-85°CA, IVO=85°CA, n=1800rpm, CR=9:1)

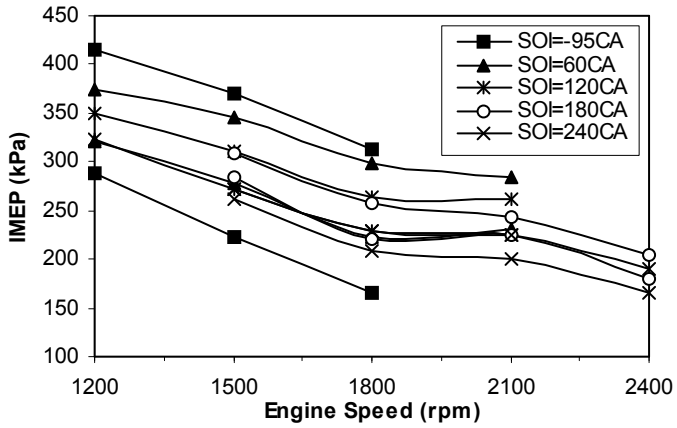

Figure 6.13 Effect of injection timing on CAI operation range at different engine speeds (EVC= -85°CA, IVO=85°CA, CR=9:1)

Figure 6.13 presents the effect injection timing has on CAI operation range at different engine speeds and loads. It can be observed that at engine speeds of 1200 rpm, stable CAI combustion can be obtained for the early (-95ºCA) and middle (60ºCA and 120ºCA) injection timings. As fuel is injected after the BDC of the intake stroke (180ºCA and 240ºCA), the minimum engine speed required for CAI operation is shifted to 1500 rpm. It can be therefore assumed that CAI operation range deteriorates as fuel injected during the intake and compression stroke. Injection before rather than after TDC of the intake, produces a wider range of CAI operation. Therefore in order to take advantage of benefits of each injection timing demonstrated above, a strategy had to be introduced that would allow fuel to be injected twice within the same cycle. These two injection effect would have to be timed as followed. The first injection should be set to occur early i.e during the recompression stroke allowing the increase of the CAI range and the second one during the compression stroke that would minimise the engine's tendency for knocking.

6.3 Effect of split injection on CAI operation

6.3.1 Overview

The sets of experiments involving two injections were performed on the same single-cylinder engine. The only parameter changed was the compression ratio which was increased from 9:1 to 11:1. This would consequently increase the risk of knocking combustion at stoichiometric operation. Furthermore IMEP levels were also expected to increase for the same EVC compared to lower compression ratio configuration. It should be underlined here that in order to directly compare and better evaluate the effect of double and single injection on CAI combustion, single injection experiments were performed chronologically after the double injection tests; the engine was configured at compression ratio of 11:1, the camshafts used had exhaust valve lift of 1.96mm and duration of 100^{o}CA and intake valve lift of 2mm and duration 110^{o}CA. The rest of the parameters were kept the same.

A necessary modification to the fuelling system was the addition of another injection control device that would allow the independent control of two rather than one injection pulse at two different timings. This setup provides the engine with a split injection of equal fuel amounts injected at various timings that can be set independently from each other. Unfortunately the existing hardware didn't allow adjustments in the fuel quantity metered in each injector before the pulse allows the fuel to be injected. Therefore while with single injection experiments a fixed amount of fuel would be injected with a single pulse, this quantity with double injection configuration was equally split into two and then injected into the cylinder. The first injection occurred before the recompression stage and during the intake stroke (referred to as early with single injection) whereas the second one ranged between 60^{o}CA and 270^{o}CA (referred to as middle and late injection with single injection).

6.3.2 Results and Analysis

In figure 6.14 the effect of double injection IMEP can be seen. The engine was operated at stoichiometric conditions; speed was kept at 1500 rpm and EVC varied from -95^{o}CA to -75^{o}CA in steps of 10^{o}CA. These were indicated as 95CA and 75CA in the graph. Single injection tests are referred to as SI in the graphs while double injection as DI.

A first look in Figure 6.14 (a) leads to a very important conclusion. Split injections can provide with higher IMEP values than single injections at the same EVC timing for every injection timing selected for both SI and DI. This is a clear indication that split injection can effectively extend the CAI operation range towards higher load values. Additionally first injection plays a more important role on increasing IMEP levels than the second one in DI configuration, while for SI retarding the injection timing tends to reduce IMEP values. It should be noted here that early first injection produces higher IMEP values at the same valve timings.

Not only does double injection offer increased IMEP range but it is also characterised by a lower cycle-to-cycle variation than single injection as shown in Figure 6.14 (b). Even at very late second injection timings, double injection provides lower COV_{IMEP} than single injection regardless of the EVC timing and thus the exhaust gas concentration in the mixture. As injection timing is retarded the increase in COV_{IMEP} is much more significant with single injection than double injection. For the same load, it is noted that the introduction of split injection (green triangle marked lines), leads to less steep pressure rise than the single injection case (colorless square and diamond marked lines). However, the rate of pressure rise does increase with higher engine output obtained from the split injection.

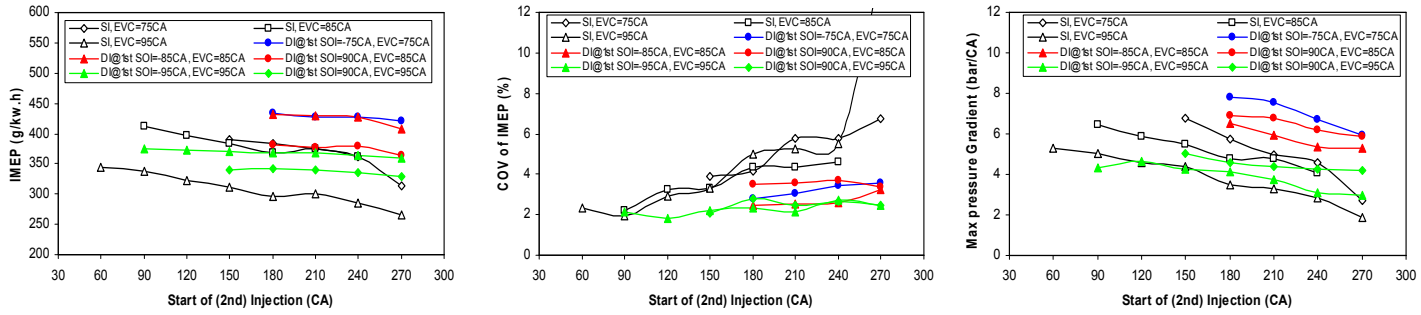

(a) IMEP (b) COV of IMEP (c) Max pressure rise rate

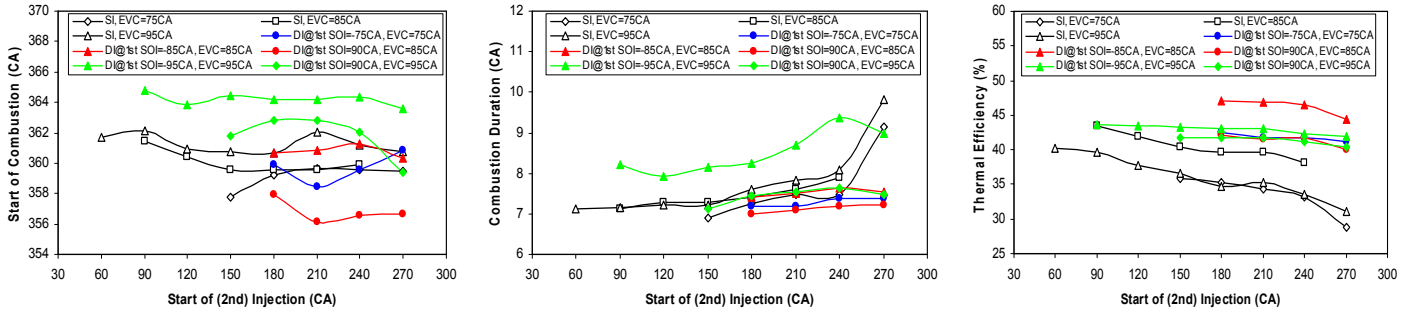

(d) Start of combustion (e) Combustion duration (f) Indicated thermal efficiency

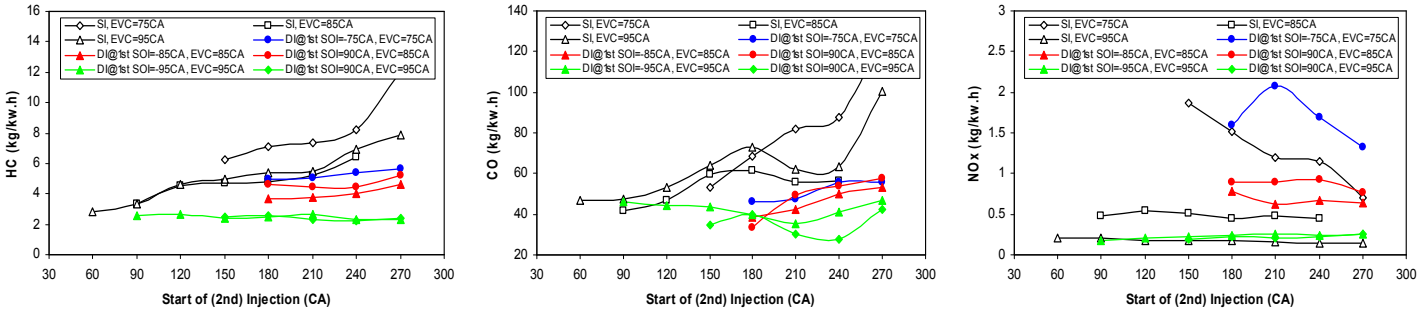

(g) HC emissions (h) CO emissions (i) NOx emissions

Figure 6.14 Combustion and emissions for single and double injections at different injection and EVC timings (1500rpm, λ=1, CR=11:1)

At EVC= -95^{o}CA double injection (green symbols) retards the start of combustion. However, with double injection at EVC -75^{o}CA, start of combustion doesn't seem to vary significantly with either injection regime. With EVC set at -85^{o}CA, start of combustion with double injection conditions is more dependant on the first injection. Compared to single injection configuration when the first of the two injections was retarded (-85^{o}CA) start of combustion is delayed whereas when the first injection advances (-90^{o}CA), start of combustion takes place earlier.

As soon as combustion commences, its duration for double injection configuration appears to be shorter than with single injection (Figure 6.14 (e)) especially for the late second injection timing. It should be noted here though that with EVC set at -95^{o}CA and advanced first injection at -95^{o}CA, combustion duration tends to last longer compared to single injection due to the delayed start of combustion.

Another significant advantage of double injection is the higher engine efficiency shown in Figure 6.14 (f). This is mainly caused by the improved combustion efficiency as indicated by lower HC and CO emissions shown in Figure 6.14 (g) and (h).

Emissions levels are shown in Figure 6.14 (g), (h) and (i). It can be stated that double injection allows reduction of both CO and HC levels compared to single injection regardless of the timing of the second injection and the EVC timings. One possible reason is that the second injection may allow more complete combustion to take place when this part of the fuel is less diluted by residuals and they are more concentrated in the air.

Furthermore NOx emissions are reduced with single injection at similar load points compared to double injection due to retarded combustion.

Following experiments conducted at λ=1, comprehensive experiments were then carried out to identify the range of CAI operation by varying the valve timings and

air/fuel ratio. The results are shown in Figure 6.15. For EVC of -75°CA and single injection tests, CAI was only achievable with injection after 180°CA due to the presence of knocking combustion with earlier injection. As far as double injection tests are concerned, first injection was coincided with EVC timing whereas the second one occurred at 240°CA during compression stroke.

A first view at the graphs shows a significantly wider range of IMEP with double injection compared to single injection conditions. However, this increase in IMEP values attainable is closely related to the change in EVC timing. With EVC -75°CA and -85°CA split injection regime enlarges IMEP operation range for both stoichiometric and lean conditions as opposed to -95°CA where a noticeable but not important increase of IMEP compared to single injection occurs between λ=1 and lean limit operation. In Figure 6.16, the operation ranges for CAI combustion with single and double injections are presented, which shows clearly the enlarged CAI operation range by the double injection, particularly the lower IMEP that could be achieved.

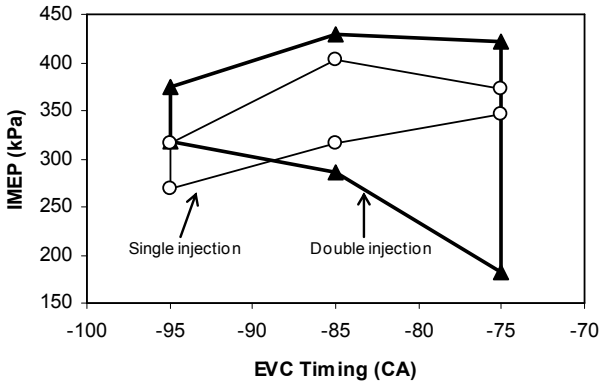

Figure 6.15 CAI operation range for single and double injection (1500rpm, CR=11:1)

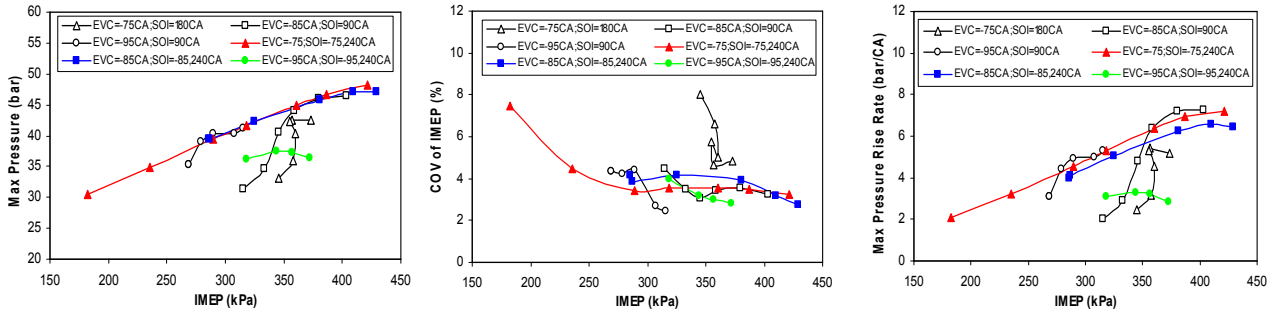

(a) Max pressure (b) COV of IMEP (c) Max pressure gradient

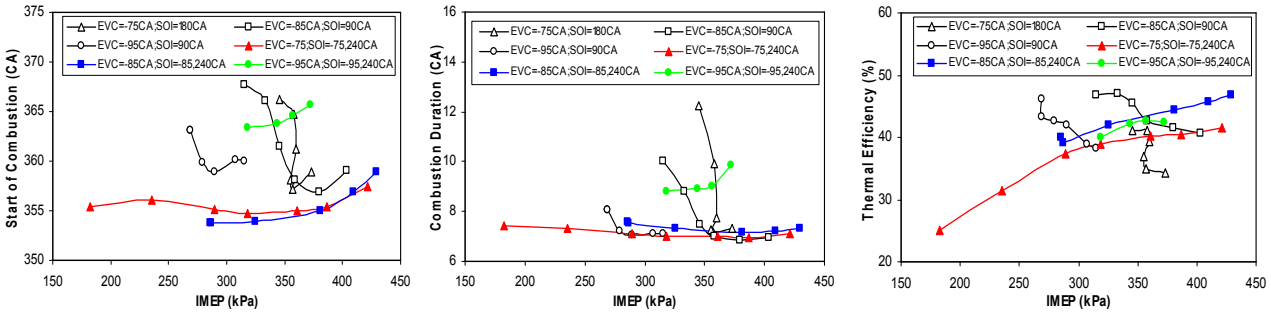

(d) Start of combustion (e) Combustion duration (f) Indicated thermal efficiency

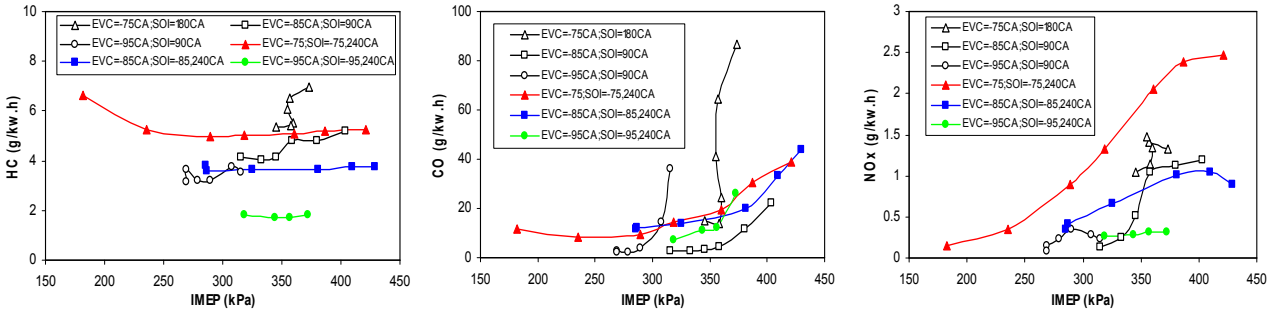

(g) HC emission (h) CO emission (i) NOx emission

Figure 6.16 Combustion and emissions for single and double injections at different EVC and injection timings (1500rpm, CR=11:1)

Other combustion characteristics such as maximum in-cylinder pressure, COV_{IMEP}, maximum pressure rise rate, start of combustion, combustion duration and indicated thermal efficiency are presented in figure 6.16 ((a)-(f)). Maximum pressure area appears similar between single and double injection for most of the load range and EVC timing. At the same time COV_{IMEP} (Figure 6.16 (b)) appears to increase as the first of the double injections takes place comparatively late (-75^{o}CA) during lean operation. However, under the same load conditions, double injections lead to lower COV_{IMEP} compared to single injection strategy.

A closer look at graphs (a) and (c) in Figure 6.16, reveals the similar trend between the maximum in cylinder pressure and inherently its rise rate curve for every EVC timing and the entire load range feasible with double and single injection. At higher load conditions the pressure rise rate reaches 6.0 bar/dCA. Figures 6.16 (d) and (e) help to explain the enlarged CAI operation with split injection. They show that combustion is brought forward and shortened with the presence of double injection so that leaner mixture and hence lower load CAI operation could be obtained.

Looking closer on graph (f) in Figure 6.16, it can be noted that there's a difference in the variation of indicated thermal efficiency when it comes to single and double injection. Under single injection conditions, thermal efficiency tends to increase with the decreasing engine load. This essentially means that the mixture becomes leaner while the opposite occurs as double injection is effective. This may be attributed to the fact that combustion under double injection regime takes place very early (5^{o}CA BTDC as shown in Figure 6.16 (d)) and combustion duration is still too short at low IMEP operation (7^{o}CA as shown in Figure 6.16 (e)). The aforementioned start of combustion and the combustion duration, clearly suggest that the biggest percentage of combustion is completed before the piston reaches TDC hence producing negative work on the piston.

Split injection rather than single injection, for the same EVC timing, tends to reduce HC and CO emissions towards higher IMEP conditions. NOx on the other hand

appear increased for split injection compared to single injection with EVC set at -75^{o} CA due to early combustion.

Particular attention should be paid to the results obtained from EVC timing of -95^{o}CA on every graph shown in Figure 6.16 for both injection strategies employed where a slight difference can be observed when compared with the other two EVC timings presented. This difference can be better seen in graphs (b), (c), (d) and (e) of Figure 6.16 where for both injection strategies there appears to be a larger difference between the values obtained at EVC -95^{o}CA when compared to EVC -85^{o}CA and -75^{o}CA. A likely explanation for this phenomenon is the actual EVC it takes place; more specifically at EVC -95^{o}CA the exhaust valve closes near the limit of valve timings that allow the engine to operate in CAI mode. At this EVC, the auto-ignition process and hence CAI combustion is very sensitive to the local thermal and flow conditions in the cylinder as well as to the ambient conditions the engine tests are taking place, therefore the injection strategy has a larger effect.

6.4 Effect of EVC timing on CAI operation

6.4.1 Overview

One of the basic principles of this study was to establish a methodology that would allow an engine to operate in CAI conditions on the one hand and on the other how to control these conditions to yield maximum benefits. The main method chosen was that of trapping hot residuals into the cylinder thus increasing the charge temperature causing the fuel to reach auto-ignition temperature levels before TDC. Earlier closure of the exhaust valve as expected would trap bigger amounts of exhaust gases and vice versa. It was therefore of paramount importance to study the effect the timing of the exhaust valve closing event had on CAI combustion characteristics and emissions.

6.4.2 Results and Analysis

Tests were performed with the engine having a compression ratio of 9:1 and start of injection was set at BDC of the intake stroke. The camshafts used for this set of experiments had Exhaust Valve Lift=1.96mm and duration 100^{o}CA and Intake Valve Lift=2mm and duration of 110^{o}CA. Meanwhile IVO was symmetric to the start of the intake for every EVC the engine was operated. The effect of EVC timing on CAI combustion at the engine speed of 1800rpm and the SOI at BDC are illustrated in Figure 6.17. In addition, the effect of EVC timing on CAI combustion at different engine speed and λ=1.0 are illustrated in Figure 6.18.

First it is noticed that fully-established CAI combustion takes place when the EVC timing ranged between -63^{o}CA and -92^{o}CA. Within this valve timing range the engine operation is stable and the mixture doesn't fail to auto-ignite even when the spark plug was turned off. As soon as the exhaust valve closed earlier than -92^{o}CA, engine operation is rather unstable and failed to reach auto-ignition due to too much residual trapped in the cylinder (Figure 6.17 (d)). In addition, when the exhaust valve timing is retarded after -63^{o}CA, the engine operates into a combined SI and CAI mode i.e partial CAI mode with increased levels of combustion variation, expressed via COV_{IMEP}, (Figure 6.17 (b)).

Engine output is controlled mainly by the timing the exhaust valve closed as illustrated at Figure 6.17 (a). If graph (a) is compared with the results shown in the graph in Figure 6.17 (d), the close relationship between the engine output and the amount of trapped exhaust gases is apparent. Hence, the engine output can be adjusted by advancing or retarding the EVC timing that would eventually determine the proportion of residuals in the mixture. What is surprising is the constant IMEP values at different lambda values. One would expect the IMEP to drop as less fuel is burned. However, as shown in Figure 6.8 (g), at each EVC timing the engine's efficiency increases with leaner mixture, due to lower CO emissions, lower pumping work and

less advanced combustion. Therefore, greater work is produced by less fuel with leaner mixture.

It should be further underlined that with the EVC timing ranging between -70°CA and -92°CA, the amount of residuals is adequate to allow a stable CAI combustion even for the mixture becoming lean reaching values of up to 1.38. Within this operational range, COV_{IMEP} values are very low (Figure 6.17 (b)) and combustion duration i.e the crank angle between 10% and 50% fuel burnt rate, is very short leading to a very stable combustion regime that is hardly affected by the mixture strength variation. On the other hand, start of combustion (Figure 6.17 (e)) varies not only with mixture strength but with EVC. Combustion starts comparatively early with the most advanced EVC and near stoichiometric mixture. Meanwhile the highest maximum pressure gradients (Figure 6.17 (c)) and peak pressure cylinder share a similar contour plot. Both of them happen only in a small area around EVC of 70°CA and λ=1.0, where the quantity of residuals is the appropriate one to obtain stable CAI combustion.

Meanwhile emissions demonstrate two types of variation; HC and NOx appear to be much more dependant on the changes of EVC/load (Figure 6.17 (g) and (i)), while CO emissions vary more with mixture composition (Figure 6.17 (h)). With the first two types of emissions, advanced EVC timing and leaner conditions are beneficial to reducing their levels. More specifically HC emissions are reduced by up to 75% and NOx by up to 10 times with advanced EVC (-92^{o}CA) and leaner mixture. CO on the other hand is found to be minimal when lambda reaches above 1.22 for EVC -92^{o}CA and 1.27 for EVC of -75^{o}CA. Those results indicate that HC and CO emissions are of different origin. It seems that increased CO levels are most likely caused by the presence of fuel rich pockets while increased rates of unburned HC emissions are probably a result of late and slower combustion.

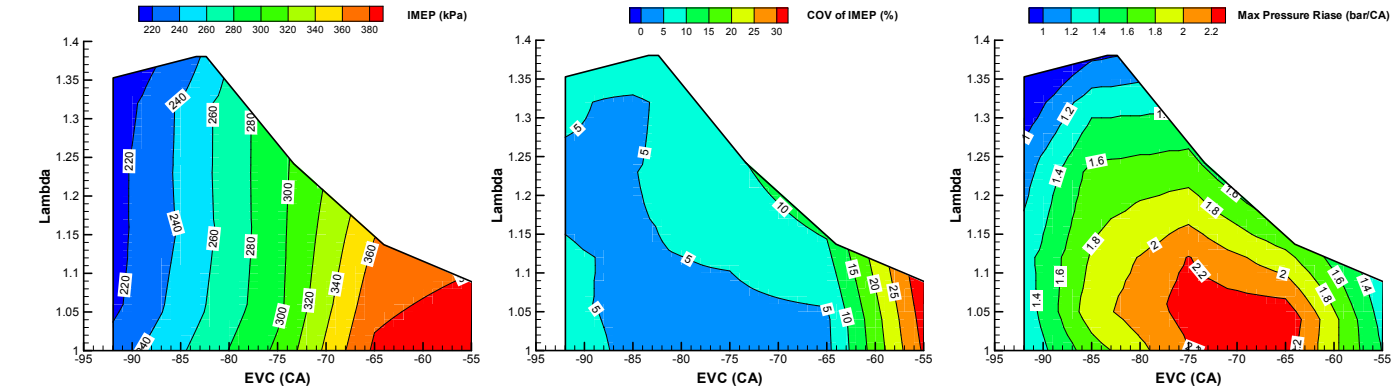

(a) IMEP (b) COV of IMEP (c) Max pressure gradient

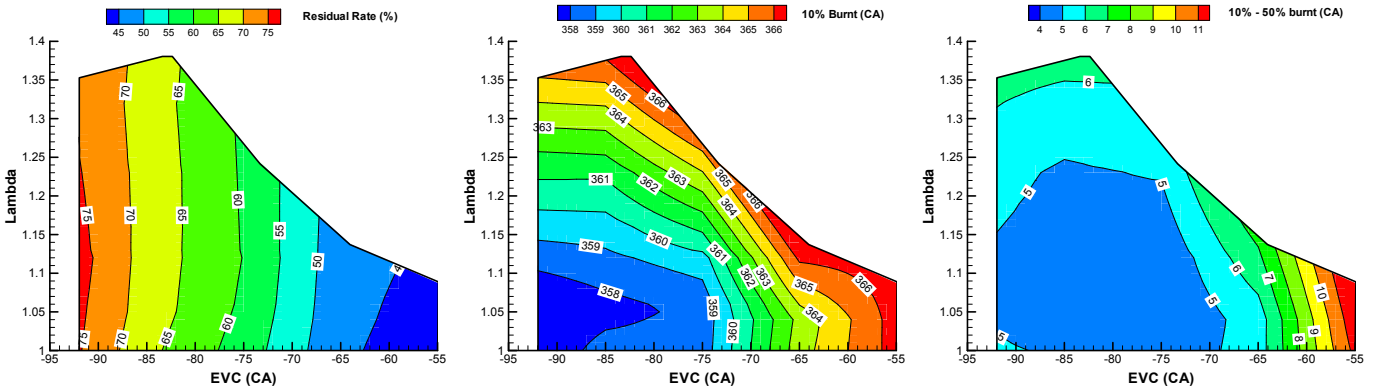

(d) Residual percentage (e) Crank angle of combustion start (f) Fast combustion period

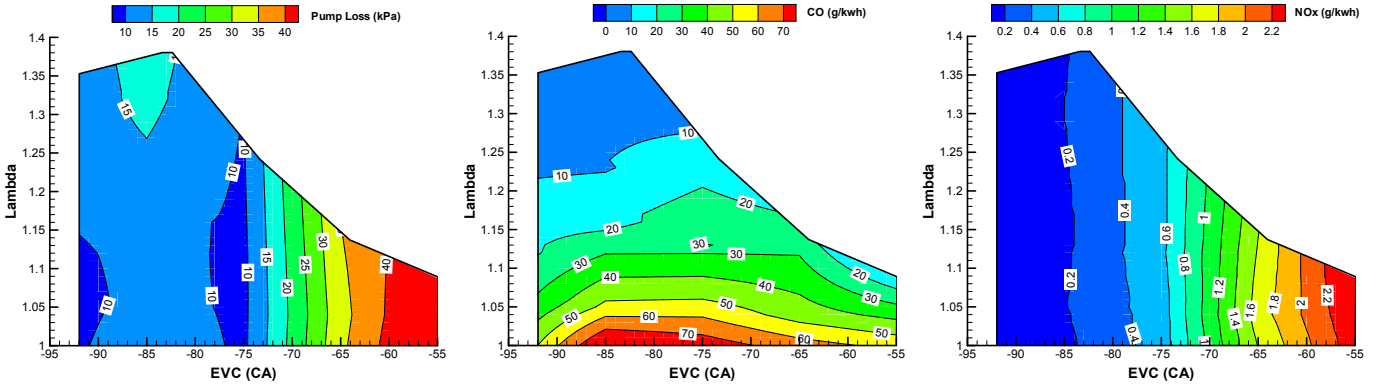

(g) HC emission (h) CO emission (i) NOx emission

Figure 6.17 Effects of EVC timing on CAI combustion (n=1800rpm, SOI=180°CA, CR=9)

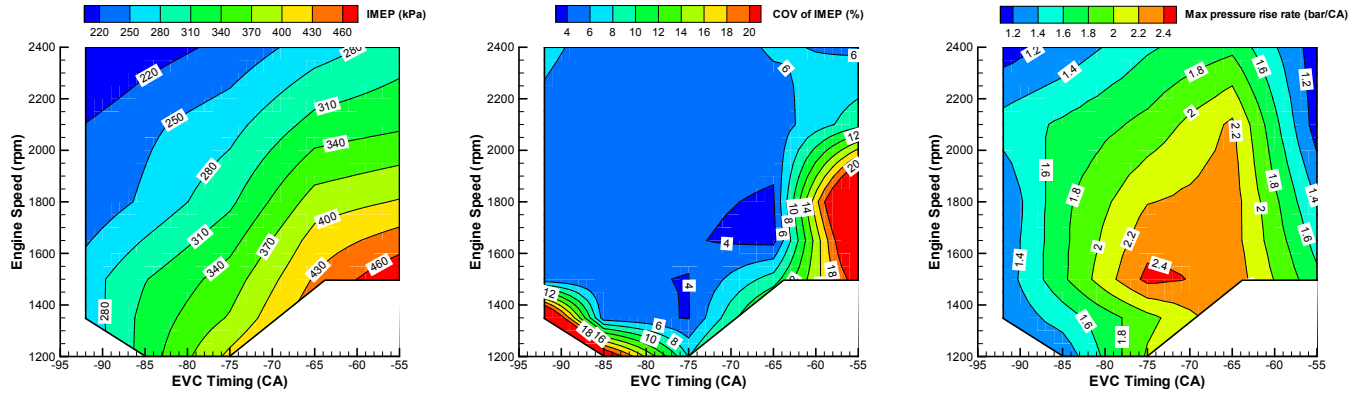

(a) IMEP (b) COV of IMEP (c) Max pressure gradient

Figure 6.18 Effects of EVC timing on CAI combustion (λ=1.0, SOI=180°CA, CR=9)

Furthermore in Figure 6.18 it is noted that CAI could be achieved between -55^{o}CA and -90^{o}CA above 1500rpm. It wasn't possible to operate the engine below 1500rpm when EVC was retarded beyond -70^{o}CA due to insufficient amount of trapped residuals. Very early EVC timing (-92^{o}CA), engine operation was also unstable featuring large COV_{IMEP} values (Figure 6.18 (b)) at speeds below 1350 rpm due to too much burned gases trapped in the cylinder. The EVC timing window and engine speed range where exhaust residuals allowed low cyclic variation CAI combustion to be achieved, is limited and it is found to vary between EVC -92^{o}CA to -70^{o}CA and speed from 1500 rpm to 2400 rpm. Within this region the point around 1800 rpm and EVC -75^{o}CA is found to feature maximum pressure rise rate whereas around this point the distribution pressure rise rates appear to distribute evenly varying mostly with EVC timing rather than with engine speed.

6.5 Effect of Compression Ratio (CR) on CAI operation

6.5.1 Overview

One of the useful capabilities of the engine used in this study was the ability to change CR rather easily. As mentioned already in Chapter 4, a 3mm thick steel plate was positioned between the cylinder block and the crank case that allowed the clearance volume to be adjusted. With the steel plate in place, the engine's CR was found to be 9:1 and without it 11:1. This advantage allowed further experiments that would provide with better insight on the effects CR may have on CAI combustion along with a consistent and immediate comparison of results obtained with both configurations. A main drawback, however, of elevated CR, is the eventual increased tendency for knocking that eventually led to employing only late injection strategies. Any other injection timing than late, is found to be harmful to the engine as the high levels of knocking emerged during every speed the engine is operated at, is a major risk to the engine's parts and consequently injection timing had to be retarded from BDC, used during lower CR of 9:1 tests, to 240^{o} CA to minimise the knocking effect.

6.5.2 Results and Analysis

As with EVC timing effect tests, engine speed varied from 1200 rpm to 2400 rpm and similarly lambda swung between stoichiometric and the leanest limit possible. Exhaust and Intake Valve Lifts were 1.96mm and 2mm respectively. Valve duration for Exhaust and Intake cams were 100^{o}CA and 110^{o}CA respectively. At the same time IVO was kept, just like with every other test, symmetrical to the EVC with respect to the TDC of the intake. Results obtained with CR of 11:1, are illustrated in Figures 6.19 where EVC timing varies versus lambda and 6.20 where EVC timing varies with engine speed. These two figures are directly comparable to Figures 6.17 and 6.18 that correspond to the equivalent results obtained with CR of 9:1.

Results shown in Figures 6.17 and Figure 6.19 demonstrate that the EVC range where CAI combustion is made possible is narrower with higher CR i.e maximum IMEP is lower and minimum IMEP is higher. With CR of 9:1 the earliest EVC (-92^{o}CA) where CAI combustion is attainable, shifted at -85^{o}CA when CR became 11:1. It appears that the same amount of residuals trapped with EVC at -92^{o}CA at lower CR, isn't adequate enough to initiate CAI combustion with higher CR. However, when smaller amounts of residuals are trapped in the cylinder with EVC -85^{o}CA, stable CAI combustion is present. Such difference may be related to the drop in the burned gas temperature with higher CR. As a result less dilution is needed to increase burned gas temperature to achieve CAI combustion.

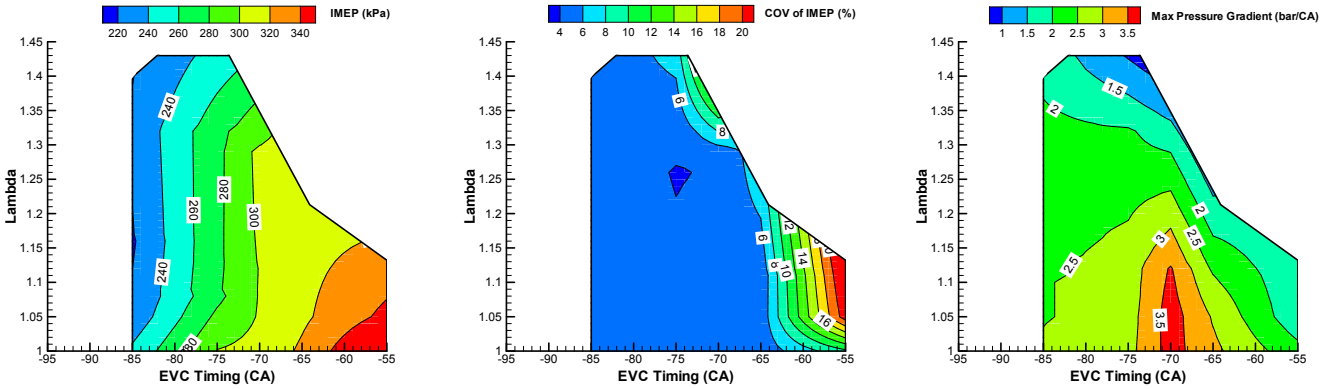

(a) IMEP (b) COV of IMEP (c) Max pressure gradient

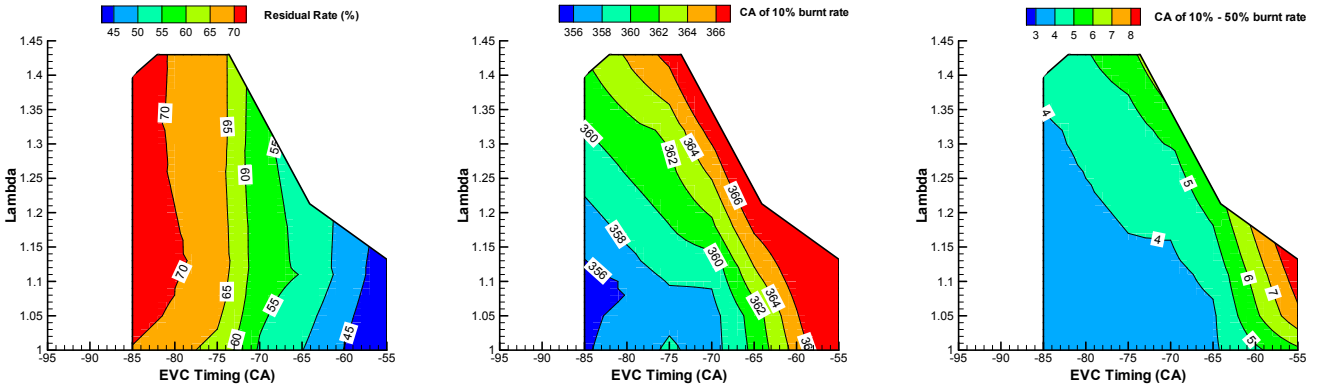

(d) Residual percentage (e) Start of combustion (f) Fast combustion period

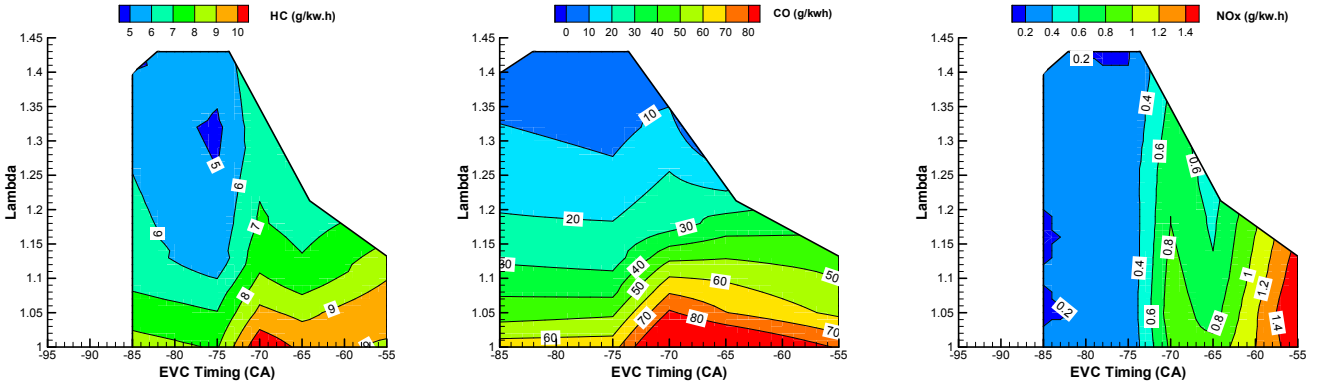

(g) HC emission (h) CO emission (i) NOx emission

Figure 6.19 Effects of EVC timing on CAI combustion (n=1800rpm, SOI=240°CA, CR=11)

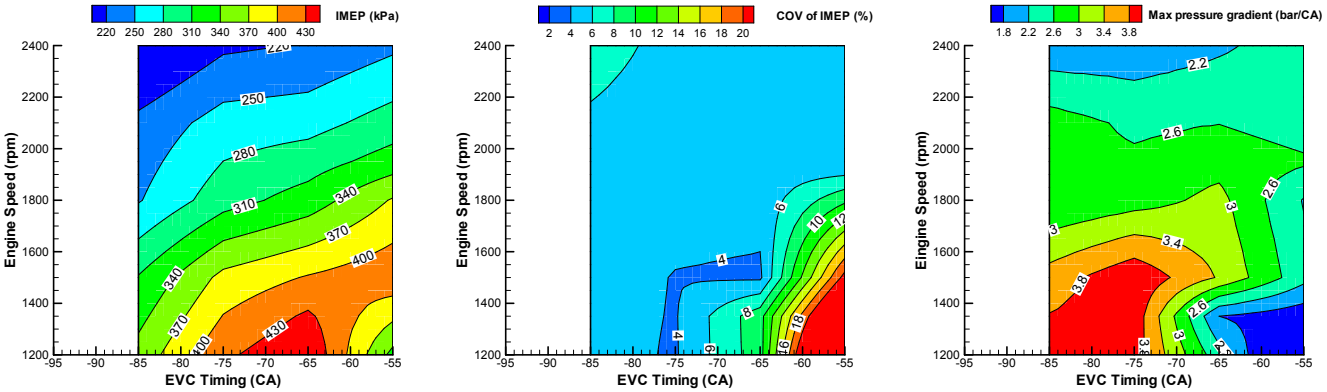

(a) IMEP (b) COV of IMEP (c) Max pressure gradient

Figure 6.20 Effects of EVC timing on CAI combustion (λ=1.0, SOI=240°CA, CR=11:1)

Similar lower CR results, IMEP with higher CR as shown in Figure 6.19 (a) tends to vary mostly with EVC timing rather than mixture concentration. The range of IMEP with higher CR is smaller mainly because of the retarded injection timing. Even though maximum pressure gradient still increased by 1bar/CA (Figure 6.19 (c)).

Furthermore a noticeable extension of the leanest limit the engine can operate at is observed with increased CR. More specifically the vertical axis representing lambda values in Figure 6.19 the maximum value attainable is extended by 0.1 when compared to lower compression ratio results and the leanest limit the engine could operate at (Figure 6.18). Even though it would be expected for IMEP to diminish as the mixture becomes leaner, it however remains constant throughout the different lambda values. Figure 6.8 shows that at EVC timing, lean mixture conditions cause increased engine efficiency due to lower CO emissions, lower pumping work and less advanced combustion. As a result, greater work is produced with reduced fuelling and bigger lambda values. Furthermore higher CR applied in these set of experiments, allows the engine to operate at even leaner conditions. Figure 6.19 (b) shows that combustion variation is kept at similar levels for most EVC timings and mixture concentrations to those in Figure 6.17.

Another effect increased compression ratio has on CAI combustion, is the earlier crank angle of 10% MFB took place during increased CR. In particular as shown in Figure 6.19 (e), the crank angle of 10% MFB is advanced by up to 2^{o}CA when compared to Figure 6.17 (e) that corresponds to CR of 9:1 for each EVC timing applied. Simultaneously, the first half of combustion as expressed by the crank angle of 10% - 50% MFB is also reduced by 1^{o}CA for higher CR (Figure 6.19 (f)). It should be underlined that the start of combustion as well as combustion duration is mostly dependant on EVC timing variation rather than on lambda swinging.

As far as emission levels are concerned, it can generally be concluded that HC levels seem to benefit from increased CR. More specifically HC emissions (Figure 6.19 (g)) are reduced by up to 50% compared to lower CR. A possible explanation for this occurrence may be on the one hand the fact that with increased compression ratio

combustion is more complete as more HC molecules are burned and therefore less unburned are measured at the exhaust pipe. In addition it is noted that HC emission variation shows a similar pattern to CO and it decreases with leaner mixture. Both HC and CO are therefore a result of rich fuel pockets that could have been formed with late injection.

A comparison between Figures 6.20 (a) and 6.18 (a) reveals that CAI combustion is feasible from engine speeds as low as 1200 rpm when CR increases due to the increased charge temperatures. IMEP variation remains similar between the two different CR settings However, with increased CR and the same EVC timing and engine speed, IMEP is higher than the equivalent operating point with CR 9:1. Figure 6.20 (b) also demonstrates the capability of increased CR to stabilise combustion i.e smaller COV_{IMEP} at earlier EVC timings when compared to lower CR. At later EVC settings higher CR appears to also improve combustion stability. This increased stability exhibited with higher CR throughout the engine speed range may be attributed to the better thermal regime installed when the engine mixture is compressed to a higher extent thus increasing the conditions for the fuel to reach auto-ignition conditions. However, the benefits of increased IMEP and lower COV_{IMEP} values came with the penalty of increased maximum pressure gradient even with early EVC and lower speeds, where burned gas and hence temperature is highest. The minimum value in the high CR range is almost equal to the maximum pressure gradient rate with CR of 9:1 (Figure 6.18 (c), 6.20 (c)).

6.6 Effect of Valve Lift and Cam Duration on CAI operation

6.6.1 Overview

As it is already mentioned in Chapter 4, in order to change the combustion regime from SI to CAI two different sets of CAI camshafts were employed in order to evaluate the effect of longer cams duration and higher valve lift on CAI combustion. Details as shown in Figure 4.1, illustrate the different properties of each camshaft

used as a means of trapping exhaust gas residuals and thus increasing the potential of the engine to operate under CAI conditions.

6.6.2 Results and Analysis

Data were taken at compression ratio of 11:1 with late injection timing of 240^{o}CA so that the results presented below in Figures 6.21 and 6.22 were directly comparable to the ones exhibited in Figure 6.19 and 6.20. The latter were obtained during experiments with engine operating on short valve lift and short duration camshafts.

A first approach to the results in Figure 6.21 reveals what is expected with the change of camshafts. Longer exhaust valve timings result in smaller amounts of exhaust gases trapped (Figure 6.19 (d)) hence the narrower EVC timing range is feasible. It can be seen that CAI is made possible when EVC lied in between -85^{o}CA and -60^{o}CA. As soon as it is attempted to operate the engine at the latest EVC of -55^{o}CA where the engine could operate during shorter duration camshafts configuration, CAI combustion couldn't be realised due to less amount of exhaust gases residuals available at the beginning of the cycle to initiate it. On the other hand the engine couldn't enter SI mode either because there are increased amounts of exhaust gases in the cylinder at the time of ignition that wouldn't allow spark discharge to lead into combustion.

At the same time the prolonged opening of the inlet valve lead to more fresh air entering the cylinder allowing the engine to operate at even leaner mixture with lambda reaching up to 1.45. This increase in air mass flow also resulted in higher IMEP values especially with EVC ranging from -75^{o}CA to -60^{o}CA (Figure 6.19 (a)) when compared to the same EVC range when lower valve lift camshafts were employed (Figure 6.21 (a)). Throughout the CAI operational range the cyclic variation is very low as shown in Figure 6.21 (b). However, the penalty for this improvement is the significant increase of the maximum pressure rise rate for each lambda (Figure 6.19 (c)) in relation with lower valve lift results (Figure 6.21 (c)).

An explanation for the aforementioned conditions may be found in the contents of Figures 6.21 (e) and (f) where combustion commences earlier by 2^{o}CA when compared to lower valve lift results (Figure 6.19 (e)). This is caused by the higher burned gas temperature of higher load operation with higher valve lifts. As a result it also leads to the shorter interval between 10% and 50% of mass fraction burnt as shown in Figure 6.21 (f).

Inherently NOx emissions are considerably increased (Figure 6.21 (i)) due to increased work output at the same EVC. NOx emissions varied according to the amount of trapped residuals in the cylinder as previous results. On the other hand there appears to be an increase in the HC emissions (Figure 6.21 (g)) probably due to more rich pockets formed from earlier fuelling. HC emissions vary with both EVC and lambda values rather than EVC timing solely as with the low lift cams. The presence of more fuel rich pockets can also explain why slightly higher CO is also noticed (Figure 6.21 (h)).

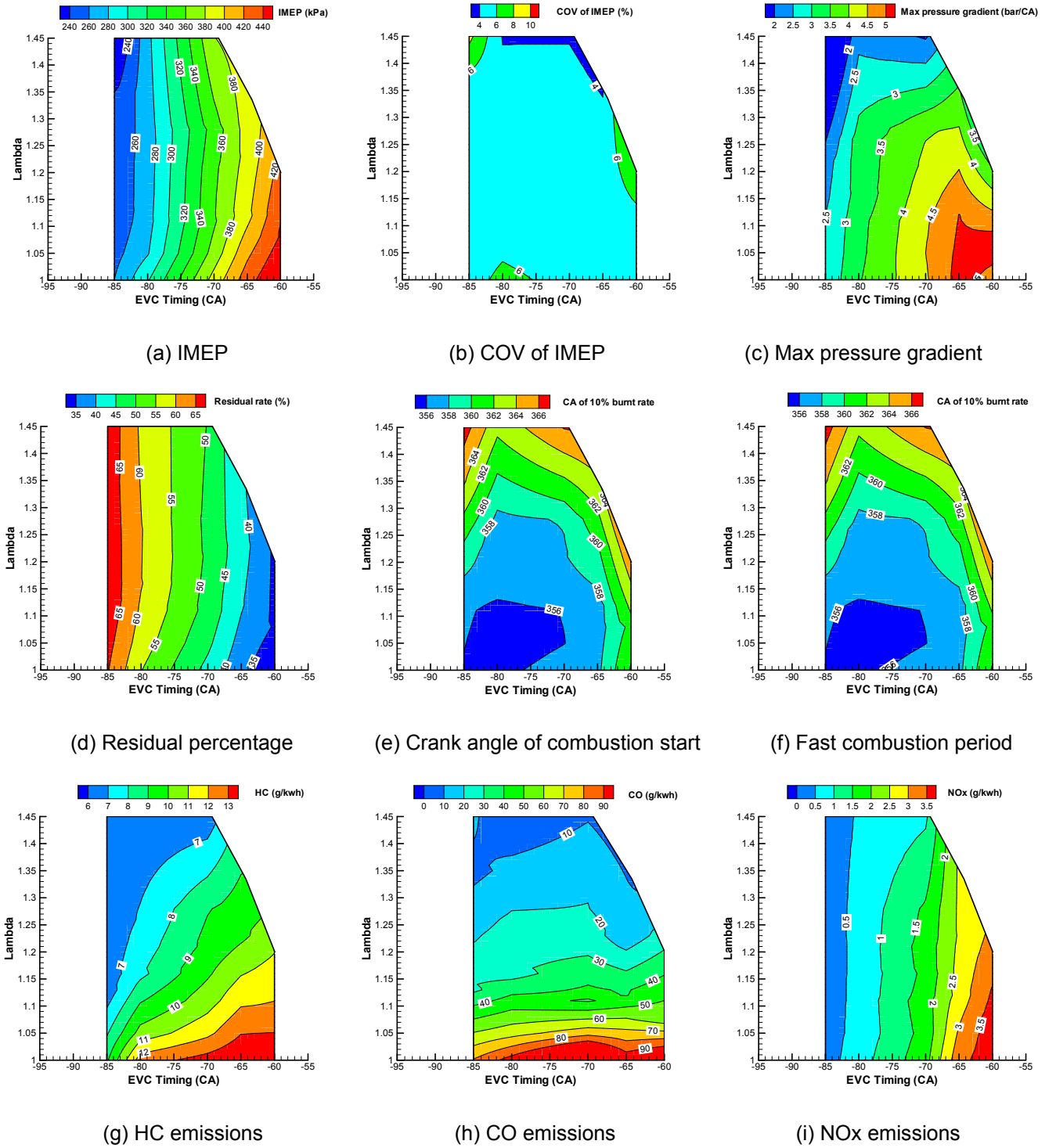

(a) IMEP (b) COV of IMEP (c) Max pressure gradient

(d) Residual percentage (e) Crank angle of combustion start (f) Fast combustion period

(g) HC emissions (h) CO emissions (i) NOx emissions

Figure 6.21 Effects of EVC timing on CAI combustion (n=1800rpm, SOI=240°CA, CR=11, Higher lift cam)

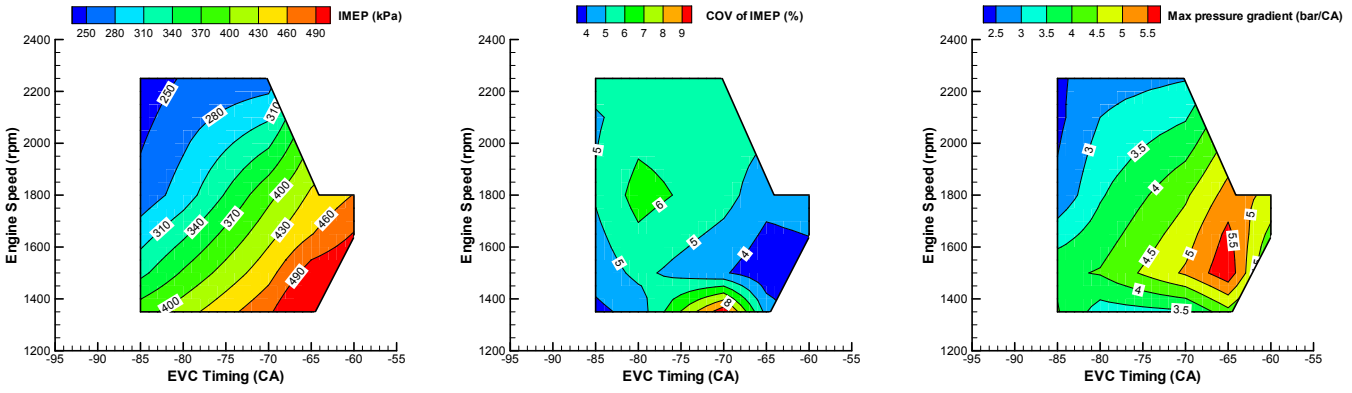

(a) IMEP (b) COV of IMEP (c) Max pressure gradient

Figure 6.22 Effects of EVC timing on CAI combustion (λ=1.0, SOI=240°CA, CR=11, Higher lift cam)

Perhaps the most dramatic effect of the higher lift cam is the CAI operational range that is significantly diminished as both speed and load vary as shown in Figure 6.22. The CAI operational range is limited above 1350 rpm and load range between 250 and 490 kPa with higher lift cams, whereas the low lift cam allows CAI operation down to 1200 rpm and load range from 220 up to 430 kPa.

6.7 Summary

This chapter has devoted to presenting the results obtained with experiments involving the effect of single and split injection, of EVC timing, compression ratio, and the effect of increased valve lift and duration on CAI combustion. The main findings can be summarised as follows.

- Single injection timing is an effective means of controlling mixture formation in the cylinder thus effecting CAI combustion control on a GDI engine that employs negative overlap approach for trapping exhaust gases. Early injection timings, during the recompression process and the intake stroke, provide with earlier onset of the auto-ignition, faster and more stable combustion, higher combustion and thermal efficiencies, less HC and CO emissions. On the other hand it provided increased knocking occurrence as well as higher NOx emissions. Fuel injection into the compression stroke, gave narrower IMEP range, delayed, extended and unstable combustion, especially towards leaner operation. Overall, the load range, over which CAI operation is feasible, is extended significantly over fixed injection timing. Early injection under lean mixture causes the fuel injected to go through a reformation procedure where a part of it, under high temperatures, can be oxidised by the oxygen present in the hot residuals. As a result it increases the pressure in the re-expansion process leading to negative pumping loss values or positive work output.

- With split injection configuration, first injection occurred at the crank angle when the exhaust valve closed and the second at middle of the compression stroke. Split injection can give extended range of CAI operation for both

stoichiometric and lean mixtures, lower cyclic variations and smoother heat release. Additionally, with split injection, thermal efficiency is improved and HC and CO emissions are significantly reduced compared to single injections. The improved performance observed with split injection, is attributed to the earlier onset of combustion and shorter combustion duration than single injection especially for leaner mixtures. The downside of it is the slightly higher NOx emissions due to earlier and faster combustion.

- Variation in EVC timings provides a direct way of controlling the engines output as it controls directly the amount of exhaust residuals trapped in the cylinder and hence the amount of air inducted in the next cycle. Exhaust gas temperatures increase with increasing engine speed and load leading to the mixture autoigniting earlier in the compression stroke. Earlier closure of the exhaust valve, traps larger amounts of residuals that increase the ignitability of stoichiometric mixtures advancing start of CAI combustion. However, at speeds below 1350 rpm, the increased amounts of residuals retained with early EVC timing, lead to unstable combustion. As engine speed increases, unstable operation is replaced by stable CAI operation with low cyclic variation. It is also found that when EVC timing ranges between -92^{o}CA and -63^{o}CA, fully developed CAI combustion is present in the cylinder. HC and NOx emissions vary mostly with EVC timings with early EVC reducing HC and NOx levels. Especially with NOx levels, early EVC seems to offer an improvement of up to 10 times. CO emissions on the other hand change with air/fuel concentration rather than with EVC timing.

- The sources of HC and CO emissions can be of different origin. CO depends on the A/F ration and is mostly caused by the fuel rich pockets present with late injection whereas HC is primarily affected by the EVC timing and they are most influenced by the combustion process.

- Increasing compression ratio, forced fuel injection to be retarded in order to minimise knocking occurrence. Higher compression ratio enables CAI operation at lower engine speeds and leaner mixtures/lower load which are caused by earlier and faster combustion. More complete combustion at higher compression ratio also helps to reduce HC emissions. However, the accelerated combustion restricts the maximum load and leads to higher combustion noise.

- With valve lift becoming greater and opening duration prolonged, the range of EVC timings range where CAI could be attained, became narrower, (-85^{o}CA to -60^{o}CA), allowing at the same time operation at leaner conditions (λ=1.45). The higher valve lift camshaft helps to extend the CAI operation to higher load. However, it can be accompanied by a narrower CAI range both in speed and load.

Chapter 7

Conclusions and Recommendations for Further Work

Chapter 7 Conclusions and Recommendations for Further Work

7.1 Conclusions

7.1.1 Engine Experiments with CAI Combustion

The concept of investigating the potential benefits of an engine combining Direct Injection and CAI combustion lies within the context of the worldwide researchers' efforts to develop an efficient and environmental friendly engine. Advantages offered by Direct Injection technology on the one hand and the merits that CAI combustion has to exhibit on the other, could theoretically provide improved results in terms of engine efficiency and reduced emissions. Developing and optimising such an engine, equipped with the appropriate control systems, seems like a really promising solution for future automotive applications where according to the load conditions the engine could enter either SI or CAI mode. This theoretical flexibility needed further investigation in order to understand the nature CAI combustion and gain insight of the complex phenomena involved especially during the transition period from SI to CAI. With the above into consideration, this study attempted to provide essential comprehension and examine in detail how engine related parameters and injection control could affect the onset CAI combustion along with analysis of the engine's behavior in terms of efficiency and emissions as soon as it was operated in CAI mode. At the same time the transition from SI to CAI mode was further examined. The results obtained could offer to engine manufacturers and researchers, a significant amount of elementary information that could assist in the optimisation and eventual implementation of CAI combustion in a GDI engine.

The aforementioned experiments were performed on a single cylinder HYDRA engine able to operate both at SI and at CAI combustion regime. Initially a comparison between SI and CAI combustion was performed followed by studies on the effect of timing of certain events on CAI combustion. Parameters such as spark discharge, IVO, fuel injection timing, EVC timing, along with coolant fluid temperature, compression ratio and valve lift effects

were investigated. Results with both combustion types were obtained under the same operating conditions so that consistency and repeatability in results are ensured.

7.2 Variable Timing Parameters' Effect on CAI combustion

7.2.1 Spark Timing Effect

Engine operation under certain conditions known as partial or spark assisted CAI, requires the presence of spark discharge to assist in firing the cycles that failed to autoignite.

Spark discharge's effect on CAI combustion is noticeable during the engine operation at low engine speed conditions where the spark discharge is necessary for firing the cycles that failed to autoignite.

As soon as fully developed CAI combustion is established, spark discharge and its timing have a minimal impact.

7.2.2 IVO Timing Effect

IVO timing appeared to play a less important role in CAI combustion contrary to what happens with engine speed.

Engine speeds above 1650rpm allow full development of CAI combustion and IMEP values, for earlier IVO timings, appear to slightly diminish.

This can be explained primarily by the less air mass inducted as in-cylinder pressure is higher than in the intake port by the time inlet valves open.

7.2.3 Fuel Injection Timing Effect

Single and double injection timing tests were performed and have shown that injection timing plays an important role in controlling CAI combustion in a GDI engine that employs negative valve overlap as a means of trapping hot residual gases in the cylinder.

Single injection effect

Injection during the recompression and the intake stroke, allows earlier, faster and more stable CAI combustion resulting into increased engine and combustion efficiency, reduced HC and CO emissions levels.

However, these advantages came with a penalty of increased levels of knocking occurrence and NOx emissions. With injection during the compression stroke on the other hand, CAI combustion is delayed, extended and unstable, especially towards leaner operation, resulting in narrower IMEP range attainable. Overall, CAI operation load levels appear to increase noticeably for a set injection timing value.

Early injection, especially under lean conditions, causes the fuel injected to go through a reformation process during which a part of it can be oxidised, under high temperatures, by the oxygen present in the hot residuals. This can result in increased pressure in the re-expansion process leading to positive work output.

Double injection effect

Split injection configuration involved fuel injection twice during each cycle in quantities and timings controlled independently. In this study equal fuel quantities were injected in every cycle, with the first injection taking place at the crank angle when exhaust valves close and the second one during the compression stroke. Split injection offers the following benefits:

i. Extended range of CAI operation for both stoichiometric and lean mixtures
ii. Lower cyclic variation
iii. Smoother heat release
iv. Improved thermal efficiency
v. Significantly reduced HC and CO emissions are compared to single injection

All the aforementioned advantages can be explained by the earlier onset of combustion and shorter combustion duration than single injection especially for leaner conditions. On the other hand, higher NOx emissions caused by earlier and faster combustion were observed with split injection configuration.

7.2.4 EVC timing effect

Varying the EVC timings, was recognised as a means of controlling the engine's output by determining directly the amount of exhaust residuals trapped and subsequently the amount of fresh air available in the next cycle. Different EVC timings were used and the effect of the inherently different amount of trapped residuals on CAI combustion was evaluated.

Results have shown that by trapping larger amounts of burnt gases, less fresh charge is available for the next cycle reducing the load and advancing the start of CAI combustion especially for stoichiometric conditions.

After 1350 rpm, unstable CAI combustion present until then, is replaced by stable CAI operation with low cyclic variation. Additionally, EVC timings between -92^{o}CA to -55^{o}CA allowed fast and stable CAI combustion.

Early EVC timings tend to reduce HC and NOx levels. NOx levels in particular seem to reduce of up to 10 times with early EVC timings. CO emissions on the other hand appear to vary more with air/fuel ratio rather than with EVC timing.

7.3 Engine Related Parameters' Effect

7.3.1 Coolant Water Temperature Effect

CAI combustion is a type of combustion closely dependent on the creation of the appropriate thermal conditions that would promote mixture autoignition. Coolant water temperatures can contribute to establishing the appropriate thermal regime for CAI initiation. More specifically, temperatures above 65^{o}C enable the engine to operate in CAI mode at a lower critical speed. As water temperatures increase, the lean limit of CAI combustion is extended; a 20^{o}C increase of coolant temperature leads to an increase in lambda of up to 0.06.

7.3.2 Compression Ratio Effect

The effect of various compression ratios on CAI combustion was investigated. For the purposes of the tests, engine variable were kept constant throughout the course of the experiments, so that accurate and reliable results could be obtained. By increasing compression ratio, fuel injection had to be retarded so that knocking occurrence could be minimised.

Higher compression ratio enables CAI operation at lower engine speeds and load mainly due to earlier and faster combustion. More complete combustion occurring at higher compression ratio helps reducing HC emissions. However, the accelerated combustion restricts the maximum load and leads to higher combustion noise.

7.3.3 Cam Lift and Valve Duration effect

Apart from the standard pair of camshafts that allowed the GDI engine to operate in SI mode, two sets of camshafts allowing CAI operation were also used. The effect of the different valve lift and duration, offered by each camshaft, on CAI combustion were investigated.

Higher valve lift and longer valve duration, diminishes the EVC timings range, (-85^{o}CA to -60^{o}CA), where CAI is feasible, allowing the engine to operate at leaner conditions (λ=1.45).

Higher valve lift camshaft helps to extend the CAI operation to higher load. However, it can be accompanied by a narrower CAI range both in speed and load.

7.4 Further Work Recommendations

Even though the results presented in these study are detailed and cover a wide range of parameters that can be altered during engine tests, a number of issues raised haven't either been adequately investigated due to time constraints or haven't been studied at all. Furthermore, past studies of similar content, have left questions unanswered that require attention to the extent that combustion theory can be successfully applied. Based on the aforementioned, below a number of suggestions for future research is proposed.

i. CAI combustion control in this study was found to be dependant on the optimum combination of various parameters including EVC and fuel injection timing as well as compression ratio. Even though the process of controlling autoignition has been studied through engine experiments, it would be really useful to be able to visualise the conditions leading to the formation of autoignition hot spots in the cylinder. Methods for visualisation such as PIV and LIEF have been successfully employed in the past, could really contribute towards visualising in-cylinder contents when the engine operates in CAI mode. Furthermore hybrid SI/CAI operation along with spark assisted CAI, could become fields of investigation using qualitative optical methods so that the phenomena taking place when flame propagation is replaced by rapid autoignition without the need for spark discharge can be studied. Furthermore, the in-cylinder phenomena that occur before, during and after CAI combustions require further study so that better insight into the conditions that lead to CAI and how they can be manipulated and can be achieved.

ii. Double injection tests have been performed during this study with equal fuel injections occurring in every cycle. Nonetheless, the equipment used for controlling

the opening of the injector allowing fuel to be injected, only offered limited capabilities. Injection timing could be controlled independently for each injection effect while the quantity of fuel injected during each of this event was always half compared to the one injected during single injection tests. This constraint didn't allow tests to be performed with varying fuel quantities injected with each pulse entering the injector. It is therefore suggested that further test with split injection takes place with varying fuel quantities injected in the mean time. This investigation can be further extended with the use of visualisation techniques mentioned before (PIV, LIEF) so that a even better understanding of the phenomena that differentiate in-cylinder interactions and conditions between single and double injection configurations can be better understood.

References

1. European Environmental Agency, Press Release, 22 June 2006, http://www.eea.europa.eu/pressroom/newsreleases/GHG2006-en

2. "The Kyoto Protocol to the United Nations Framework Convention on Climate Change" UNFCCC Document No. FCCC/CP/1997/Add.1, March 1998.

3. Information obtained at www.carbonmonoxidekills.com

4. "California Exhaust Emissions Standards and Test Procedures for 2004 and Subsequent Model Passenger Cars. Light Duty Trucks and Medium Duty Vehicles, California Environmental Protection Agency Air Resources Board" (CARB), June 2004.

5. European Commission proposal for Euro V for passenger cars COM(2005) 683 obtained from http://europa.eu

6. Johnson, T. V., "Mobile Emissions Control technologies in review, International Conference on 21st Century Emissions Technology." IMechE Conference Transactions 2000-2, ISBN 186058 322 9 , 2000.

7. European Council Directive 2003/96/EC of 27 /10/2003 restructuring the Community framework for the taxation of energy products and electricity obtained at http://europa.eu

8. European Commission Press Release Reference: IP/07/155 Date: 07/02/2007 obtained at http://europa.eu

9. Ellinger, R., et al., "Comparison of CO Emission Levels for Internal Combustion 2 Engine and Fuel Cell Automotive Propulsion Systems", SAE paper, No. 2001-01-3751, 2001.

10. Weiss, M., et al., “Comparative Assessment of Fuel Cell Cars, Report MIT LFEE, Laboratory for Energy and the Environment”, MIT http://lfee.mit.edu/publications/, 2003-001 RP, 2003.

11. California Environmental Protection Agency Air Resources Board” (CARB) obtained at www.cars.com

12. Weiss, M., Heywood, J., et al., “On the Road in 2020: A Life Cycle Analysis of New Automobile Technologies,” MIT Energy Laboratory Report EL00-003, MIT, Cambridge, MA., 2000.

13. Statistics by R. L. Polk & Co obtained at http://usa.polk.com/site/news_popup.asp?link=2006_0504_hybrids

14. Stone, R,. “Introduction to internal combustion engines”, Third Edition, p.171, Macmillan Press, ISBN 0-333-86058 322 9, 2000.

15. Searles, R.A., “Emission catalyst technology – challenges and opportunities in the 21st century.” International conference on 21st century emissions technology, IMechE, Conference Transactions 2000-2, ISBN 1 86058 322 9, 2000.

16. United States Air and Radiation Environmental Protection Agency, EPA420-F-03-017, June 2003.

17. Salvat, O., et al., “Passenger car serial application of a particulate filter system on a common rail direct injection diesel engine,” SAE paper 2000-01-0473, 2000.

18. Ogink, R., “Computer Modeling of HCCI Combustion.” p.2, Division of Thermo and Fluid Dynamics Chalmers University of Technology, ISBN: 91-7291-458-0, 2004.

19. Johansson, B., “Homogeneous Charge Compression Ignition – the future of IC engines?,” Lund Institute of Technology at Lund University (obtained at http://www.osd.org.tr)

20. Thirouard, B., Cherel, J., Knop, V., "Investigation of Mixture Quality Effect on CAI Combustion," SAE paper 2005-01-0141, 2005.

21. Zhao, H., Peng, Z., Williams, J. and Ladommatos, N., "Understanding the effects of recycled burnt gases on the controlled auto-ignition (CAI) combustion in a 4-stroke gasoline engines," SAE paper 2001-01-3607, 2001.

22. Onishi, S., Hong Jo, S., Shoda, K., Do Jo, P. and Kato, S., "Active thermo-atmosphere combustion (ATAC) – A new combustion process for internal combustion engines," SAE paper 790507, 1979.

23. Noguchi, M., Tanaka, Y., Tanaka, T. and Takeuchi, Y. A, "Study on gasoline engine combustion by observation of intemediate reactive products during combustion," SAE paper 790840, 1979.

24. Najt, P. and Foster, D. E., "Compression-ignited homogeneous charge combustion," SAE paper 830264, 1983.

25. Thring. R. H., "Homogeneous-charge compression-ignition (HCCl) engine," SAE paper 892068, 1989.

26. Ishibashi, Y. and Asai, M., "Improving the exhaust emissions of two-stroke engines by applying the activated radical combustion", SAE paper 960742, 1996.

27. Aoyama, T., Hattori, Y., Mizuta, J. and Sato, Y., "An experimental study on premixed-charge compression ignition gasoline engine," SAE paper 960081, 1996.

28. Duret, P. and Venturi, S., "Automotive calibration of the IAPAC fluid dynamically controlled two-stroke combustion process," SAE paper 960363, 1996.

29. Lavy, J., Dabadie, J., Angelberger, C., Duret, P. (IFP), Willand, J., Juretzka, A., Schaflien, J. (Daimler Chrysler), Ma, T. (Ford), Lendress, Y., Satre, A.(PSA Peugeot Citroen), Shultz, C., Kramer, H. (PCI – Hiedelberg University), Zhao, H., Damiano, L. (Brunel University), "Innovative ultra-low NOx controlled auto-

ignition combustion process for gasoline engines: the 4-SPACE project," SAE paper 2000-01-1837, 2000.

30. Zhao, H., Peng, Z., Williams, J. and Ladommatos, N., "Understanding the effects of recycled burnt gases on the controlled auto-ignition (CAI) combustion in a 4-stroke gasoline engines," SAE paper 2001-01-3607, 2001.

31. Oppenheim, A. K., "The knocking syndrome: its cures and its victims," SAE paper 841339, 1984.

32. Onishi, S., Hong Jo, S., Shoda, K., Do Jo, P. and Kato, S., "Active thermo-atmosphere combustion (ATAC) – A new combustion process for internal combustion engines," SAE paper 790507, 1979.

33. Flynn, P., et al., "The Inevitability of Engine-Out NOx Emissions from Spark Ignited and Diesel Engines," Proc. of the Comb. Inst., Vol. 28, pp. 1211-12, 2000.

34. Stanglmaier, R. and Roberts, C., "Homogeneous Charge Compression Ignition (HCCI): Benefits, Compromises, and Future Engine Applications," SAE paper, No. 1999-01-3682, 1999.

35. Pucher, G. R., Gardiner, D. P., Bardon, M. F. and Batissa, V., "Alternative combustion systems for piston engines involving homogenous charge compression ignition concepts – a review of studies using methanol, gasoline and diesel fuel," SAE paper 962063, 1996.

36. Kluting, M., Flierl, R., Grudno, A., and Luttermann, C., "Drosselfrei Laststeurung mit vollvariablen Ventiltrieben," in MTZ Motortechnische Zeitschrift, vol. 60, pp.476-485, 1999.

37. Pischinger, M., Hagen, J., Salber, W., and Esch, T., "Moglichkeiten der ottomotorischen Prozessfuhrung bei Verwendung des elektromechanischen Ventiltriebes," 7. Aachener Kolloquium Fahzeug- and Motorentechnik, pp. 987-1015, 1998.

38. Olsson, J. Johansson, B., “Closed loop control of an HCCI engine,” SAE paper 2001-01-1031, 2001.

39. Christensen, M., Hultqvist, A., and Johansson, B., “Demonstrating the Multi Fuel Capability of a Homogeneous Charge Compression Ignition Engine with Variable Compression Ratio,” SAE paper, No. 1999-01-3679, 1999.

40. Christensen, M. and Johansson, B., “Influence of Mixture Quality on Homogeneous Charge Compression Ignition, SAE paper,” No. 982454, 1998.

41. Urushihara, T., Hiraya, K., Kakuhou, A., Itoh, T., “Expansion of HCCI operating region by the combination of direct injection, negative valve overlap and internal fuel reformation,” SAE paper 2003-01-0749, 2003.

42. Aoyama, T., Hattori, Y., Mizuto, J., Sato, Y., “An experimental study on premixed-charge compression ignition gasoline engine,” SAE paper 960363, 1996.

43. Koopmans, L. and Denbratt, I., “Cycle to Cycle Variations: Their Influence on Cycle Resolved Gas Temperature and Unburned Hydrocarbons from a Camles Gasoline Compression Ignition Engine,” SAE paper, No. 2002-01-0110, 2002.

44. Koopmans, L., Ogink, R., and Denbratt, I., “Direct Gasoline Injection in the Negative Valve Overlap of a Homogeneous Charge Compression Ignition Engine,” SAE paper, No. 2003-01-1854, JSAE 20030195, 2003.

45. Li, J., Zhao, H., Ladommatos, N. and Ma, T. “Research and development of controlled auto-ignition (CAI) combustion in a 4-stroke multi-cylinder gasoline engine,” SAE Paper 2001-01-3608, 2001.

46. Koopmans, L., Strom, H., Lundgren, S., Backlund, O and Denbratt, I., “Demonstrating a SI-HCCI-SI mode change on a Volvo 5-cylinder electronic valve control engine,” SAE Paper 2003-01-0753,2003.

47. Zhao, H., Ladommatos, N., and Ma, T., New Generation "Direct Injection Gasoline Engine with Controlled Autoignition," School of Engineering and Design, Brunel University, 2002.

48. Oakley, A., "Experimental investigations on controlled auto ignition combustion in a four-stroke engine," PhD Thesis, Brunel University, 2001.

49. Sjöberg, M., Edling, L., Eliassen, T., Magnusson, L. and Angstrom, H., "GDI HCCI: Effects of injection timing and air swirl on fuel stratification, combustion and emissions formation." SAE Paper 2002-01-0106, 2002.

50. Li, Y., Zhao, H., Peng, Z., Ladommatos, N., "Particle image velocimetry measurement of in-cylinder flow in internal combustion engines - experiment and flow structure analysis," Proceedings of the I MECH E Part D, Journal of Automobile Engineering, Volume 216, Number 1, pp. 65-81(17), 2002.

51. B. Johansson: "Cycle to Cycle Variation in SI Engines - The Effects of Fluid Flow and Gas Composition in the Vicinity of the Spark Plug on Early Combustion", SAE 962084, 1996.

52. Koopmans, L., et al., "Location of the First Auto-Ignition Sites for Two HCCI Systems in a Direct Injection Engine," SAE paper, No. 2004-01-0564, 2004.

53. Dec, J.E., Sjöberg, M., "A parametric Study of HCCI Combustion – the Sources of Emissions at Low Loads and the Effects of GDI Fuel Injection," SAE paper 2003-01-0752, 2003.

54. Li, Y., Zhao, H., Brouzos, N., Ma, T., and Leach B., "Effect of Injection Timing on Mixture and CAI Combustion in a GDI Engine with an Air-Assisted Injector," SAE paper 2006-01-0206, 2006.

55. Kontarakis, G. K., Collings, N. C. and Ma, T. H. (2000), "Demonstration of Hcci Using a Single-Cylinder, Four-Stroke SI Engine With Modified Valve Timing," SAE Paper No.2000-01-2870.

56. Cao, L., Zhao, H., Jiang, X. and Kalian, N., “Mixture formation and controlled auto-ignition combustion in four-stroke gasoline engines with port and direct fuel injections,” International Journal of Engine Research, Volume 6, Number 4, pp. 311-329(19), 2005.

57. Wang, Z., Shuai, SJ., Wang, JX., Tian, GH., “A computational study of direct injection gasoline HCCI engine with secondary injection,” Fuel, Volume 85, Issues 12-13, Pages 1831-1841, 2006.

58. Zhao, H., Li, J., Ma, T. and Ladommatos, N., “Performance and analysis of a 4-stroke multi –cylinder gasoline engine with CAI combustion” SAE paper 2002-01-0420, 2001.

59. Flowers, D., Aceves, S., Smith. R., Torres, J., Girard. J, and Dibble, R., “HCCI in a CFR engine: experiments and detailed kinetic modelling,” SAE paper 2000-01-0328, 2000.

60. Christensen, M., B. Johansson, and Einewall P., "Homogeneous Charge Compression Ignition (HCCI) Using Isooctane, Ethanol and Natural Gas- A Comparison with Spark Ignition Operation," SAE Paper 972874, 1997.

61. Gray III, A. W, and T. W. Ryan III (1997), "Homogeneous Charge Compression Ignition (HCCI) of Diesel Fuel," SAE Paper 971676, 1997.

62. Aoyama, T., Yoshiaki, H., Mizuta, J., Sato, Y., “An experimental study on premixed-charge compression ignition gasoline engine,” SAE paper 960081, 1996

63. Christensen, M, and Johansson, B, "The Effect of Piston Topland Geometry on Emissions of Unburned Hydrocarbons from a Homogeneous Charge Compression Ignition (HCCI) Engine," SAE Paper 200101-1893, 2001.

64. Aceves, S.M., Flowers, D.L., Espinosa-Loza, F., Martinez-Frias, J., Dibble, R.W., Christensen, M., Johansson, B., Hessel, R.P., “Piston-Liner Crevice Geometry Effect on HCCI Combustion by Multi-Zone Analysis,” SAE Paper 2002-01-2869, 2002.

65. Dec, J. E., "A Computational Study of the Effects of Low Fuel Loading and EGR on Heat Release Rates and Combustion Limits in HCCI Engines," SAE Paper 2002-01-1309, 2002.

66. Kaiser, E. W., Yang, J., Culp, T., Xu, N., and Maricq, M. M., "HCCI Engine-Out Emissions – Does Flame Propagation Occur in HCCI," International Journal of Engine Research, Vol. 3, pp. 185-195, 2002.

67. Sjoberg, M. and Dec, J. E., "Combined Effects of Fuel-Type and Engine Speed on Intake Temperature Requirements and Completeness of Bulk-Gas Reactions in an HCCI Engine," SAE Paper 2003-01-3173, 2003.

68. Sjoberg, M. and Dec, J. E., "An Investigation into Lowest Acceptable Combustion Temperatures for Hydrocarbon Fuels in HCCI Engines," Submitted to the 30 International Symposium on Combustion, Chicago, IL, July 25-30, 2004.

69. Aceves, S. M., Flowers, D. L., Espinosa-Loza, F., Martinez-Frias, J., Dec, J. E., Sjoberg, M., R.W. and Hessel, R. P., "Spatial Analysis of Emissions Sources for HCCI Combustion at Low Loads Using a Multi-Zone Model," SAE Paper 2004-01-1910, (2004).

70. Zhao, H. and Ladommatos, N., "Engine Combustion Instrumentation and Diagnostics", p. 74, ISBN 0-7680-0665-1, SAE International, 2001.

71. Randolph, A., "Methods of processing cylinder pressure transducer signals to maximise data accuracy," SAE Paper 900170, 1990.

72. Heywood, J.B., "Internal Combustion Engine Fundamentals McGraw-Hill," ISBN 0071004998

73. Stone, R,. "Introduction to internal combustion engines", third edition, p.526, Macmillan Press, ISBN 0-333-86058 322 9, 2000.

74. Leach, B.T., “In Cylinder Flow and Combustion Studies in an Air-assisted Direct Injection Gasoline Engine.”, PhD Thesis, Brunel University, 2004.

75. R.J. Osborne, G. Li, S.M. Sapsford, J. Stokes, T.H. Lake and M.R. Heikal, “Evaluation of HCCI for Future Gasoline Powertrains,” SAE paper 2003-01-0750, 2003.

76. R. H. Standing, N. Kalian, T. Ma, H. Zhao, M. Wirth and A. R. Schamel, “Effects of Injection Timing and Valve Timing on CAI Operation in a Multi-Cylinder DI Gasoline Engine,” SAE paper 2005-01-0132, 2005.

77. Leach B., Zhao, H., Li, J., and Ma, T., “Control of CAI Combustion Through Injection Timing in a GDI Engine with an Air- Assisted Injector,” SAE paper 2005-01-0134, 2005.

78. Saijyo, K., Kojima T., and Nishiwaki, K., “A Numerical Analysis of the Effect of Mixture Heterogeneity on Combustion in a Premixed Charge Compression Ignition Engine,” Proceeding of the 6th COMODIA, p239-246, 2004.

79. G. Cathcart and C. Zavier, “Fundamental Characteristics of an Air-Assisted Direct Injection Combustion System as Applied to a 4 Stroke Automotive Gasoline Engines,” SAE paper 2000-01-0256, 2000.

80. Li, J., Zhao, H., Brouzos, N., and Ma, T., “Parametric Study on CAI Combustion in a GDI Engine with an Air-Assisted Injector”, 2007-01-0196, 2007.

81. Christensen, M., Johansson, B., and Hultquist, A., ‘‘The Effect of Combustion Chamber Geometry on HCCI Operation,’’ SAE Paper 2002-01-0425, 2002.

82. Maigaard, P., Mauss, F., and Kraft, M.,“Homogeneous Charge Compression Ignition Engine: A Simulation Study on the Effectsof Inhomogeneities” Journal of Engineering for Gas Turbines and Power, Volume 125, Issue 2, pp. 466-471, 2003.

83. Kim, J.U., Harold, B.G., Philip, J.S., Daniel K., and Nocera, G., "Exciplex Fluorescence Visualization Systems for Pre-Combustion Diagnosis of An Automotive Gasoline Engine," SAE paper 960826, 1996.

84. Kornmesser, C., Muller, T., Beushausen, V., Hentschel W., and Andresen, P., "Applicability of Different Exciplex Tracers and Model Fuels for Investigation of Mixture Formation in Direct Injection Gasoline," the 5th COMODIA, 2001.

85. Leach B., Zhao, H., Li, Y., and Ma, T., "Two-Phase Fuel Distribution in an Air assisted DI Gasoline Engine," the 6th COMODIA, 2004.

86. Li, Y., Zhao, H., Leach, B., Ma T., and Ladommatos, N., "In-Cylinder Measurements of Fuel Stratification in a Twin-Spark Three-Valve SI Engine," SAE paper 2004-01-1354, 2004.

87. Zhao, F., Laia, M.C. and Harrington, D.L. (1999), "Automotive spark-ignited direct-injection gasoline engines," Prog. Energy Combust. Sci. 25, ISSN 0360-1285, 437-562.

88. Shimotani, K., Oikawa K., Horada O., Kagawa Y., "Characteristics of gasoline in-cylinder direct injection engine," JSAE Review paper, No 17-267-272, 1996.

89. Santoso, H., "Managing transient behaviours of a Dual Mode Spark Ignition / Controlled Auto Ignition Engine with a Variable Valve Timing System", PhD Thesis, S.M. Mechanical Engineering, MIT, 2002.

90. Cao L., Zhao H., Ziang X., "Investigation into Controlled Auto-Ignition Combustion in a GDI Engine with Single and Split Fuel Injections", SAE 2007-01-0211

Appendix A

Engine Component Detail Drawings

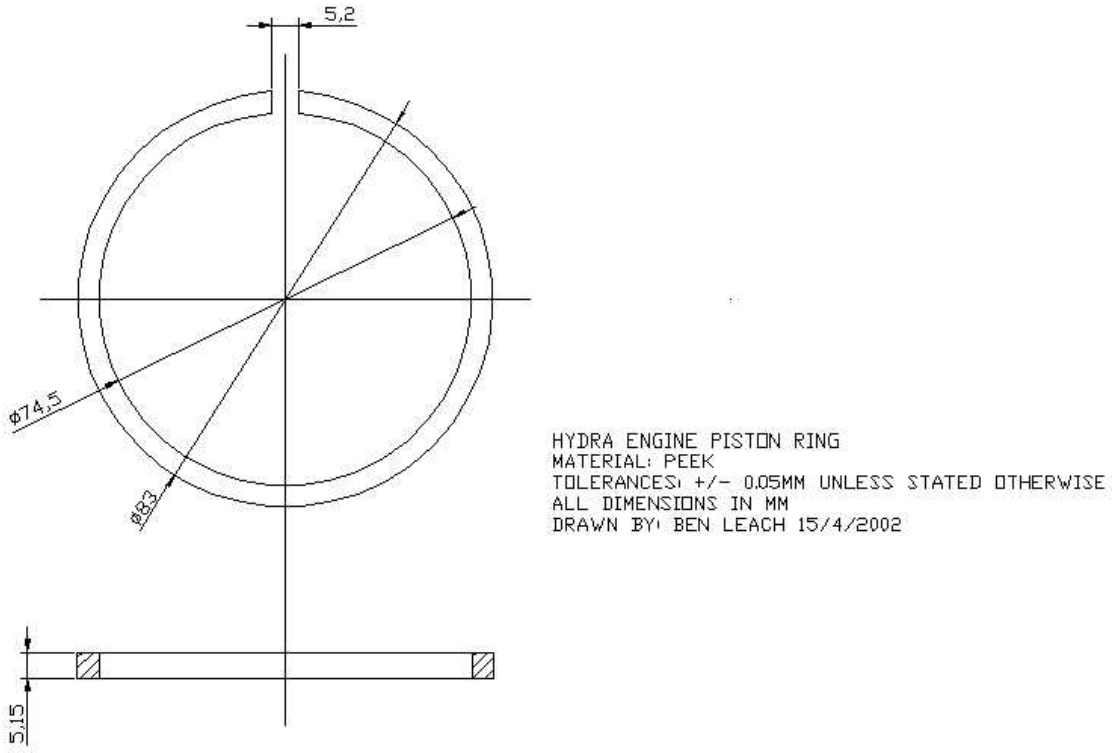

Figure A1 Detail Drawing of Piston Rings

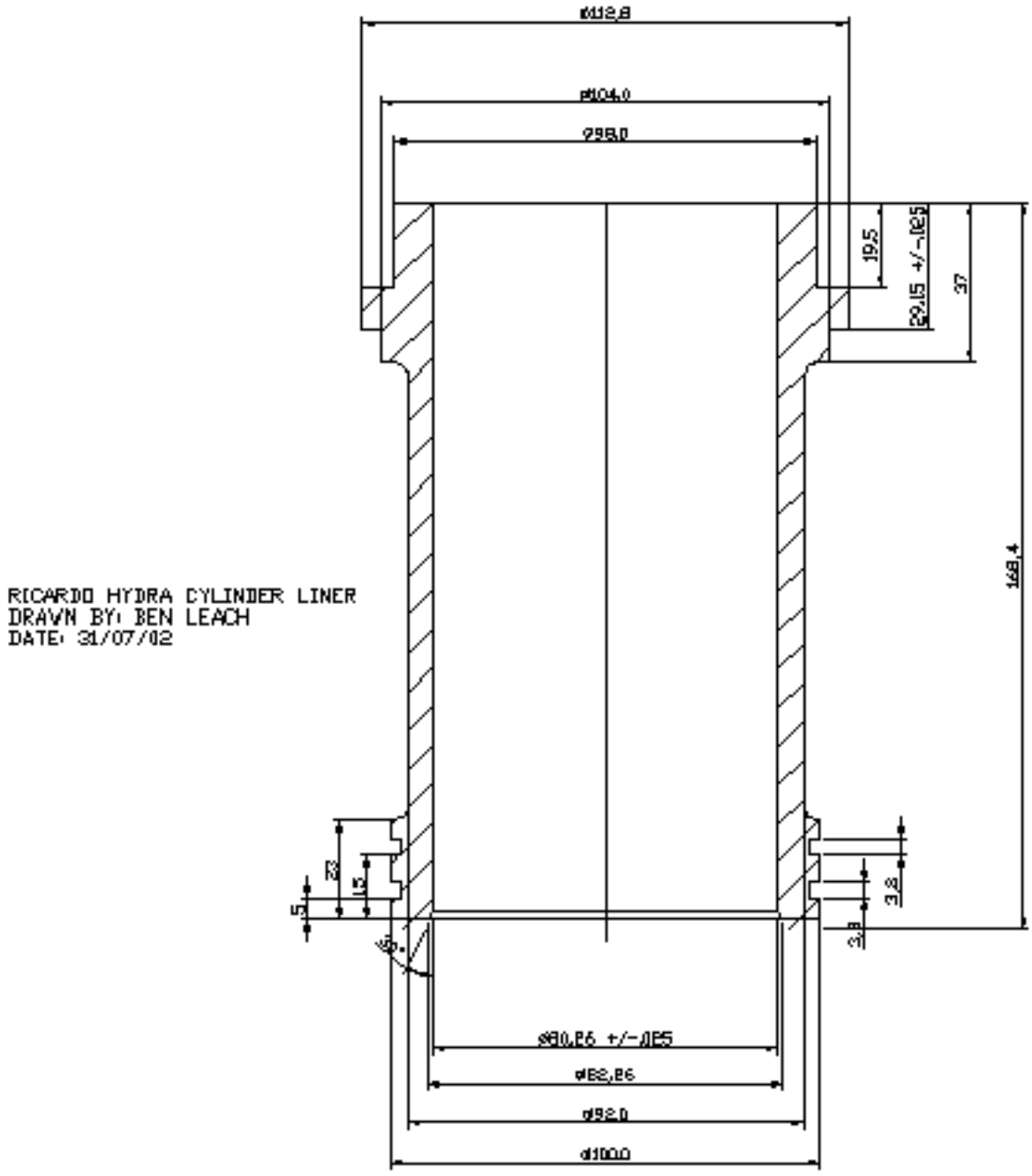

Figure A2 Detail Drawing of Cylinder Replacement Cylinder Liner

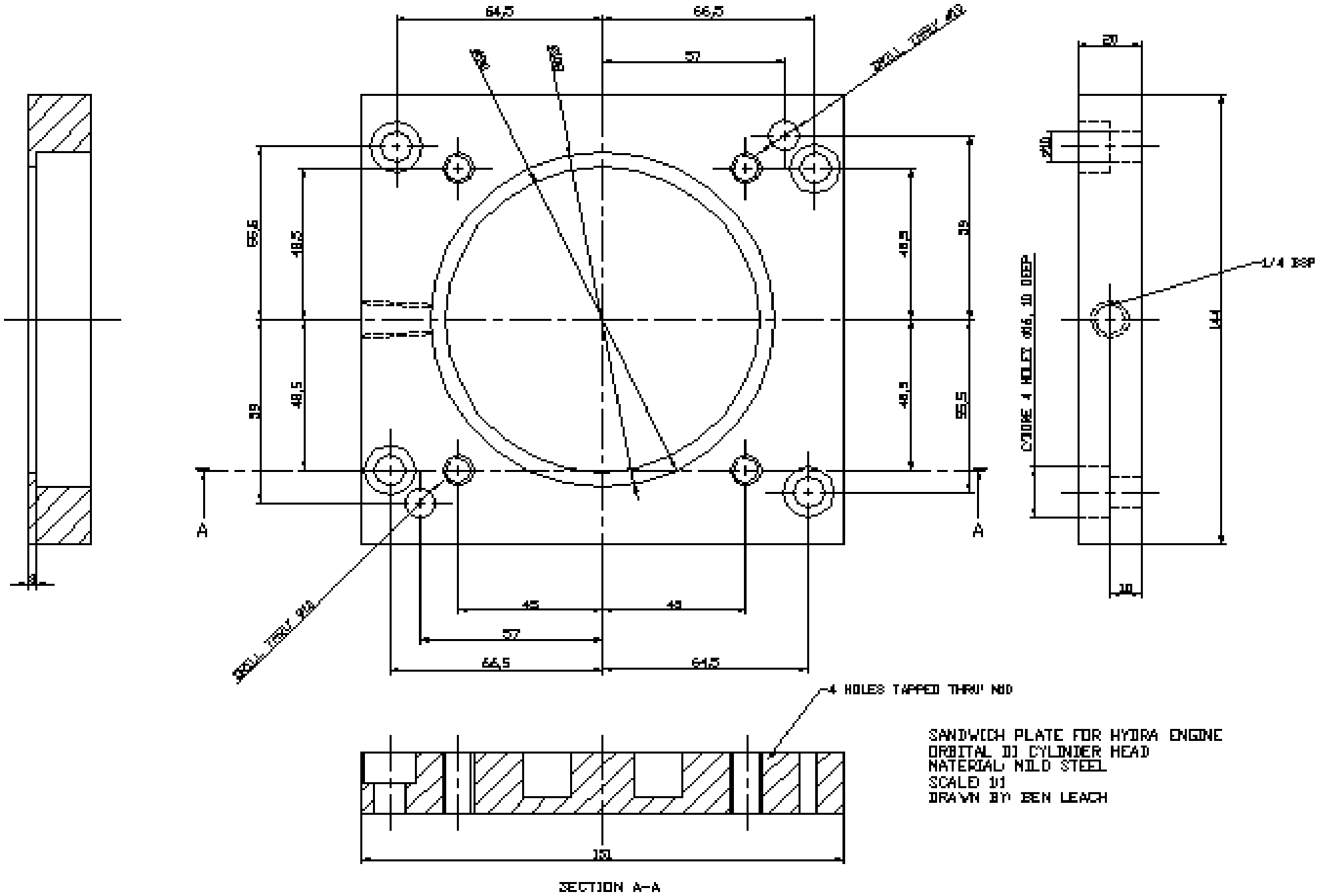

Figure A3 Detail Drawing of Cylinder Head Sandwich Adaptor Plate

Appendix B
Fuel Injector Calibration Curves

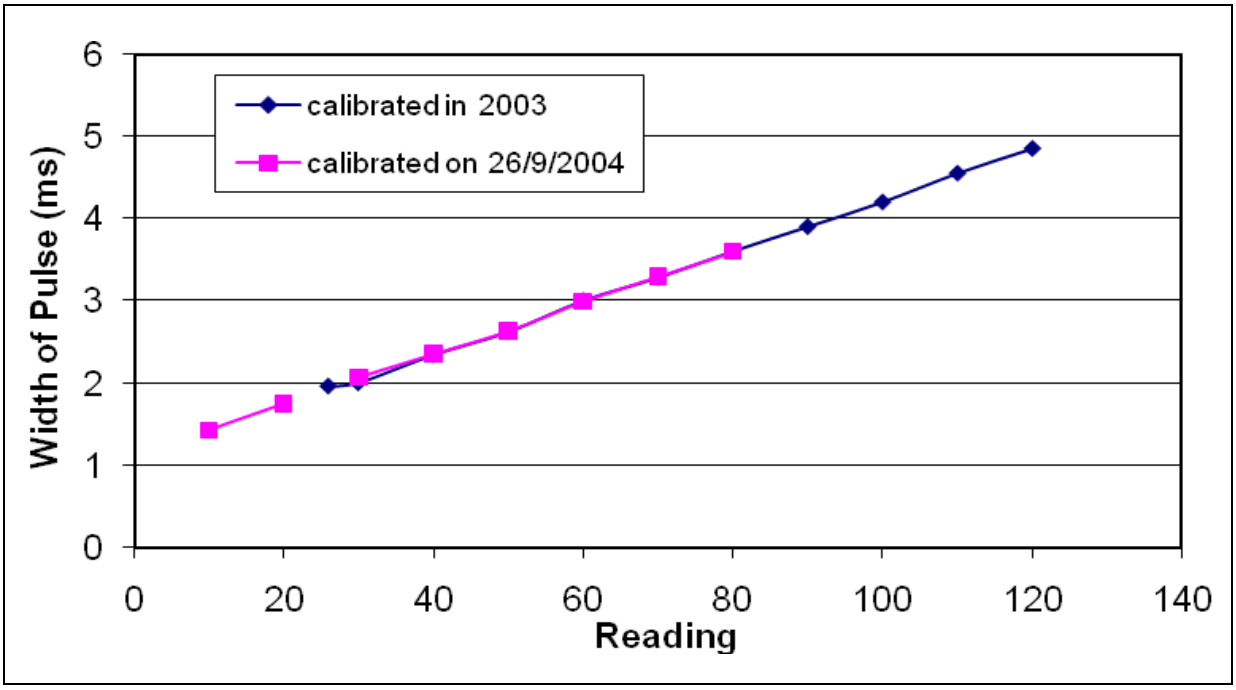

Figure B1 Injector Pulse Duration Versus Reading on the Instrument Dial Obtained Yearly

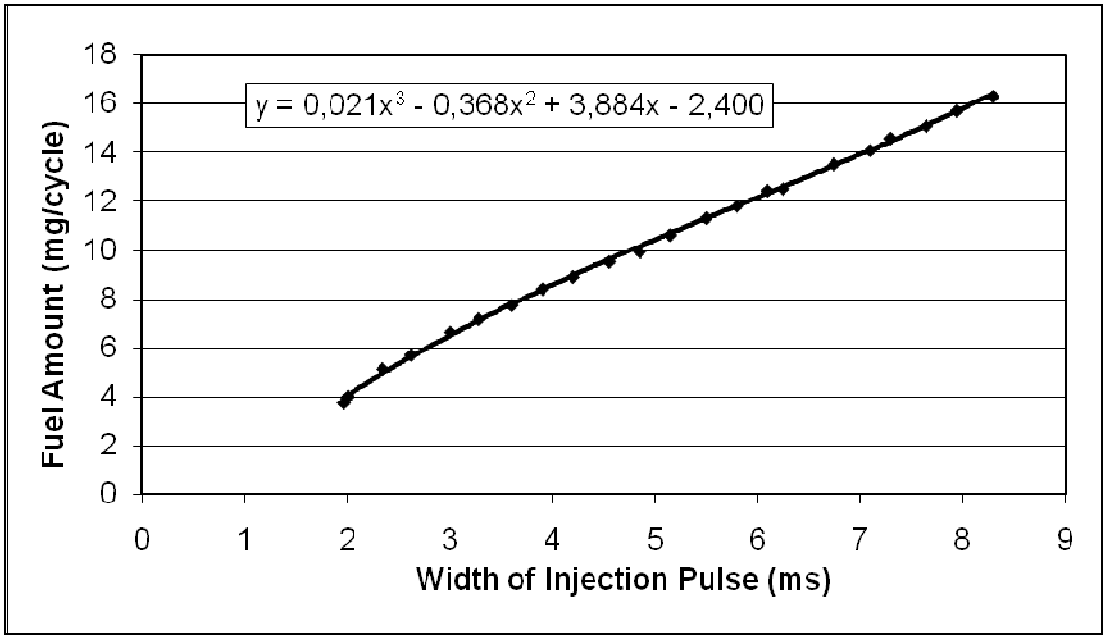

Figure B2 Injector Pulse Duration Versus Fuel Amount Injected. Regression Data Adapted in 3rd Degree Polynomial Regression Line.

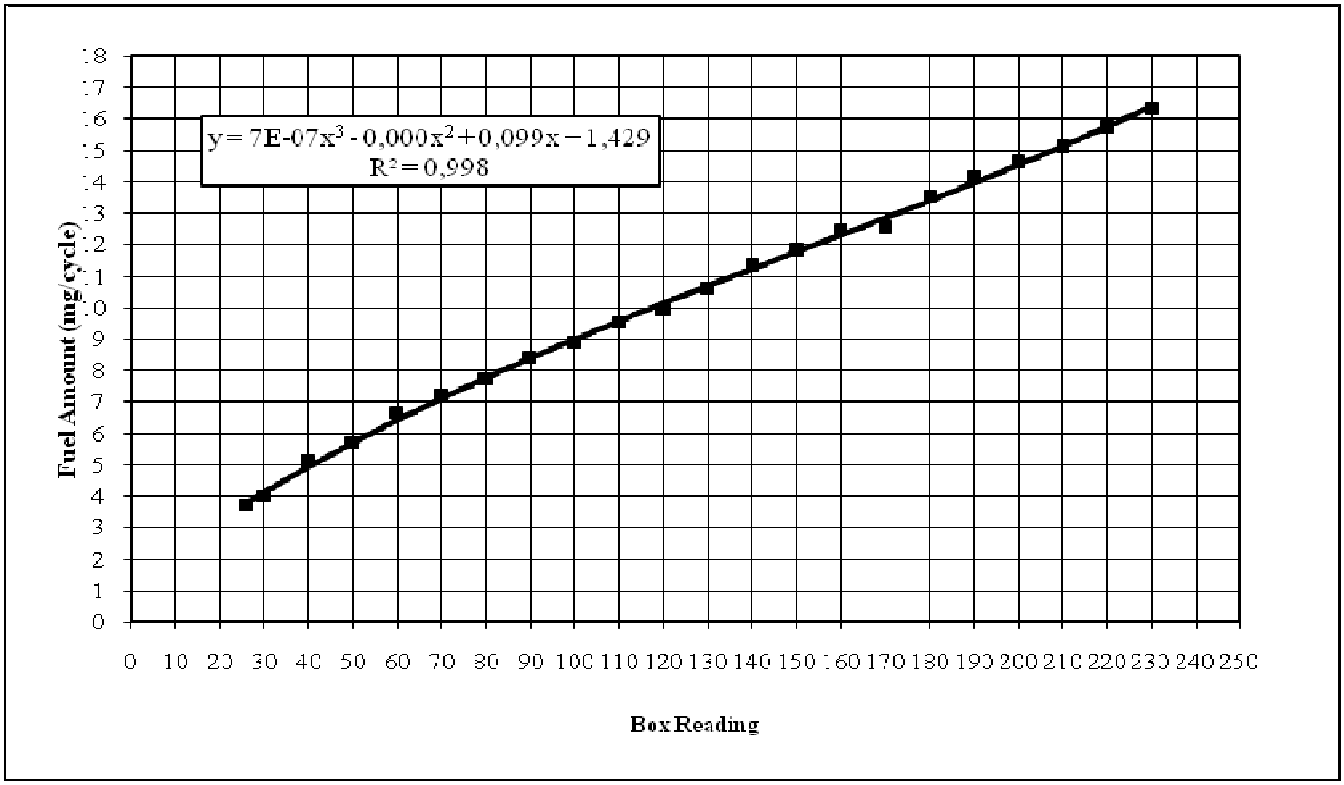

Figure B3 Fuel Amount Injected versus Reading on the Instrument Dial. Regression Data Adapted in 3rd Degree Polynomial Equation

Appendix C
Compression Ratio Calculations

Table C1 Compression Ratio Calculations for Different Plate Thicknesses

bore	stroke	swept volume	cham volume	max.compression ratio	deck clearance volume	deck volume	Compression ratio	bowl diameter	bowl depth	bowl volume	
80,26	89,00	450275,38	38700,00	12,64	0,00	0,00	12,64	46,00	0,00	0,00	
80,26	89,00	450275,38	38700,00	12,64	1,00	5059,27	11,29	46,00	0,00	0,00	
80,26	89,00	450275,38	38700,00	12,64	2,00	10118,55	10,22	46,00	0,00	0,00	
80,26	89,00	450275,38	38700,00	12,64	3,00	15177,82	9,36	46,00	0,00	0,00	0.5mm plate
80,26	89,00	450275,38	38700,00	12,64	2,03	10270,33	10,19	46,00	0,00	0,00	0mm plate
80,26	89,00	450275,38	38700,00	12,64	1,53	7740,69	10,70	46,00	0,00	0,00	2.37mm plate
80,26	89,00	450275,38	38700,00	12,64	3,90	19731,17	8,71	46,00	0,00	0,00	
80,26	89,00	450275,38	38700,00	12,64	4,00	20237,10	8,64	46,00	0,00	0,00	
80,26	89,00	450275,38	38700,00	12,64	5,00	25296,37	8,04	46,00	0,00	0,00	
80,26	89,00	450275,38	38700,00	12,64	6,00	30355,64	7,52	46,00	0,00	0,00	

The plate thickness is 2.37mm

Appendix D – Source Code of Calculations Software Used

Heat release programme written in FORTRAN Programming language
written on 12/07/2004 by Dr. Yufeng Li.
Last edited by Dr. Yufeng Li on 3/4/2005.

This program is used to calculate indicated work, IMEP,
COV of IMEP, Temperature, separate SI and CAI cycles
And calculate heat release from 300 recorded cylinder pressure traces

```
      integer tdc,cycl,logic,contr,misfir_no,si_no,cai_no,ivc,evo
      integer misfir(305),si(305),cai(305),remov_no
      dimension a0(305),a1(305),alpha0(305),alpha1(305),a_Tmax(305)
      character*50 filename,char
      real power,p0,p_inlet,Vc,Vh,B,S,ss,L,cr,speed
      real cov_imep,gama
      dimension p(730,305),pp(730,305),vol(730),w(305),p_mean(730)
      dimension p_max(305),dpdt_max(305),heatrate(730,305),heat(730,305)
      dimension heat5(305),heat10(305),heat50(305),heat90(305)
      dimension p_misfir(730),p_si(730),p_cai(730),pump(305),T_mean(730)
      dimension heat_mean(730),heat_misfir(730),heat_si(730),heat_cai(730)
      dimension hr_mean(730),hr_misfir(730),hr_si(730),hr_cai(730),T5(305)
      dimension pm_hr(730),pm_heat(730),pm_T(730),T(730,305),Tmax(305)
      real mass5,mass10,mass50,mass90,mass5_misfir,mass5_si,mass5_cai
      real mass10_misfir,mass10_si,mass10_cai,mass50_misfir,mass50_si
      real mass50_cai,mass90_misfir,mass90_si,mass90_cai
      real imep(305),imep_mean,imep_misfir,imep_si,imep_cai,imep_sigma
      real pmax_mean,dpdt_mean,cov_pmax,cov_dpdt,cov_a0
      real cov_a1,a0_mean,a1_mean,plus,plus1,plus2,plus3
      real isfc,fuel,air,egr,af,co,hc,nox,nr,np


C     calculate displacing volume at each crank angle, (cm3)
      PI=3.14159
C     write(*,*) 'Input bore, stroke and con-rod length. B,S,L=?(mm) '
C     read(*,*) B,S,L
C     write(*,*) 'input the compression ratio? '
C     read(*,*) cr
      B=80.2
      S=89
      L=155
      cr=8.7
C     write(*,*) 'Ratio of specific heat & Calorific Value(MJ/kg), gama,CV=? '
C     read(*,*) gama,CV
      gama=1.31
      CV=44


C     open and read cylinder pressure data file
      write(*,*) 'Input the cylinder pressure data file name:'
      read(*,*) filename
      open(unit=11,file=filename,status='unknown')
      write(*,*) 'How many cycles in pressure data:'
      read(*,*) cycl
      do i=1,720
            if(i.le.520) then
                  read(11,*) p0,p0,p0,(pp(i,j),j=1,cycl)
            else
                  read(11,*) p0,char,p0,(pp(i,j),j=1,cycl)
            end if
      end do
      close(11)
```

```
C       remove those cycles that have a discontinuous pressure value at the start and the end of the cycle
C       remove those cycles having max. pressure near the beginning of the cycle, i.e. 0-30 CA
        remov_no=0
        j=1
19      if(j.gt.cycl) goto 18
c                       plus1=(pp(1,j)+pp(3,j)+pp(5,j)+pp(7,j)+pp(9,j))/5
c                       plus2=(pp(361,j)+pp(363,j)+pp(365,j)+pp(367,j)+pp(369,j))/5
c               if((plus1-plus2).gt.0.0) then
c                       remov_no=remov_no+1
c                       cycl=cycl-1
c                       do k=j,cycl
c                               do i=1,720
c                                       pp(i,k)=pp(i,k+1)
c                               end do
c                       end do
c                       j=j-1
c               end if
c               j=j+1
c               goto 19
c               if((abs(pp(1,j)-pp(720,j)).gt.2.0)) then
                if((abs(pp(1,j)-pp(720,j)).gt.2.0).or.(pp(677,j).gt.pp(720,j))) then
                        remov_no=remov_no+1
                        cycl=cycl-1
                        do k=j,cycl
                                do i=1,720
                                        pp(i,k)=pp(i,k+1)
                                end do
                        end do
                        j=j-1
                end if
                j=j+1
                goto 19
18      continue
        write(*,*)
        write(*,499) remov_no,cycl
499     format(i3,' cycles have been removed,' i4,' cycles are left')
        write(*,*)


C       correcting TDC shift
        write(*,*) ' Input actual TDC (360) obtaind from motored pressure:'
        read (*,*) tdc
        do 20 j=1,cycl
                do i=1,720
                        k=i+(tdc-360)
                        if(k.gt.720) k=k-720
                        if(k.le.0) k=k+720
                        p(i,j)=pp(k,j)
                end do
20      continue


C       shift the pressure data when the phase changes during the data acquisition
        do j=1,cycl
                plus1=(pp(1,j)+pp(3,j)+pp(5,j)+pp(7,j)+pp(9,j))/5
                plus2=(pp(361,j)+pp(363,j)+pp(365,j)+pp(367,j)+pp(369,j))/5
                if(plus1.gt.plus2*1.1) then
                        do i=1,720
                                if(i.le.360) pp(i,j)=p(i+360,j)
                                if(i.gt.360) pp(i,j)=p(i-360,j)
                        end do
                        do i=1,720
                                p(i,j)=pp(i,j)
                        end do
```

```
            end if
        end do

C       determination of the absolute pressure
        write(*,*) 'Input inlet pressrue p0(mmHg):'
        read(*,*) p0
        p0=10.1325*p0/(760*9.81)
        do 30 j=1,cycl
            p_inlet=0.0;
            do i=220,230
                p_inlet=p_inlet+p(i,j);
            end do
            p_inlet=p_inlet/11.0;
            do i=1,720
                p(i,j)=p(i,j)-(p_inlet-p0);
            end do
30      continue


C       extend the pressure data 10 CA into next cycle
        do j=1,cycl
            do i=1,10
                p(720+i,j)=p(i,j)
            end do
        end do

C       Smoothing the pressure data by removing burrs and averaging in shifing window with a changeable
width
        do 35 j=1,cycl
            do i=2,730
                vol(i)=0.0
                if(p(i,j).lt.5) then
                    if(abs(p(i,j)-p(i-1,j))/p(i-1,j).gt.0.80) vol(i)=1.0
                end if
            end do
            do 36 i=2,730
                if(vol(i).eq.0.0) goto 36
                k=1
37              if(vol(i+k).eq.1.0) then
                    k=k+1
                    goto 37
                else
                    p(i,j)=(p(i+k,j)-p(i-1,j))/(k+1)+p(i-1,j)
                end if
36          continue
            do 38 i=3,727
                if(p(i,j).lt.p(340,j)) then
                    pp(i,j)=(p(i-2,j)+p(i-1,j)+p(i,j)+p(i+1,j)+p(i+2,j))/5
                else
                    pp(i,j)=(p(i-1,j)+p(i,j)+p(i+1,j))/3
                end if
38          continue
35      continue
        do j=1,cycl
            do i=3,727
                p(i,j)=pp(i,j)
            end do
            p(1,j)=pp(721,j)
            p(2,j)=pp(722,j)
        end do

C       extend the pressure data 10 CA into next cycle
        do j=1,cycl
            do i=1,10
                p(720+i,j)=p(i,j)
```

```
            end do
        end do

C       calculate the average pressure p_mean(i,j) and Pmax, dpdt_max
        do i=1,730
            plus=0.0
            do j=1,cycl
                plus=plus+p(i,j)
            end do
            p_mean(i)=plus/cycl
        end do
        pm_max=1.0
        pm_dpdt=0.0
        do i=320,450
            if(p_mean(i).gt.pm_max) then
                pm_max=p_mean(i)
                pm_alpha0=i
            end if
            plus=(p_mean(i+1)-p_mean(i))/1.0
            if(plus.gt.pm_dpdt)then
                pm_dpdt=plus
                pm_alpha1=i
            end if
        end do

C       calculate the Pmax & its crank angle, (dp/dt)max & its crank angle for each cycle
        do 40 j=1,cycl
            p_max(j)=1.0
            dpdt_max(j)=0.0
            do i=320,450
                if (p(i,j).gt.p_max(j)) then
                    p_max(j)=p(i,j)
                    alpha0(j)=i
                end if
                plus=(p(i+1,j)-p(i,j))/1.0
                if(plus.gt.dpdt_max(j)) then
                    dpdt_max(j)=plus
                    alpha1(j)=i
                end if
            end do
40      continue


C       judge and separate the SI cycle, CAI cycle and slow-burn/misfire cycle.
C       rearrange data in the order of slow-burn/misfire cycles, SI cycles and CAI cycles
C       misfire/slow-burn cycle is obtained when the first derivative is less than 0 during expension stroke.
C       the CAI cycle is obtained when the Pmax is 20% higher than P(360)
        write(*,*) 'Want to separate slow-burn,CAI,SI cycle? (1-yes,2=no)'
        read(*,*) logic
        if(logic.ne.1) goto 51
        do i=1,cycl
            si(i)=0
            cai(i)=0
            misfir(i)=0
        end do

C       judge the misfire, SI and CAI cycles by max pressure
        p_motor=p0*cr**gama
        do 50 j=1,cycl
            k=0
            if(p_max(j).lt.p_motor) then
                do i=362,450
                    plus=p(i+1,j)-p(i,j)
                    if(plus.ge.0.0) k=k+1
                end do
```

```
                        if(k.lt.8) then
                                misfir(j)=misfir(j)+1
                                goto 50
                        else
                                si(j)=si(j)+1
                                goto 50
                        end if
                else
                        cai(j)=cai(j)+1
                        goto 50
                end if
50      continue
        misfir_no=0
        si_no=0
        cai_no=0
        do i=1,cycl
                misfir_no=misfir_no+misfir(i)
                si_no=si_no+si(i)
                cai_no=cai_no+cai(i)
        end do
        write(*,*)
        write(*,500) misfir_no,si_no,cai_no
500     format('Misfire/slow-burn, SI, CAI cycles is:',3(i4,1x))

C       rearrange p(i,j),p_max(j),dpdt_max(j).alpha0(j),alpha1(j) in the order of misfire/slow-burn, SI and
CAI
        court=0
        do j=1,cycl
                do i=1,730
                        pp(i,j)=0.0
                end do
                w(j)=0.0
                imep(j)=0.0
                a0(j)=0
                a1(j)=0
        end do
        do j=1,cycl
                if (misfir(j).eq.1) then
                        court=court+1
                        do i=1,730
                                pp(i,court)=p(i,j)
                        end do
                        w(court)=p_max(j)
                        imep(court)=dpdt_max(j)
                        a0(court)=alpha0(j)
                        a1(court)=alpha1(j)
                end if
        end do
        do j=1,cycl
                if (si(j).eq.1) then
                        court=court+1
                        do i=1,730
                                pp(i,court)=p(i,j)
                        end do
                        w(court)=p_max(j)
                        imep(court)=dpdt_max(j)
                        a0(court)=alpha0(j)
                        a1(court)=alpha1(j)
                end if
        end do
        do j=1,cycl
                if (cai(j).eq.1) then
                        court=court+1
                        do i=1,730
                                pp(i,court)=p(i,j)
```

```
                    end do
                    w(court)=p_max(j)
                    imep(court)=dpdt_max(j)
                    a0(court)=alpha0(j)
                    a1(court)=alpha1(j)
            end if
    end do
    do j=1,cycl
            do i=1,730
                    p(i,j)=pp(i,j)
            end do
            p_max(j)=w(j)
            dpdt_max(j)=imep(j)
            alpha0(j)=a0(j)
            alpha1(j)=a1(j)
    end do
51  continue


C   Mean value of Pmax and (dp/dt)max, and their rms values over cycles
    pmax_mean=0.0
    dpdt_mean=0.0
    a0_mean=0.0
    a1_mean=0.0
    do i=1,cycl
            pmax_mean=pmax_mean+p_max(i)
            dpdt_mean=dpdt_mean+dpdt_max(i)
            a0_mean=a0_mean+alpha0(i)
            a1_mean=a1_mean+alpha1(i)
    end do
    pmax_mean=pmax_mean/cycl
    dpdt_mean=dpdt_mean/cycl
    a0_mean=a0_mean/cycl
    a1_mean=a1_mean/cycl
    plus=0.0
    plus1=0.0
    plus2=0.0
    plus3=0.0
    do i=1,cycl
            plus=plus+(p_max(i)-pmax_mean)*(p_max(i)-pmax_mean)
            plus1=plus1+(dpdt_max(i)-dpdt_mean)*(dpdt_max(i)-dpdt_mean)
            plus2=plus2+(alpha0(i)-a0_mean)*(alpha0(i)-a0_mean)
            plus3=plus3+(alpha1(i)-a1_mean)*(alpha1(i)-a1_mean)
    end do
    plus=sqrt(plus/cycl)
    plus1=sqrt(plus1/cycl)
    plus2=sqrt(plus2/cycl)
    plus3=sqrt(plus3/cycl)
    cov_pmax=plus*100/pmax_mean
    cov_dpdt=plus1*100/dpdt_mean
    cov_a0=plus2*100/a0_mean
    cov_a1=plus3*100/a1_mean

C   compute mean pressure over all misfire, SI and CAI cycles recorded
    if (logic.eq.1) then
            do 60 i=1,720
                    plus1=0.0
                    plus2=0.0
                    plus3=0.0
                    do j=1,cycl
                            if(j.le.misfir_no) then
                                    plus1=plus1+p(i,j)
                            else if(j.gt.(cycl-cai_no)) then
                                    plus3=plus3+p(i,j)
                            else
```

```
                                        plus2=plus2+p(i,j)
                                end if
                        end do
                        p_misfir(i)=plus1/misfir_no
                        p_si(i)=plus2/si_no
                        p_cai(i)=plus3/cai_no
60              continue
        end if

        write(*,*) 'input the engine speed (Hz)? '
        read(*,*) speed
        Vh=PI*B*B*S/4
        S=S/2
        Vc=Vh/(cr-1)
        do i=1,720
                ss=S*cos(PI*i/180)+sqrt(L*L-S*S*sin(PI*i/180)*sin(PI*i/180))
                vol(i)=Vc+PI*B*B*(L+S-ss)/4
                vol(i)=vol(i)/1000
        end do

C       extend the volume data 10 CA into next cycle
        do i=1,10
                vol(720+i)=vol(i)
        end do

C       calculate indicate work per cycle (J), power (kW) and IMEP (kPa) for each cycle
        do 70 j=1,cycl
                plus=0.0
                do i=1,720
                        plus=plus+(p(i,j)+p(i+1,j))*(vol(i+1)-vol(i))/2
                end do
                w(j)=plus*9.81/100
                imep(j)=w(j)*1000000/Vh
70      continue
        plus1=0.0
        plus2=0.0
        do j=1,cycl
                plus1=plus1+w(j)
                plus2=plus2+imep(j)
        end do
        w_mean=plus1/cycl
        imep_mean=plus2/cycl
        power=w_mean*speed/(2*1000)
        write(*,*)
        write(*,502) w_mean,power,imep_mean
502     format('W(J), P(kw),IMEP(kPa) averaged over cycles:',3(1x,f5.1))

C       calculate indicate work per cycle (J), power (kW) and IMEP (kPa) from mean pressure
        plus=0.0
        do i=1,720
                plus=plus+(p_mean(i)+p_mean(i+1))*(vol(i+1)-vol(i))/2
        end do
        pm_work=plus*9.81/100
        pm_imep=pm_work*1000000/Vh
        pm_power=pm_work*speed/(2*1000)
        write(*,503) pm_work,pm_power,pm_imep
503     format('W(J),P(kw),IMEP(kPa) from mean pressure:',3(1x,f5.1))


C       calculate the COV of imep
        plus=0.0
        do j=1,cycl
                plus=plus+(imep(j)-imep_mean)*(imep(j)-imep_mean)
        end do
        plus=sqrt(plus/cycl)
```

```
      cov_imep=plus*100/imep_mean

C     calculate the pump loss (J) for each cycle
      do 75 j=1,cycl
            plus=0.0
            plus1=0.0
            do i=1,180
                  plus=plus+(p(i,j)+p(i+1,j))*(vol(i+1)-vol(i))/2
            end do
            do i=541,720
                  plus1=plus1+(p(i,j)+p(i+1,j))*(vol(i+1)-vol(i))/2
            end do
            pump(j)=plus+plus1
            pump(j)=pump(j)*9.81*(-1)/100
75    continue
      plus=0.0
      do j=1,cycl
            plus=plus+pump(j)
      end do
      pump_mean=plus/cycl

C     calculate the pump loss (J) from mean pressure
      plus=0.0
      plus1=0.0
      do i=1,180
            plus=plus+(p_mean(i)+p_mean(i+1))*(vol(i+1)-vol(i))/2
      end do
      do i=541,720
            plus1=plus1+(p_mean(i)+p_mean(i+1))*(vol(i+1)-vol(i))/2
      end do
      pm_pump=plus+plus1
      pm_pump=pm_pump*9.81*(-1)/100

      write(*,*) 'Reading of fuel control box? (0 for motored)'
      read(*,*) x
      fuel=7e-7*x*x*x-0.0003*x+0.0992*x+1.4297

C     write(*,*) '\n Input valve timing ivc and evo=?  '
C     read(*,*) ivc,evo
      ivc=240
      evo=500

C     calculate gross heat release rate (J/CA) from 1 to 720 for each cycle
      do j=1,cycl
            do i=1,730
                  heatrate(i,j)=0.0
                  heat(i,j)=0.0
                  pp(i,j)=0.0
            end do
            heat5(j)=0.0
            heat10(j)=0.0
            heat50(j)=0.0
            heat90(j)=0.0
      end do
      do 80 j=1,cycl
            do i=1+1,730
                  plus1=gama*p(i,j)*(vol(i)-vol(i-1))/(gama-1)
                  plus2=vol(i)*(p(i,j)-p(i-1,j))/(gama-1)
                  heatrate(i,j)=plus1+plus2
                  heatrate(i,j)=heatrate(i,j)*9.81/100
            end do
C     smooth the heat release rate curve
            do i=5,725
                  plus1=0.0
                  do k=-3,3
```

```
                        plus1=plus1+heatrate(i+k,j)
                    end do
                    pp(i,j)=plus1/7
                end do

                do i=5,720
                    heatrate(i,j)=pp(i,j)
                end do
                do i=1,4
                    heatrate(i,j)=pp(720+i,j)
                end do

C       calculate the integrated heat release from 240CA to 500CA for each cycle
                plus=0.0
                do i=ivc+1,evo+1
                    plus=plus+(heatrate(i-1,j)+heatrate(i,j))*1/2
                    heat(i,j)=plus
                end do
                heat(ivc,j)=heatrate(ivc,j)
C       give percentage of burnt rate, assume max heat release is 100%
                plus1=0.0
                do i=ivc,evo
                    if(heat(i,j).gt.plus1) then
                        plus1=heat(i,j)
                        k=i
                    end if
                end do
                plus2=(heat(ivc+1,j)+heat(ivc+2,j)+heat(ivc+3,j))/3
                plus1=(plus1+heat(k-1,j)+heat(k+1,j))/3
                do i=ivc,evo+1
                    heat(i,j)=(heat(i,j)-plus2)*100/(plus1-plus2)
                end do
                do i=ivc+1,evo
                    heat(i,j)=(heat(i-1,j)+heat(i,j)+heat(i+1,j))/3
                end do
80      continue

C       calculate gross heat release rate (J/CA) from 1 to 720 from mean pressure
        do i=1,730
                pm_hr(i)=0.0
                pm_heat(i)=0.0
        end do
                pm_heat5=0.0
                pm_heat10=0.0
                pm_heat50=0.0
                pm_heat90=0.0
        do i=1+1,730
                plus1=gama*p_mean(i)*(vol(i)-vol(i-1))/(gama-1)
                plus2=vol(i)*(p_mean(i)-p_mean(i-1))/(gama-1)
                pm_hr(i)=plus1+plus2
                pm_hr(i)=pm_hr(i)*9.81/100
        end do
C       smooth the heat release rate curve
        do i=5,725
                plus1=0.0
                do k=-2,2
                    plus1=plus1+pm_hr(i+k)
                end do
                pm_heat(i)=plus1/5
        end do
        do i=5,720
                pm_hr(i)=pm_heat(i)
        end do
        do i=1,4
                pm_hr(i)=pm_heat(720+i)
```

```
        end do

        do i=1,730
                pm_heat(i)=0.0
        end do

C       calculate Percent of integrated heat release over fuel energy during 240CA to 500CA from mean
pressure
        plus=0.0
        do i=ivc+1,evo+1
                plus=plus+(pm_hr(i-1)+pm_hr(i))*1/2
                pm_heat(i)=plus
        end do
                pm_heat(ivc)=pm_hr(ivc)
C               plus1=0.0
C       do i=ivc,evo
C               if(pm_heat(i).gt.plus1) then
C                       plus1=pm_heat(i)
C                       k=i
C               end if
C       end do
C       plus2=(pm_heat(ivc+1)+pm_heat(ivc+2)+pm_heat(ivc+3))/3
C       plus1=(plus1+pm_heat(k-1)+pm_heat(k+1))/3
        do i=ivc,evo+1
C                       pm_heat(i)=(pm_heat(i)-plus2)*100/(plus1-plus2)
                if (fuel.ne.0) pm_heat(i)=pm_heat(i)*100/(fuel*CV)
        end do


C       calculate the crank angle of 1%, 10%, 50% and 90% mass fraction burnt
C       and the period of early combustion, fast combustion and late combustion
C       critical point at which fast burnt stage end for CAI cycles
        do 90 j=1,cycl
                plus=0.0
                do i=ivc,evo
                        if((heat(i,j).lt.1).and.(heat(i+1,j).gt.1)) then
                                heat5(j)=i+(1-heat(i,j))/(heat(i+1,j)-heat(i,j))
                        else if((heat(i,j).lt.10).and.(heat(i+1,j).gt.10)) then
                                heat10(j)=i+(10-heat(i,j))/(heat(i+1,j)-heat(i,j))
                        else if((heat(i,j).lt.50).and.(heat(i+1,j).gt.50)) then
                                heat50(j)=i+(50-heat(i,j))/(heat(i+1,j)-heat(i,j))
                        else if((heat(i,j).le.90).and.(heat(i+1,j).gt.90)) then
                                heat90(j)=i+(90-heat(i,j))/(heat(i+1,j)-heat(i,j))
                                goto 90
                        end if
                end do
90      continue
        plus=0.0
        plus1=0.0
        plus2=0.0
        plus3=0.0
        k=0
        do j=1,cycl
                if((heat90(j).gt.360).and.(heat10(j).gt.300)) then
                        k=k+1
                        plus=plus+heat5(j)
                        plus1=plus1+heat10(j)
                        plus2=plus2+heat50(j)
                        plus3=plus3+heat90(j)
                end if
        end do
        mass5=plus/k
        mass10=plus1/k
        mass50=plus2/k
        mass90=plus3/k
```

```
C       calculate the crank angle of 1%, 10%, 50% and 90% burnt rate form mean pressure data
        plus=0.0
        do i=ivc,evo
                if((pm_heat(i).lt.1).and.(pm_heat(i+1).gt.1)) then
                        pm_heat5=i+(1-pm_heat(i))/(pm_heat(i+1)-pm_heat(i))
                else if((pm_heat(i).lt.10).and.(pm_heat(i+1).gt.10)) then
                        pm_heat10=i+(10-pm_heat(i))/(pm_heat(i+1)-pm_heat(i))
                else if((pm_heat(i).lt.50).and.(pm_heat(i+1).gt.50)) then
                        pm_heat50=i+(50-pm_heat(i))/(pm_heat(i+1)-pm_heat(i))
                else if((pm_heat(i).le.90).and.(pm_heat(i+1).gt.90)) then
                        pm_heat90=i+(90-pm_heat(i))/(pm_heat(i+1)-pm_heat(i))
                end if
        end do
C       Find max burnt rate (actual) if it is less than 90%
        if(pm_heat90.eq.0) then
                plus1=0.0
                do i=ivc,evo
                        if(pm_heat(i).gt.plus1) plus1=pm_heat(i)
                end do
                pm_heat90=plus1
        end if

C       calculate the mean heat release (total, misfire, SI, CAI cycles)
        do 100 i=1,720
                plus1=0.0
                plus2=0.0
                plus3=0.0
                plus4=0.0
                plus5=0.0
                plus6=0.0
                plus7=0.0
                plus8=0.0
                do j=1,cycl
                        plus1=plus1+heatrate(i,j)
                        plus2=plus2+heat(i,j)
                end do
                if(logic.eq.1) then
                        do j=1,misfir_no
                                plus3=plus3+heatrate(i,j)
                                plus4=plus4+heat(i,j)
                        end do
                        do j=misfir_no+1,misfir_no+si_no
                                plus5=plus5+heatrate(i,j)
                                plus6=plus6+heat(i,j)
                        end do
                        do j=cycl-cai_no+1,cycl
                                plus7=plus7+heatrate(i,j)
                                plus8=plus8+heat(i,j)
                        end do
                end if
                hr_mean(i)=plus1/cycl
                heat_mean(i)=plus2/cycl
                if(logic.eq.1) then
                        hr_misfir(i)=plus3/misfir_no
                        heat_misfir(i)=plus4/misfir_no
                        hr_si(i)=plus5/si_no
                        heat_si(i)=plus6/si_no
                        hr_cai(i)=plus7/cai_no
                        heat_cai(i)=plus8/cai_no
                end if
100     continue


C       calculate Mean value of w(j), imep(j), pumploss(j),... over cycles if logic=1
```

```
if(logic.eq.1) then
        if(misfir_no.gt.0) then
                plus1=0.0
                plus2=0.0
                plus3=0.0
                plus4=0.0
                plus5=0.0
                plus6=0.0
                plus7=0.0
                plus8=0.0
                plus9=0.0
                plus10=0.0
                plus11=0.0
                k=0
                do j=1,misfir_no
                        plus1=plus1+w(j)
                        plus2=plus2+imep(j)
                        plus3=plus3+pump(j)
                        plus4=plus4+p_max(j)
                        plus5=plus5+dpdt_max(j)
                        plus6=plus6+alpha0(j)
                        plus7=plus7+alpha1(j)
                        if(heat90(j).gt.360) then
                                plus8=plus8+heat5(j)
                                plus9=plus9+heat10(j)
                                plus10=plus10+heat50(j)
                                plus11=plus11+heat90(j)
                                k=k+1
                        end if
                end do
                w_misfir=plus1/misfir_no
                imep_misfir=plus2/misfir_no
                pump_misfir=plus3/misfir_no
                pmax_misfir=plus4/misfir_no
                dpdt_misfir=plus5/misfir_no
                a0_misfir=plus6/misfir_no
                a1_misfir=plus7/misfir_no
                mass5_misfir=plus8/k
                mass10_misfir=plus9/k
                mass50_misfir=plus10/k
                mass90_misfir=plus11/k
        end if
        if(si_no.gt.0) then
                plus1=0.0
                plus2=0.0
                plus3=0.0
                plus4=0.0
                plus5=0.0
                plus6=0.0
                plus7=0.0
                plus8=0.0
                plus9=0.0
                plus10=0.0
                plus11=0.0
                k=0
                do j=misfir_no+1,misfir_no+si_no
                        plus1=plus1+w(j)
                        plus2=plus2+imep(j)
                        plus3=plus3+pump(j)
                        plus4=plus4+p_max(j)
                        plus5=plus5+dpdt_max(j)
                        plus6=plus6+alpha0(j)
                        plus7=plus7+alpha1(j)
                        if(heat90(j).gt.360) then
                                plus8=plus8+heat5(j)
```

```
                                    plus9=plus9+heat10(j)
                                    plus10=plus10+heat50(j)
                                    plus11=plus11+heat90(j)
                                    k=k+1
                            end if
                    end do
                    w_si=plus1/si_no
                    imep_si=plus2/si_no
                    pump_si=plus3/si_no
                    pmax_si=plus4/si_no
                    dpdt_si=plus5/si_no
                    a0_si=plus6/si_no
                    a1_si=plus7/si_no
                    mass5_si=plus8/k
                    mass10_si=plus9/k
                    mass50_si=plus10/k
                    mass90_si=plus11/k
            end     if
            if(cai_no.gt.0) then
                    plus1=0.0
                    plus2=0.0
                    plus3=0.0
                    plus4=0.0
                    plus5=0.0
                    plus6=0.0
                    plus7=0.0
                    plus8=0.0
                    plus9=0.0
                    plus10=0.0
                    plus11=0.0
                    k=0
                    do j=cycl-cai_no+1,cycl
                            plus1=plus1+w(j)
                            plus2=plus2+imep(j)
                            plus3=plus3+pump(j)
                            plus4=plus4+p_max(j)
                            plus5=plus5+dpdt_max(j)
                            plus6=plus6+alpha0(j)
                            plus7=plus7+alpha1(j)
                            if(heat90(j).gt.360) then
                                    k=k+1
                                    plus8=plus8+heat5(j)
                                    plus9=plus9+heat10(j)
                                    plus10=plus10+heat50(j)
                                    plus11=plus11+heat90(j)
                            end if
                    end do
                    w_cai=plus1/cai_no
                    imep_cai=plus2/cai_no
                    pump_cai=plus3/cai_no
                    pmax_cai=plus4/cai_no
                    dpdt_cai=plus5/cai_no
                    a0_cai=plus6/cai_no
                    a1_cai=plus7/cai_no
                    mass5_cai=plus8/k
                    mass10_cai=plus9/k
                    mass50_cai=plus10/k
                    mass90_cai=plus11/k
            end if
    end if

    write(*,*) 'Heat release calculateion has been finished.'
    write(*,*) 'Input 1 to save the results and end the program, or'
write(*,*)'input 2 to get ISFC,specific emissions and tmeperature'
    read(*,*) logic1
```

```
        if(logic1.eq.1) goto 110

C       calculating the fuel consumption,ISFC (g/kw.h) using power averaged over cycles and from mean
pressure, respectively
        fuel=fuel*speed/2/1000
        isfc=fuel*3600/power
        pm_isfc=fuel*3600/pm_power

C       calculating the air flow rate (g/s)
        write(*,*) 'Input the A/F ratio:'
        read(*,*) af
        air=af*fuel

C       estimating the inner EGR percent and total mass per cycle(g/cycle)
        write(*,*) 'Input exhaust valve close timing (CA from intake TDC):'
        read(*,*) evc
        write(*,*) 'Input the exhaust temperature (C):'
        read(*,*) temp
        temp=temp+273
        Rb=8314/28.65
        egr=p_mean(evc)*vol(evc)/(Rb*temp)*9.81/100*speed*1000/2
        t_mass=(air+fuel+egr)*2/speed
        egr=egr/(air+fuel+egr)*100
        write(*,*)
        write(*,810) isfc,pm_isfc,egr
810     format('Two ISFC(g/kw.h): ',2(f6.1,1x),'EGR rate(%)=',f5.1)
        write(*,*)

C       *   *   *   *
C       Estimate the cylinder temperature (C) and max temperature from mean pressure
        Tmax_pm=0.0
        do i=1,720
                pm_T(i)=p_mean(i)*vol(i)*9.81*10/t_mass/Rb-273
                if(pm_T(i).gt.Tmax_pm) then
                        Tmax_pm=pm_T(i)
                        atmax_pm=i
                end if
        end do
C       temperature at 5% burnt rate
        do i=1,720
                if((mass5.ge.i).and.(mass5.lt.i+1)) then
                        T5_pm=pm_T(i)+(pm_T(i+1)-pm_T(i))*(mass5-i)
                end if
        end do
        write(*,811) Tmax_pm,atmax_pm
811     format('Max Temperature(C): ',f6.1,1x,'at CA=',f5.1)

C       Estimate the cylinder temperature (C) and max temperature for each cycle
        do i=1,305
                Tmax(i)=0.0
                a_Tmax(i)=0.0
        end do
        do j=1,cycl
                do i=1,720
                        T(i,j)=p(i,j)*vol(i)*9.81*10/t_mass/Rb-273
                        if(T(i,j).gt.Tmax(j)) then
                                Tmax(j)=T(i,j)
                                a_Tmax(j)=i
                        end if
                end do
        end do
C       temperature at 1% burnt rate
        do j=1,cycl
                do i=1,720
                        if((heat5(j).ge.i).and.(heat5(j).lt.i+1)) then
```

```
                        T5(j)=T(i,j)+(T(i+1,j)-T(i,j))*(heat5(j)-i)
                        end if
                end do
        end do
C       calculate mean temperature at 1% burnt rate over total cycles
        plus=0.0
        do j=1,cycl
                plus=plus+T5(j)
        end do
                T5_mean=plus/cycl

C       calculate the mean temperature over total cycles
        do i=1,720
                plus1=0.0
                do j=1,cycl
                        plus1=plus1+T(i,j)
                end do
                T_mean(i)=plus1/cycl
        end do
C       mean Max Temperarue (Tmax) and its CA
        plus=0.0
        plus1=0.0
        do j=1,cycl
                plus=plus+Tmax(j)
                plus1=plus1+a_Tmax(j)
        end do
        Tmax_mean=plus/cycl
        atmax_mean=plus1/cycl
C       COV of Tmax and T5
        plus=0.0
        plus1=0.0
        do j=1,cycl
                plus=plus+(Tmax(j)-Tmax_mean)*(Tmax(j)-Tmax_mean)
                plus1=plus1+(T5(j)-T5_mean)*(T5(j)-T5_mean)
        end do
        plus=sqrt(plus/cycl)
        plus1=sqrt(plus1/cycl)
        cov_Tmax=plus*100/Tmax_mean
        cov_T5=plus1*100/T5_mean
        write(*,812) Tmax_mean,cov_Tmax,T5_mean,cov_T5
812     format('Tmax & COV:',2(f6.1),3x,'T@1% & COV:',2(f6.1))
C       *   *   *   *



C       calculating the specific emissions using averaged power over cycles and from mean pressure,
respectively
        write(*,*) 'Input emission readings, CO(%),HC(ppm),NOx(ppm),CO2(%)'
        read(*,*) co,hc,nox,co2
        a=7.94
        b=1.85
        c=0.0
        tc=co+co2+hc/10000
C       plus=a*(12+1*b+16*c)
        plus=12+1*b+16*c
        pm_co=co*(12+16)*pm_isfc/(plus*tc)
        pm_hc=hc*(b*1+12)*pm_isfc/(plus*tc)/10000
        pm_nox=nox*(14+16*2)*pm_isfc/(plus*tc)/10000
        co=co*(12+16)*isfc/(plus*tc)
        hc=hc*(b*1+12)*isfc/(plus*tc)/10000
        nox=nox*(14+16*2)*isfc/(plus*tc)/10000

C       nr=1+a*(1+b/4)*(1+3.773)
C       np=a*(1+b/2)+a*(1+b/4)*3.773
C       plus=a*(12+1*b+16*c)
```

```
C       c_mole=a/plus*100
C       co=co*(12+16)*isfc/(plus*c_mole)
C       hc=hc*(b*1.008+12)*isfc/(plus*c_mole)/10000
C       nox=nox*(14+16*2)*isfc/(plus*c_mole)/10000
        write(*,820) co,hc,nox
820     format('CO, HC, NOx (averaged over cycles): ',3(f7.2,1x))
        write(*,821) pm_co,pm_hc,pm_nox
821     format('CO, HC, NOx (calculated from mean pressure): ',3(f7.2,1x))

C       calculate some variables
        hcci=1000*cai_no*0.1/cycl
        grosswork=(w_mean+pump_mean)*1000000/vh
        pup=pump_mean*1000000/vh

C       output the results
110     write(*,*) 'Input the filename for saving heat release results:'
        read(*,*) filename
        open(12,file=filename,status='unknown')
        write(12,599) cycl


C       *       *   *   *
        if(logic1.ne.1) then
        write(12,598) hcci,imep_mean,cov_imep,isfc
        write(12,597) Tmax_mean,T5_mean,cov_T5,co,hc,nox,mass5,mass10,
     &  mass50,mass90,pmax_mean,dpdt_mean,grosswork,pup,power,egr
        end if
598     format(4(1x,f7.2))
597     format(17(1x,f7.2))
C       *       *   *   *

        write(12,*) '***** Parameters averaged over cycles *****'
        write(12,600) pmax_mean,a0_mean,dpdt_mean,a1_mean,Tmax_mean,
     &  atmax_mean,T5_mean
        write(12,601) w_mean,power,imep_mean,pump_mean
        write(12,614) mass5,mass10,mass50,mass90
        if(logic1.ne.1) then
                write(12,620) isfc,egr,air,fuel
                write(12,621) co,hc,nox
        end if
        write(12,*)
        write(12,*) '***** Parameters calculated from mean pressure *****'
        write(12,600) pm_max,pm_alpha0,pm_dpdt,pm_alpha1,Tmax_pm,
     &  atmax_pm,T5_pm
        write(12,601) pm_work,pm_power,pm_imep,pm_pump
        write(12,614) pm_heat5,pm_heat10,pm_heat50,pm_heat90
        if(logic1.ne.1) then
                write(12,620) pm_isfc,egr,air,fuel
                write(12,621) pm_co,pm_hc,pm_nox
        end if
        write(12,*)
        write(12,602) cov_imep,cov_pmax,cov_dpdt,cov_a0,cov_a1,cov_Tmax,cov_T5
        write(12,*)
        if(logic.eq.1) then
                write(*,*)
                write(12,615) misfir_no,si_no,cai_no
                write(12,603) w_misfir,w_si,w_cai
                write(12,604) pump_misfir,pump_si,pump_cai
                write(12,605) imep_misfir,imep_si,imep_cai
                write(12,606) pmax_misfir,pmax_si,pmax_cai
                write(12,607) dpdt_misfir,dpdt_si,dpdt_cai
                write(12,608) a0_misfir,a0_si,a0_cai
                write(12,609) a1_misfir,a1_si,a1_cai
                write(12,610) mass5_misfir,mass5_si,mass5_cai
                write(12,611) mass10_misfir,mass10_si,mass10_cai
```

```
                write(12,612) mass50_misfir,mass50_si,mass50_cai
                write(12,613) mass90_misfir,mass90_si,mass90_cai
        end if
        write(12,*)
        write(12,*)'********** Cycle-resolved results **********'
        write(12,*)'Cycl,Work,Imep,Pump,Pmax,dp/dt,CA_Pmax,
    &CA_dp/dt,1%,10%,50%,90%,Tmax,CA_Tmax,T1%'
        do j=1,cycl
        write(12,700) j,w(j),imep(j),pump(j),p_max(j),dpdt_max(j),
    &alpha0(j),alpha1(j),heat5(j),heat10(j),heat50(j),heat90(j),
    &Tmax(j),a_Tmax(j),T5(j)
        end do
        write(12,*)
        if(logic.ne.1) then
                write(12,*) '***Cylinder pressure (mean + vol + 50 cycles)***'
                do i=1,720
                        write(12,701) i,p_mean(i),vol(i),(p(i,j),j=1,50)
                end do
                if(logic1.ne.1) then
                        write(12,*)
                        write(12,*) '****** Cylinder Temperature ******'
                        write(12,*) 'T (mean pres.) + T (over cycles) + 50 cycles)'
                        do i=1,720
                                write(12,701) i,pm_T(i),T_mean(i),(T(i,j),j=1,50)
                        end do
                end if
                write(12,*)
                write(12,*) '******* Rate of Heat Release (HRR) *******'
                write(12,*) 'HRR (mean pres.) + HRR (over cycles) + 50 cycles)'
                do i=1,720
                write(12,701) i,pm_hr(i),hr_mean(i),(heatrate(i,j),j=1,50)
                end do
                write(12,*)
                write(12,*) '******* Integrated Heat Release (IHR) *******'
                write(12,*) 'IHR (mean pres.) + IHR (over cycles) + 50 cycles)'
                do i=ivc,evo
                        write(12,701) i,pm_heat(i),heat_mean(i),(heat(i,j),j=1,50)
                end do
        else
                write(12,*)'***Pressure list (slow-burn,SI and CAI cycles)***'
                k1=20
                k2=20
                k3=50
                if(misfir_no.lt.30) k1=misfir_no
                if(si_no.lt.30) k2=si_no
                if(cai_no.lt.30) k3=cai_no
C               if((misfir_no+si_no).le.30) k3=50
C               if((misfir_no+cai_no).le.30) k2=50
C               if((si_no+cai_no).le.30) k3=50
                write(12,800) k1,k2,k3
                do i=1,720
                write(12,701) i,p_mean(i),vol(i),p_misfir(i),p_si(i),p_cai(i),
    &           (p(i,j),j=1,k1),(p(i,j),j=misfir_no+1,misfir_no+k2),
    &           (p(i,j),j=cycl-k3+1,cycl)
                end do
                if (logic1.ne.1) then
                        write(12,*)
                        write(12,*) '***** Temperature List *****'
                        write(12,802) k1,k2,k3
                        do i=1,720
                          write(12,701) i,pm_T(i),T_mean(i),(T(i,j),j=1,k1),(T(i,j),
    &                     j=misfir_no+1,misfir_no+k2),(T(i,j),j=cycl-k3+1,cycl)
                        end do
                end if
                write(12,*)
```

```
                write(12,*) '**** Rate of Heat Release List ****'
                write(12,801) k1,k2,k3
                do i=1,720
                  write(12,701) i,pm_hr(i),hr_mean(i),hr_misfir(i),hr_si(i),
     &     hr_cai(i),(heatrate(i,j),j=1,k1),(heatrate(i,j),
     &     j=misfir_no+1,misfir_no+k2),(heatrate(i,j),j=cycl-k3+1,cycl)
                end do
                write(12,*)
                write(12,*) '******** Heat Release List ********'
                write(12,801) k1,k2,k3
                do i=ivc,evo
                  write(12,701) i,pm_heat(i),heat_mean(i),heat_misfir(i),heat_si(i),
     &      heat_cai(i),(heat(i,j),j=1,k1),(heat(i,j),
     &      j=misfir_no+1,misfir_no+k2),(heat(i,j),j=cycl-k3+1,cycl)
                end do
        end if
        close(12)
599     format('Total cycles are:',i4)
600     format('Pmax,CA_Pmax,dp/dt,CA_dp/dt,Tmax,CA_Tmax,T1%=',7(f7.2,1x))
601     format('W(J), P(kw), imep(kPa), pump(kPa)=',4(f7.2,1x))
602     format('COV of imep,Pmax,dp/dt,CA_Pmax,CA_dp/dt,Tmax,T1%=',7(f6.1))
603     format('WORK (J) for slow-burn, SI and CAI is:',3(f7.2,1x))
604     format('PUMPLOSS (J) for slow-burn, SI and CAI is:',3(f7.2,1x))
605     format('IMEP (kPa) for slow-burn, SI and CAI is:',3(f7.2,1x))
606     format('Pmax (kg/cm2) for slow-burn, SI and CAI is:',3(f7.2,1x))
607     format('dp/dt_max for slow-burn, SI and CAI is:',3(f7.2,1x))
608     format('CA_Pmax (deg) for slow-burn, SI and CAI is:',3(f7.2,1x))
609     format('CA_dp/dt_max for slow-burn, SI and CAI is:',3(f7.2,1x))
610     format('CA of 1% HR for slow-burn, SI and CAI is:',3(f7.2,1x))
611     format('CA of 10% HR for slow-burn, SI and CAI is:',3(f7.2,1x))
612     format('CA of 50% HR for slow-burn, SI and CAI is:',3(f7.2,1x))
613     format('CA of 90% HR for slow-burn, SI and CAI is:',3(f7.2,1x))
614     format('CA of 1%,10%,50%,90% Heat Release (HR)=',4(f7.2,1x))
615     format('misfire/slow-burn, SI, CAI cycles=',3(i4,1x))
620     format('ISFC(g/kw.h),EGR(%),air & fuel flow(g/s)=',4(f7.2,1x))
621     format('Specific emissions CO,HC,NOx (g/kw.h)=',3(f7.2,1x))
700     format(i4,21(1x,f7.2))
701     format(i4,100(1x,f7.2))
800     format('Mean,volume,mean_misfir,mean_si,mean_cai,following
   &  with slow-burn, SI and CAI combustion cycles=',3(i4,1x))
801     format('Mean+avg.+mean_misfir +mean_si +mean_cai following
   &  with slow-burn, SI and CAI combustion cycles=',3(i4,1x))
802     format('Mean+avg. following
   &  with slow-burn, SI and CAI combustion cycles=',3(i4,1x))


        write(*,*) 'OK, input any key to complete the calculation. '
        read(*,*)

        END
```